UNIVERSITY OF CALIFORNIA, SAN DIEGO

Selective attention and its roles in enhancing sensory information processing and perceptual performance

A dissertation submitted in partial satisfaction of the requirements for the degree

Doctor of Philosophy

in

Neurosciences

by

Sirawaj Itthipuripat

Committee in charge:

Professor John Serences, Chair
Professor Karen Dobkins
Professor Timothy Gentner
Professor John Reynolds
Professor Ayse Saygin

2017

The dissertation of Sirawaj Itthipuripat is approved, and it is acceptable in quality and form for publication on microfilm and electronically:

_____

_____

_____

_____

_____
Chair

University of California, San Diego

2017

DEDICATION

To family and friends

TABLE OF CONTENTS

LIST OF ABBREVIATIONS

BOLD: blood-oxygenation level dependent

CRF: contrast response function

EEG: electroencephalography

EOI: electrode-of-interest

ERP: event-related potential

fMRI: functional magnetic resonance imaging

GLM: general linear model

ITI: intertrial interval

LPD: late positive deflection

NMA: The normalization model of attention

RF: receptive field

RT: response time

SDT: signal detection theory

SNR: signal-to-noise ratio

SSVEP: steady-state visual evoked potential

TvC: threshold versus contrast curve

VSDI: voltage-sensitive dye imaging

LIST OF FIGURES

LIST OF TABLES

ACKNOWLEDGMENTS

First, I would like to thank my mother, Quanratt Itthipuripat, who has fostered me with love and has always believed in my talent and determination. Second, I would like to thank my father, Tanamet Itthipuripat, whose hard work has provided me opportunities to pursue higher levels of education. Third, I would like to thank my aunt, Dr. Iyarint Itthipuripat, who has inspired me to pursue a career in science. Fourth, I would like to thank my younger brother and sister, Dr. Siratarn Itthipuripat and soon-to-be-Dr. Sirarat Itthipuripat, for always having my back— I am so proud of you both.

Next, I would like to thank Dr. Marty Woldorff for giving me 4 years worth of research experience at Duke University. You instilled in me valuable knowledge related to cognitive neuroscience and equipped me with a research skillset that made me ready for graduate school.

I would like to give a special thank you to Dr. John Serences for being an awesome advisor, a respectable role model, and a great friend. For 6 years at UCSD, you have guided me to establish myself as an independent and successful scholar. You have allowed me to explore my research interests and have helped me reach my full potential during graduate school. Thank you John! Moreover, I would like to give special thanks to Howard Hughes Medical Institute for recognizing the importance of supporting international students in the United State of America and for granting me financial support for my research and education at UCSD.

I would also like to thank Dr. Adam Aron for the many opportunities to collaborate with your research team at UCSD, and thank to my thesis committees including Dr. Karen Dobkins, Dr. John Reynolds, Dr. Timothy Gentner, and Dr. Ayse Saygin for your valuable time and advice. Moreover, I would like to thank all the staff, faculty members, and students

at the UCSD Neurosciences graduate program for making our program a great platform for me not only to develop my research career but also to thrive in the Neuroscience community in a broader sense.

Next, I would like to thank my past and current lab mates, including Dr. Thomas Sprague, Dr. Anna Byers, Dr. Javier Garcia, Dr. Edward Ester, Dr. Rosy Cowell, Dr. Mary Smith, Dr. Miranda Scolari, Dr. Tiffany Ho, Dr. Rosy Cowell, Dr. Chaipat Chunharas, Dr. Rosanne Readmaker, Vy Vo, Stephanie Nelli, Nuttida Rungratsameetweemana, Margaret Henderson, Kimberly Kay, and Anna Shafer Skelton for your intellectual inputs, help with many technical challenges, and friendship. Here, I would also like to give a special thank you to Dr. Thomas Sprague for being such an awesome science buddy!

I would also like to give special thanks to my superstar research assistants, including Sean Deering, Kexin Cha, Kai-yu Chang, Annalisa Salazar, and Napat Rungsipat for your significant contributions to our research projects, and our previous and future publications. And thanks to all other research assistants including Vianey Perez, Suzana Wong, Ivan Macias, Isabel Asp, Emily Baker, Naomi Lee, Kevin Diep, Ashley Bong, Amanda Du, Cherin Kim, Metta Nguyen, Arthi Venkat, Cecillia Chow, Siyi Chen, Jhankhana Jan, Kevin Wu, Fairlie Reese, Candace Linscheid, Tony Abuyo, and Danna Lee. Without your help, I would not have been able to succeed.

Last but not least, I would like to thank all my dear friends including Dr. Scott Freeman, Dr. Evan Carr, Dr. Anna Byers, Dr. Kristin Howell, Dr. Camille Toarmino, Stephanie Nelli, Azim Raza, Michelle Fields, Sean Deering, Adam Morgan, and Phichai Khammano. You all have taught me what true friendship is all about. I will certainly miss you and miss our good and fun times in San Diego. I love you all.

Chapter 1, in full, is a reprint of the material as it appears in a review entitled "Integrating levels of analysis in systems and cognitive neurosciences: selective attention as a case study" published in The Neuroscientist 2015. Itthipuripat, S.; Serences, John T., SAGE Publications, 2015. The dissertation author was the primary author of the manuscript. Supported by NIH-092345 and a James S. McDonnell Foundation Scholar Award to J.T.S., and by an HHMI International Fellowship to SI. We thank Kexin Cha for help producing figures; Thomas Sprague, Justin Gardner, and Franco Pestilli for useful conversions; and John Reynolds, Jude Mitchell, John Maunsell, Joonyeol Lee, Franco Pestilli, Justin Gardner, Marisa Carrasco, David Heeger, Eyal Seidemann, and Yuzhi Chen for providing materials for data figures.

Chapter 2, in full, is a reprint of the material as it appears in an article entitled "Temporal dynamics of divided spatial attention" published in Journal of Neurophysiology 2013. Itthipuripat, S.; Garcia, Javier O.; Serences, John T., American Physiological Society, 2013. The dissertation author was the primary author of the manuscript. Supported by NIMH Grant R01-MH092345 to J.S.T. and by NIMH Grant R01-MH68004 G.J.O. We thank Candace Linscheid, Tony Abuyo, and Danna Lee for help with data collection.

Chapter 3, in full, is a reprint of the material as it appears in an article entitled "Changing the spatial scope of attention alters patterns of neural gain in human cortex" published in The Journal of Neuroscience 2014. Itthipuripat, S.; Garcia, Javier O.; Rungratsameetaweemana, Nuttida; Sprague, Thomas C.; Serences, John T., Society for Neuroscience, 2014. The dissertation author was the primary author of the manuscript. Supported by NIH Grant R01-MH092345 and a James S. McDonnell Foundation grant to J.T.S. and by NIH Grant R01-MH068004 to J.O.G. We thank Kimberly Kaye and Edward F. Ester for help with data collection, Anna Byers and Mary E. Smith for assistance with

retinotopic mapping procedures, and John Reynolds, Timothy Q. Gentner, Edward Awh, Jeremy Freeman, and Scott Freeman for useful discussions.

Chapter 4, in full, is a reprint of the material as it appears in an article entitled "Sensory gain outperforms efficient readout mechanisms in predicting attention-related improvements in behavior " published in The Journal of Neuroscience 2014. Itthipuripat, S.; Ester, Edward F.; Deering, Sean; Serences, John T., Society for Neuroscience, 2014. The dissertation author was the primary author of the manuscript. Supported by National Institutes of Health Grant R01-MH092345 to J.T.S., by a James S. McDonnell Foundation grant to J.T.S, and by a Howard Hughes Medical Institute international student fellowship to S.I. We thank Suzanna K. Wong and Ivan Macias for help with data collection; Javier Garcia and Franco Pestilli for technical support; and Steven Hillyard, Franco Pestilli, Justin Gardner, Thomas C. Sprague, and Anna Byers for useful discussions.

VITA

2011, Bachelor of Science with Summa Cum Luade, Neuroscience, Duke University

2011, Bachelor of Science with Summa Cum Luade, Psychology, Duke University

2013, Master of Science, Neurosciences, University of California, San Diego

2017, Doctor of Philosophy, Neurosciences, University of California, San Diego

PUBLICATIONS

Itthipuripat, S., Garcia, J.O., Serences, J.T. (2013). "Temporal dynamics of divided spatial attention." *Journal of Neurophysiology*. 109(9): 2364-73.

Itthipuripat, S., Garcia, J.O., Rungratsameetaweemana, N., Sprague, T., Serences, J.T. (2014) "Changing the scope of attention alters patterns of neural gain in human cortex." *The Journal of Neuroscience*. 34(1):112-123

Itthipuripat, S., Ester E.F., Deering, S., Serences, J.T., (2014) "Sensory gain outperforms efficient read-out mechanisms in predicting attention-related improvements in behavior." *The Journal of Neuroscience*. 34 (40): 13384-98.

Itthipuripat, S., Serences, J.T. (2015) "Integrating levels of analysis in systems and cognitive neuroscience: selective attention as a case study." *The Neuroscientist*. pii: 1073858415603312.

ABSTRACT OF THE DISSERTATION

Selective attention and its roles in enhancing

sensory information processing and perceptual performance

by

Sirawaj Itthipuripat

Doctor of Philosophy in Neurosciences

University of California, San Diego, 2017

Professor John Serences, Chair

In a complex visual environment—such as a crowed street—driving would be impossible if drivers do not have an intact attentional system. They have to monitor surrounding vehicles, while attending to traffic lights and pedestrians. Under this scenario, drivers need to divide their attention into multiple spotlights and flexibly change the size of their attention field such that only relevant information is efficiently processed. In the first experiment (Chapter 2), we provided neural evidence showing that attention could be divided into multiple spotlights. Using a stimulus-frequency-tagging technique where we flashed two visual targets and a distractor at the

intermediate location at different frequencies, we were able to monitor changes of steady state visually evoked potentials (SSVEPs) that oscillated at the same frequencies as the target and distractor stimuli. We found the significant divergence of the target-related and distractor-related SSVEPs ~150-350ms before human participants correctly discriminated the two targets. In the second experiment (Chapter 3), we examined the neural basis underlying changes of the spatial scope of attention and studied how such changes may alter the way sensory information is encoded in the visual cortex. By manipulating the spatial extent of visual target in a stream of flickering non-target stimuli, we observed changes in the spread of cortical activity in the contralateral visual cortex measured using functional magnetic resonance imaging (fMRI). Importantly, we found that this attentional spread modulated the magnitude of sensory signals measured via SSVEPs in the way that was consistent with predictions from computational models based on divisive normalization. Lastly, in the third experiment (Chapter 4), we made a further step to examine the quantitative relationship between attentional gain modulations of neural signals and attention-related improvements in behavioral performance. We found that attentional gain modulations of early visually evoked responses could sufficiently predict attention-related improvements in perceptual performance, without the need to invoke other alternative mechanisms, such as noise reduction or efficient read-out mechanisms. Taken together, the results from these three experiments suggest that selective attention enhances sensory information processing via changes in gain modulations of early sensory signals and these attentional gain modulations play a critical role in supporting attention-related improvement in perceptual performance.

Chapter 1:

Integrating levels of analysis in systems and cognitive neurosciences: selective attention as a case study

Integrating Levels of Analysis in Systems and Cognitive Neurosciences: Selective Attention as a Case Study

Sirawaj Itthipuripat [1] and John T. Serences [1,2,3]

Abstract
Neuroscience is inherently interdisciplinary, rapidly expanding beyond its roots in biological sciences to many areas of the social and physical sciences. This expansion has led to more sophisticated ways of thinking about the links between brains and behavior and has inspired the development of increasingly advanced tools to characterize the activity of large populations of neurons. However, along with these advances comes a heightened risk of fostering confusion unless efforts are made to better integrate findings across different model systems and to develop a better understanding about how different measurement techniques provide mutually constraining information. Here we use selective visuospatial attention as a case study to highlight the importance of these issues, and we suggest that exploiting multiple measures can better constrain models that relate neural activity to animal behavior.

Keywords
attention, systems neuroscience, cognitive neuroscience, levels of analysis, behavior

Introduction

The ultimate goal of neuroscience is to understand links between brain activity and behavior from micro to macro levels of analysis (Sejnowski 1991; Sejnowski and others 2014). This goal is being pursued using ever more advanced tools to assay neural activity, coupled with increasingly nuanced computational models to link neural data to behavioral outcomes. However, these advances also pose a formidable set of challenges as new technology is often deployed before we fully understand how the new measurements relate to more traditional assays of neural activity. For example, there is still an unclear link between single-unit spiking activity and the pattern of responses observed with large-scale measurements such as electroencephalography (EEG), the blood-oxygenation level dependent (BOLD) response as measured using functional magnetic resonance imaging (fMRI), voltage-sensitive dye imaging (VSDI), and calcium imaging. Whereas the severity of this problem varies, each method comes with its own unique set of inference issues. Moreover, different methods are often sensitive to at least partially independent aspects of neuronal and cortical activity (e.g., membrane potentials, action potentials, calcium concentrations, neurovascular activity), so failing to formally link data collected using different techniques at different spatial and temporal scales represents a significant missed opportunity.

The main purpose of this update article is to highlight these challenges by focusing on efforts to link selective attentional modulations in visual cortex with behavior. This is an ideal case study in many respects because research in this area has been done in a variety of species using a variety of techniques, and there is a long history of using quantitative models to link changes in neural activity with changes in perceptual sensitivity and behavioral performance.

Selective Attention, Neural Modulations, and Changes in Perceptual Sensitivity

Attention is an essential cognitive operation that selectively enhances the processing of relevant information

[1]Neurosciences Graduate Program, University of California, San Diego, La Jolla, CA, USA
[2]Department of Psychology, University of California, San Diego, La Jolla, CA, USA
[3]Kavli Institute for Brain and Mind, University of California, San Diego, La Jolla, CA, USA

Corresponding Author:
Sirawaj Itthipuripat, Neuroscience Graduate Program, University of California, San Diego, 9500 Gilman Dr., 92093, La Jolla, CA 92093, USA.
Email: itthipuripat.sirawaj@gmail.com

while simultaneously suppressing the processing of irrelevant information. Attention deficits are apparent in many clinical populations, including patients with schizophrenia (Heinrichs and Zakzanis 1998), attention-deficit hyperactivity disorder (Stefanatos and Baron 2007), and Parkinson's disease (Botha and Carr 2012). Given these clinical implications, it is not surprising that thousands of experiments have been carried out to examine the neural mechanisms that support selective information processing. Here we focus on three general mechanisms for illustrative purposes, but several more comprehensive reviews have recently been published and go into far more detail (e.g., Anton-Erxleben and Carrasco 2013; Carrasco 2011; Krauzlis and others 2014; Sprague and others 2015).

Generally speaking, attention has been proposed to operate by enhancing the gain of neural responses associated with relevant stimuli (*sensory gain models*), by reducing the variability of neural responses in order to increase encoding fidelity (*noise reduction models*), and by enhancing the efficiency of the "read-out" of early sensory responses by downstream decision circuits (*efficient read-out models*). Although there is considerable evidence that supports all three of these mechanisms and they are by no means mutually exclusive, it is challenging to predict when one mechanism might play a dominant role in attentional selection and this has motivated much debate in the literature. For example, differences in the physical characteristics of the stimulus can play a large role in generating different patterns of attentional modulation observed in visual cortex (Herrmann and others 2010; Itthipuripat and others 2014b; Reynolds and Heeger 2009). However, we argue that another source of variability relates directly to the methods that are used to measure neural modulations and the methods that are used to relate those modulations to behavior. We start with a brief overview of the three different models of attentional modulation that we will consider here, and we then highlight how results from different methods support different theories, even in situations where behavioral paradigms are strikingly similar.

Sensory Gain, Noise Reduction, and Efficient Read-Out Mechanisms

In one widely used attention task, subjects must determine which of two successive stimulus intervals (first or second) contains a "test" stimulus rendered in a slightly higher contrast than a "standard" stimulus (i.e., a two-interval forced choice, or 2IFC, task; see Fig. 1A). The smallest discriminable change in contrast can be measured by adjusting the difference in contrast between the test stimulus and the standard stimulus. This procedure can be repeated using standard stimuli of different contrasts to map out a full *threshold versus contrast* curve (TvC; Fig. 1B). While behavioral thresholds are assessed at each standard contrast level, neural responses in visual cortex can also be concurrently measured to estimate the magnitude of cortical responses, producing a *contrast response function* (CRF; Fig. 1C) (Boynton and others 1999). Using this general approach, studies can determine how attention changes the relationship between neural activity and behavior by systematically manipulating the focus of attention with either a focused-attention cue or with a divided-/distributed-attention cue at the beginning of each trial (Fig. 1A; Hara and Gardner 2014; Itthipuripat and others 2014a; Pestilli and others 2011).

Linking attentional modulations of neural responses and behavior can then be achieved by using signal detection theory (SDT) to relate the slope and the variability at each point along the neural CRF to the shape of the psychophysical TvC function (Boynton and others 1999; Itthipuripat and others 2014a; Pestilli and others 2011). In STD, perceptual sensitivity (termed d') is proportional to the magnitude of the differences between two neural signals (ΔR) that are evoked by two different stimuli, weighted by the variability of each signal (σ) (Boynton and others 1999; Tanner and Swets 1954). In cases of pure sensory gain, d' increases as ΔR or the slope of the CRF increases, while σ is constant (Fig. 2A). In noise reduction models, d' increases when the overlap between the signal distributions associated with each stimulus is reduced (Fig. 2B). In contrast, efficient read-out models hold that sensory gain and noise reduction are not sufficient to explain behavior. Instead, these models posit that an additional read-out rule is implemented so that the output from neural populations that encode relevant information is over-weighted compared to neural populations that encode irrelevant information (Fig. 2C and D) (Eckstein and others 2009; Hara and Gardner 2014; Palmer and others 2000; Pelli 1985; Pestilli and others 2011; Shaw 1984). Importantly for our current purposes, the link between each neural model and behavioral performance can be understood through a common, and relatively simple, theoretical framework based on SDT.

Linking Sensory Gain to Behavioral Performance

Empirical support for sensory gain models (Fig. 2A) comes primarily from single-unit recordings in monkeys and from EEG studies in human subjects (Di Russo and others 2001; Hillyard and others 1998; Itthipuripat and others 2014a; Itthipuripat and others 2014b; Kim and others 2007; Lauritzen and others 2009; Lee and Maunsell 2009, 2010; Martínez-Trujillo and Treue 2002; Reynolds and others 2000; Störmer and others 2009; Wang and Wade 2011). Early monkey single-unit recording studies reported that attention increases the gain of the CRF at

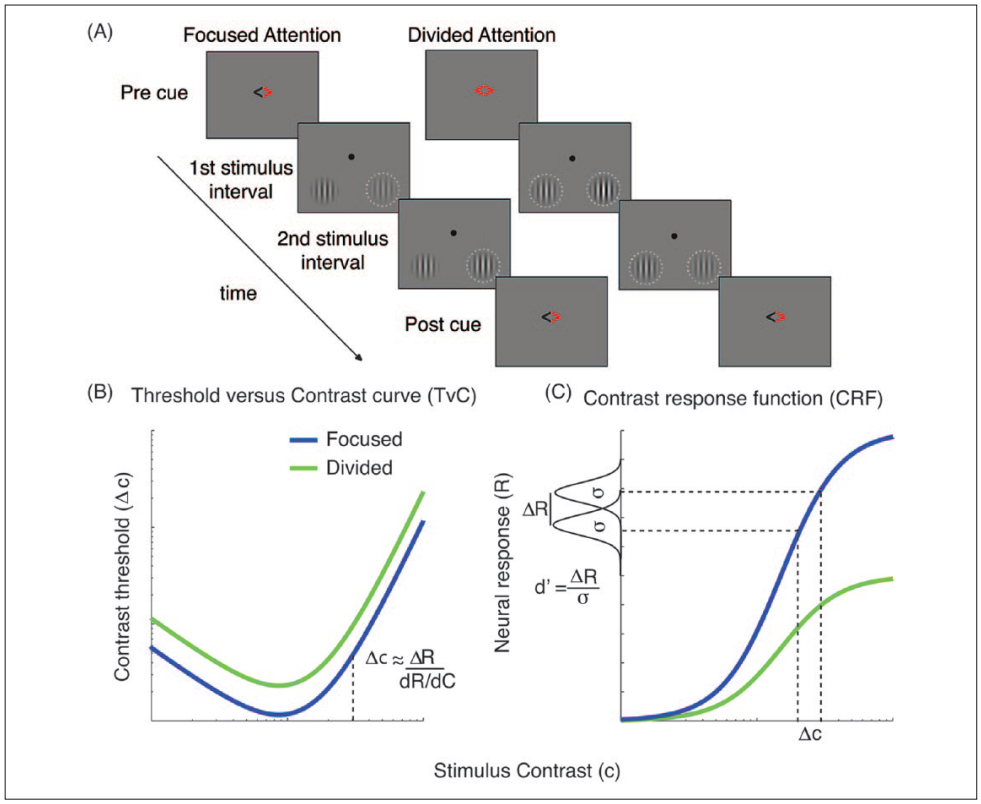

Figure 1. Linking changes in perceptual sensitivity to contrast response functions (CRFs) in visual cortex. In a standard two-interval-force choice (2IFC) contrast discrimination tasks (see panel A for example), subjects have to report which of the two successive stimulus intervals (1st or 2nd) contains a "test" stimulus that is rendered with a slightly higher contrast than a "standard" stimulus. The minimum detectable contrast change is then measured as function of each "standard" stimulus contrast (along x-axis) to estimate the minimum change in contrast (threshold) required to make an accurate discrimination. This produces "threshold versus contrast" curves (TvCs in panel B). In these tasks, responses in visual cortex can be concurrently measured, yielding neural contrast response functions (CRFs in panel C). The link between TvCs and CRFs can be made using signal detection theory (STD). For example, the psychophysical contrast threshold (Δc in panel B) at any given level of the standard contrast (c) is approximately proportional to the differential neural responses evoked by the standard stimulus and test stimuli (ΔR in panel C), divided by the derivative of the CRF (dR/dC). According to STD, perceptual sensitivity (d') will increase when ΔR increases as well as when trial-by-trial variability (σ) of neural responses decreases. This logic can be applied to link changes in TvC curves with attention-induced changes in neural CRFs. For example, in the focused-attention condition (left side of panel A), subjects were cued to attend to the location that contained the target contrast increment. In the divided-attention condition (right side of panel B), subjects were cued that either location could contain the target stimulus. In these tasks, TvCs and CRFs for both focused- and divided-attention conditions (blue and green curves in panels B and C) were measured, and the link between attention-induced changes in TvCs and CRFs could be made using quantitative modeling (see Fig. 2).

mid-level contrasts in visual areas such as V4 and MT (termed *contrast gain*) (Fig. 3A; Martínez-Trujillo and Treue 2002; Reynolds and others 2000). This attentional enhancement of responses should, in theory, facilitate contrast discrimination by creating more separable neural response distributions, particularly for mid-contrast visual stimuli (cf., Carrasco and others 2004).

While some of these studies support a link between sensory gain at mid-level contrasts and behavior, different patterns of sensory gain in the CRF have also been

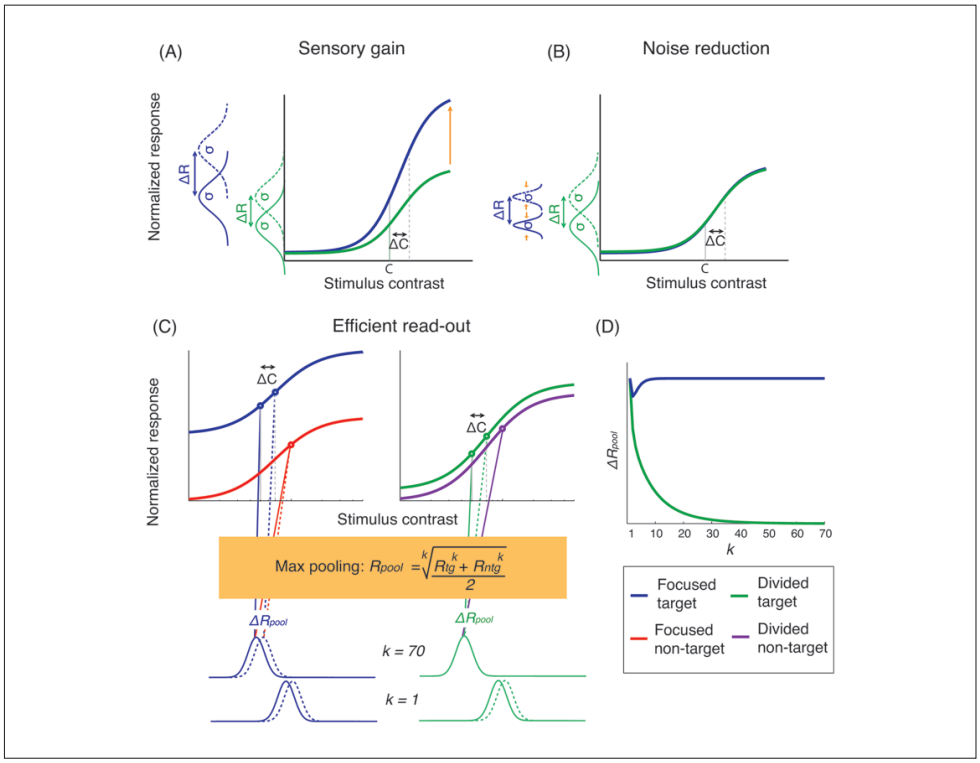

Figure 2. Alternative models of attention. (A) Sensory gain models posit that attention amplifies neural responses in sensory cortex. In a contrast discrimination task, attention-induced sensory gain will increase the slope of the CRF and thereby magnify the differential responses (ΔR) evoked by a standard stimulus and a test stimulus that has a slightly higher contrast, resulting in enhanced perceptual sensitivity. (B) In contrast, noise reduction models propose that attention achieves a similar increase in d by reducing the trial-by-trial variability of neural responses. When attention reduces the trial-by-trial variability of sensory responses (σ) associated with pedestal and test stimuli, perceptual sensitivity will increase even when if there no change in ΔR because the responses distributions will overlap less. (C) Post-sensory readout models hold that neither sensory gain nor noise modulation sufficiently accounts for attention-induced changes in behavior because using some measurement techniques such as fMRI, attention does not change the gain (slope) or the noise characteristics, but instead induces an additive shift of CRFs (also see Fig. 3G and H and right panels in Fig. 4). The read-out model proposes that the responses to all stimuli in each interval are first pooled, and then a decision is based on the interval that has the larger pooled response. Moreover, sensory responses evoked by target (R_{tg}) and nontarget stimuli (R_{ntg}) are combined into the pooled response (R_{pool}) using a max-pooling operation (see equation in the yellow box) that uses exponentiation (k) to overweight high amplitude responses. In turn, larger changes in the pooled response between the first and second interval will support better performance (ΔR_{pool}). Because of the additive shift in the fMRI-based CRFs induced by attention, this exponentiation will overweight responses to attended target stimuli over responses to ignored nontarget stimuli (blue vs. red curves). However, in the distributed-/divided-attention condition, there is a smaller additive increase in the response to the target stimulus (green vs. purple curves); thus, when nontarget stimuli happen to be rendered at higher contrasts than the target stimulus, the model will overweight responses to nontarget stimuli, resulting in lower perceptual sensitivity in the divided-/distributed-attention compared with the focused-attention condition.
(D) Simulation of the max-pooling rule showing the differential response pooled from signals evoked by the interval containing the standard stimuli and the interval containing the standards plus the target increment (ΔR_{pool}) across divided- and focused-attention conditions (green vs. blue curves). When k = 1, ΔR_{pool} is the same across divided- and focused-attention conditions. However, when k increases, ΔR_{pool} in the divided-attention condition sharply decreases and becomes much lower than ΔR_{pool} in the focused-attention condition. Thus, as k increases, perceptual sensitivity in the divided-attention condition will decrease under the assumption that the noise of the pooled responses is identical across focused- and divided-attention conditions.

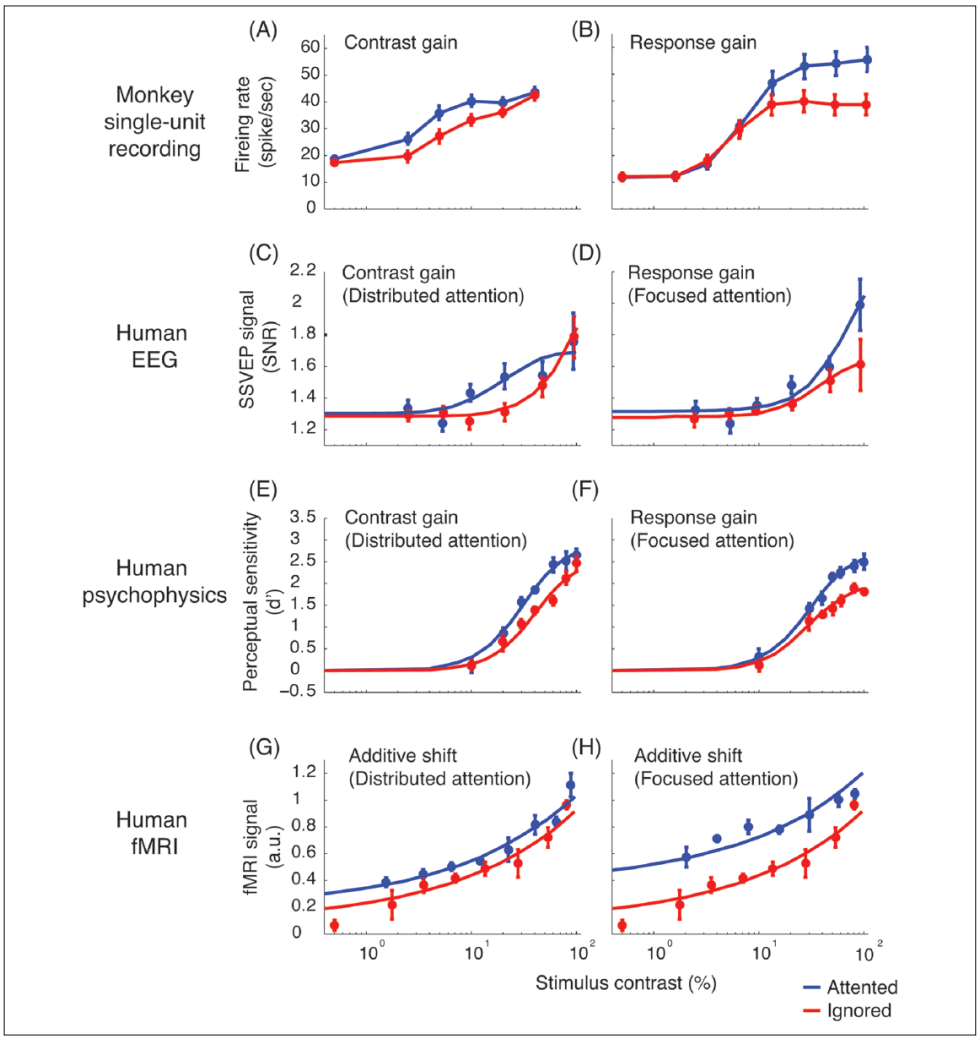

Figure 3. Different patterns of attentional gain modulation in contrast response functions (CRFs) measured using different methods. (A-B) Single-unit eletrophysiological studies in monkeys typically observe either contrast gain (Reynolds and other 2000) or response gain patterns of the CRFs measured in early visual cortices (Lee and Maunsell 2010, respectively). Similar contrast and response gain patterns have been observed in the CRFs measured using steady-state visually evoked responses (SSVEPs) in human EEG (C-D; Itthipuripat and others 2014b) and in the CRFs measured using human psychophysics (E-F; Herrmann and others 2010). These studies have found that the pattern of gain modulation (contrast or response gain) depends on the relative size between attention and a stimulus, consistent with the prediction of the normalization model of attention (Reynolds and Heeger 2009). Specifically, when the scope of attention is larger than a stimulus (C and E; distributed attention), contrast gain effects are observed. On the other hand, when the scope of attention is smaller than a stimulus (D and F; focused attention), response gain effects are observed. (G-H) On the other hand, distributed attention and focused attention do not produce contrast and response gain effects on CRFs measured using fMRI (Pestilli and others 2011). Instead, both attention conditions induced baseline increases (an additive shift) in the fMRI-based CRFs with a higher degree of baseline increase with focused-attention compared to distributed-attention conditions. All figures replotted based on original data for color consistency (with permission of authors).

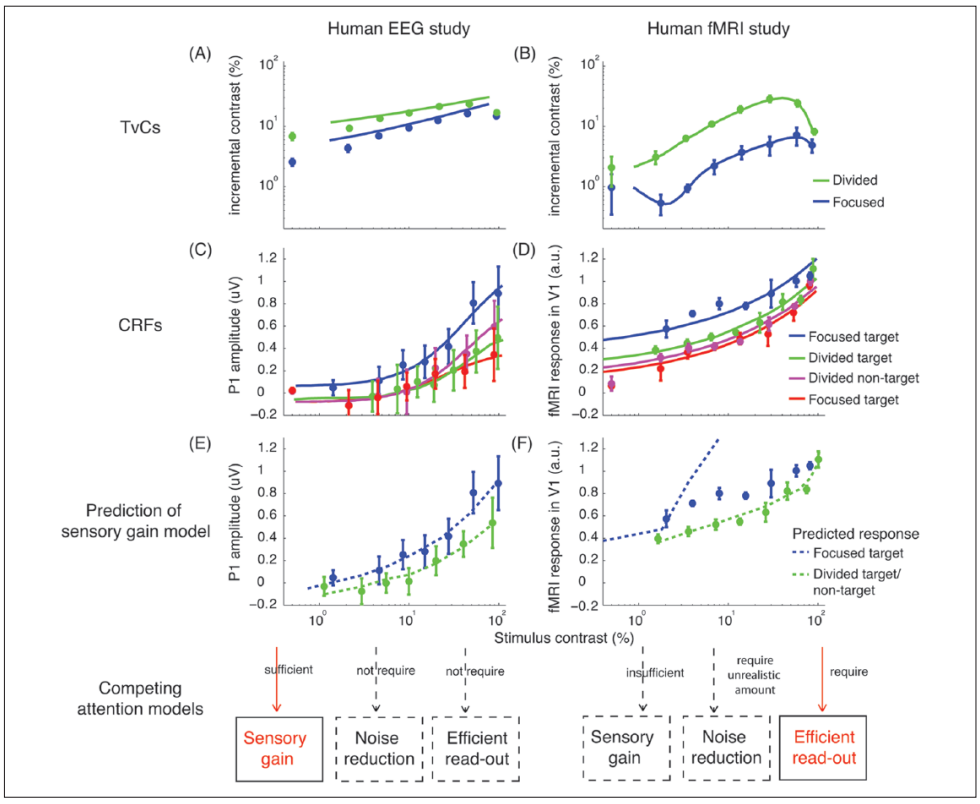

Figure 4. Comparing studies that link changes in perceptual sensitivity and attentional modulation of visual responses measured using EEG (Itthipuripat and others 2014a) and fMRI (Pestilli and others 2011). (A-B) Across both studies, focused attention reduced contrast discrimination thresholds, compared to divided/distributed attention. (C) Focused attention induced a multiplicative response gain (increase in slope) of the CRFs based on the amplitude of the early sensory P1 component (80–130 ms poststimulus) measured using EEG. (D) In contrast, focused attention induced a baseline increase of the CRFs measured using fMRI. Accordingly the sensory gain model, which relies on a change in the slope of the CRF, could sufficiently account for the relationship between changes in perceptual sensitivity and attentional modulations based on the P1 EEG response (E) but not on the fMRI response (F) To account for the baseline increase in the fMRI response, a postsensory efficient read-out mechanism based on a max-pooling rule is required (Fig. 2C). All figures replotted based on original data for color consistency (with permission of authors).

reported. For example, many single-unit electrophysiology studies in monkeys (Lee and Maunsell 2009, 2010) and EEG studies in humans (Di Russo and others 2001; Itthipuripat and others 2014a; Itthipuripat and others 2014b; Kim and others 2007; Lauritzen and others 2009; Wang and Wade 2011) have also found that spatial attention can enhance gain at higher contrasts as opposed to just inducing gain at mid-level contrasts (termed *response gain*) (Fig. 3B and D). In a recent EEG study carried out in our lab (Itthipuripat and others 2014a), we found that focused attention induced response gain of the early visually evoked response peaking at ~80 to 100 ms following a stimulus (i.e., the P1 component). Using SDT, we found that this response gain could sufficiently account for attention-induced changes in perceptual sensitivity, without the need to invoke either noise reduction or efficient read-out mechanisms (left panels in Fig. 4). Consistent with our findings, Störmer and others (2009) used EEG to show that this early sensory gain is highly correlated with subjects' reports of attention-induced increases in perceived contrast (see Carrasco and others 2004).

Even though the exact pattern of sensory gain could be different (either contrast or response gain), the same basic linking hypothesis that relates changes in the slope of the

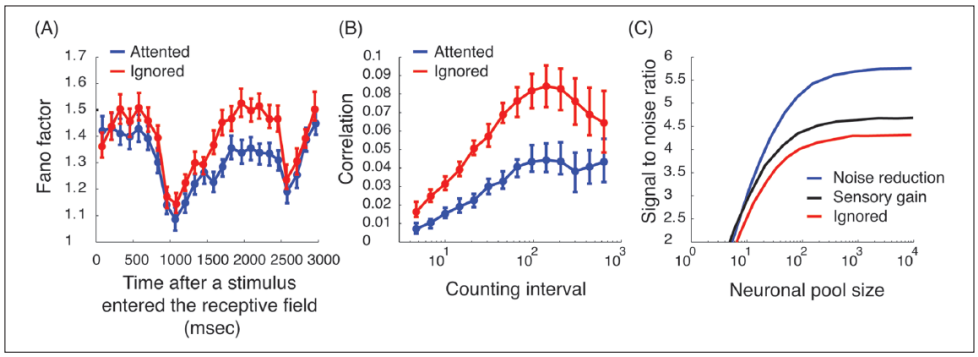

Figure 5. Attention induces reductions in neuronal noises (Mitchell and others 2009; also see Cohen and Maunsell 2009). (A) Attention reduces trial-by-trial variability of neural responses (fano factor or variance divided by the mean firing rate) in monkey V4. (B) Attention also reduces noise correlations between pairs of neurons. (C) Quantitative modeling suggests that a model-based noise reduction leads to a higher degree of signal-to-noise ratio pooled across neuronal population than a model based on sensory gain alone (i.e., the increase in firing rates). All figures replotted based on original data for color consistency (with permission of authors).

CRF and improved perceptual sensitivity still holds. In addition, it is likely that many of the subtle differences in sensory gain may be related to the size of the stimulus and the spatial scope of attention (see Reynolds and Heeger 2009 for more details). For example, human EEG (Itthipuripat and others 2014b) and human psychophysics studies (Herrmann and others 2010) provide converging evidence that when the spread of attention is larger than a stimulus (distributed attention), contrast gain effects are observed (Fig. 3C and E). On the other hand, when the spread of attention is smaller than a stimulus (focused attention), response gain effects are observed (Fig. 3D and F). However, this relationship between the spatial scope of attention and stimulus size cannot explain all differences observed in CRFs and their relationship to behavior, as studies using fMRI consistently reveal no change in the gain of fMRI-based CRFs across focused- and distributed-attention conditions (Fig. 3G and H and right panels in Fig. 4) (Hara and Gardner 2014; Pestilli and others 2011). Instead, spatial attention enhances the baseline offset of fMRI-based CRFs and does not affect the slope of these CRFs (see also Buracas and Boynton 2007; Murray 2008). Since the slope of fMRI-based CRFs does not change, it is challenging to link attentional modulations of fMRI signals to behavior within the simple SDT framework and more elaborate models have to be developed (see below).

Linking Changes in Neural Noise to Behavioral Performance

In addition to sensory gain modulations, single- and multi-unit electrophysiology studies reveal that attention can also reduce trial-to-trial variability in neuronal responses as well as modulate noise correlations between pairs of neurons (Fig. 5A and B) (Cohen and Maunsell 2009; Herrero and others 2013; Mitchell and others 2007, 2009; Niebergall and others 2011). According to SDT, the reduction in trial-to-trial variability in neuronal responses (σ) should increase perceptual sensitivity (d') (Fig. 2B). That said, previous studies have suggested that the reduction in pairwise noise correlation between neurons may have a large impact on the signal-to-noise ratio of neural populations compared to sensory gain alone, and this may contribute to higher d' by increasing the separability of population responses when discriminating two stimuli (Fig. 5C) (Cohen and Maunsell 2009; Mitchell and others 2008, 2009). However, the relationship between noise correlations and stimulus discriminability is complex, as Ruff and Cohen (2014) recently demonstrated that attention can either decrease or increase pairwise noise correlations between neurons in V4. While this finding is in line with theoretical analysis of optimal patterns of neural noise (Abbott and Dayan 1999), more work will be needed to directly link these changes to changes to behavioral performance. Moreover, different measurement techniques such as VSDI, which indexes the summed membrane potentials across larger populations of neurons, have reported that attention has no impact on neuronal noise (Chen and Seidemann 2012). The absence of attention-induced changes in trial-by-trial variability of neural activity has also been reported in studies using EEG (Itthipuripat and others 2014a) and fMRI (Pestilli and others 2011). So, as is the case with pure sensory gain accounts, these discrepant results that arise from different methodological approaches raise several questions:

(a) methods such as VSDI, EEG, and fMRI may not be sensitive to trial-to-trial response variability compared to single- and multi-unit electrophysiology, or (b) noise modulations may not play an important role in all behavioral tasks, especially when looking at activity aggregated over large neuronal populations.

Linking Changes in Efficient Read-Out to Behavioral Performance

Recently, several reports converge on the hypothesis that changes in sensory gain or neural noise may not be the primary mechanisms by which attention affects perceptual sensitivity (see an example in right panels of Fig. 4). As mentioned above, Pestilli and others (2011) found that focused attention selectively increased the baseline offset of CRFs measured using fMRI (Fig. 3G and H and Fig. 4D). Since these additive shifts are almost completely independent of stimulus contrast and do not change the slope of CRFs (see also Buracas and Boynton 2007; Murray 2008), models based on sensory gain fail to predict attention-induced changes in psychophysical data based on fMRI CRFs (Fig. 4G). When testing a noise reduction model of the fMRI data, an unrealistically large amount of noise reduction has to be implemented to explain the relationship between the fMRI signals and behavioral performance (~400% reduction; Hara and Gardner 2014; Pestilli and others 2011) compared to ~50% reduction in monkey electrophysiological studies (Cohen and Maunsell 2009; Mitchell and others 2009). Thus, Pestilli and others (2011) proposed a postsensory max-pooling rule that acts to overweight the influence of responses evoked by the attended stimulus so that these responses have a larger impact on postsensory decision mechanisms (Fig. 2C-D) (see also Eckstein and others 2009; Palmer and others 2000; Pelli 1985; Shaw 1984). Specifically, the max-pooling equation (yellow box in Fig. 2C) uses an exponent (k) to overweight high-amplitude responses. In turn, this exponentiation overamplifies responses evoked by attended target stimuli over ignored nontarget stimuli because of the large additive shift in the fMRI-based CRFs in the focused-attention condition (blue vs. red curves). However, in the distributed-/divided-attention condition, responses evoked by target and nontarget stimuli are similar in amplitude (green vs. purple curves). Thus, when nontarget stimuli happen to be rendered at higher contrasts than the target stimulus, the model will overweight responses to nontarget stimuli, resulting in lower perceptual sensitivity in the divided-/distributed-attention condition compared to focused-attention condition.

While at odds with much of the single-unit physiology data, this model raises the important possibility that studying single neurons might cloud important modulations that happen in large-scale populations that are thought to drive fMRI responses. For instance, Hara and others (2014) proposed that the summed response over a large population of neurons that undergo both contrast and response gain should give rise to an additive shift in the fMRI signal with attention, and that this additive shift should accurately predict corresponding changes in perceived contrast (Cutrone and others 2014). If true, then using measures such as fMRI may provide a more accurate picture of the link between large-scale population codes and behavior. However, this proposal still needs to be refined and extended, as other population-level measures such as EEG are more in line with observations of contrast and response gain, similar to those observed with single-unit physiology (Di Russo and others 2001; Martínez-Trujillo and Treue 2002; Reynolds and others 2000; Itthipuripat and others 2014a; Itthipuripat and others 2014b; Kim and others 2007; Lauritzen and others 2009; Lee and Maunsell 2009, 2010; Wang and Wade 2011; but see Williford and Maunsell 2006). Moreover, a recent EEG study, which employed a task similar to the task used by Cutrone and others (2014), has shown that sensory gain in the early evoked potential (P1) is closely related to subjects' reports of attention-induced increase in stimulus contrast (Störmer and others 2009). In addition, we have recently shown that this EEG component undergoes response gain modulation and not an additive shift like fMRI signals. Finally, psychophysical data, which presumably reflect the output of large population responses, is largely consistent with models that assume underlying contrast and response gain at the neural level (Herrmann and others 2010).

Reconciling Different Accounts and Different Measurements

Single-unit and multi-unit recording studies and human EEG studies point to sensory gain and noise reduction as important factors that mediate selective attention (Cohen and Maunsell 2009; Di Russo and others 2001; Herrero and others 2013; Hillyard and others 1998; Itthipuripat and others 2014a; Itthipuripat and others 2014b; Kim and others 2007; Lauritzen and others 2009; Lee and Maunsell 2009, 2010; Martínez-Trujillo and Treue 2002; Mitchell and others 2007, 2009; Niebergall and others 2011; Reynolds and others 2000; Wang and Wade 2011), and in some cases these modulations are sufficient to almost completely account for changes in perceptual sensitivity (Cohen and Maunsell 2009; Itthipuripat and others 2014a). On the other hand, some studies that use fMRI point to efficient-selection as the main mechanism of attention (Hara and Gardner 2014; Pestilli and others 2011). These conflicting findings raise an important challenge regarding how results from different neural

measures should be interpreted. Potential resolutions involve (a) developing more formal and mechanistic models to link neural activity to the outcome measure in each methodological domain and (b) making more formal and quantitative models to link neural measurements to changes in behavior (e.g., accuracy, reaction times, detection/discrimination thresholds).

For example, EEG may be more sensitive to the attentional modulation of local stimulus-evoked spiking activity than fMRI, as EEG has been closely linked to spiking activity in visual cortex (Whittingstall and Logothetis 2009), and gain patterns observed using EEG on human subjects are similar to those observed using single unit electrophysiology in nonhuman primates (Di Russo and others 2001; Martínez-Trujillo and Treue 2002; Reynolds and others 2000; Itthipuripat and others 2014a; Itthipuripat and others 2014b; Kim and others 2007; Lauritzen and others 2009; Lee and Maunsell 2009, 2010; Wang and Wade 2011; but see Williford and Maunsell 2006). Gain amplification of the EEG response has also been closely linked to perceptual reports of stimulus contrast (Störmer and others 2009) and contrast detection and discrimination thresholds (Campbell and Kulikowski 1972; Itthipuripat and others 2014a). Taken together, these findings suggest that increased spiking activity in visual cortex, which may be more accessible in humans using EEG, may be tightly linked to attention-induced changes in perception (e.g., increase in perceived stimulus contrast) and overt behavior (e.g., improved discrimination thresholds).

On the other hand, measures such as fMRI may be more sensitive to detect increased synaptic input caused by anticipatory/top-down effects of spatial attention, as opposed to the interaction between top-down signals and stimulus-evoked spiking activity per se (Cardoso and others 2012; Kastner and others 1999; Logothetis 2002, 2008; Logothetis and Wandell 2004; Serences and others 2004; Sirotin and Das 2009; Sylvester and others 2009; Viswanathan and Freeman 2007). This is consistent with the observation that changes in the gain of fMRI signals closely predict behavior in simple visual detection and discrimination tasks where there is no systematic manipulation of attention (Boynton and others 1999; Ress and Heeger 2003; Ress and others 2000). However, when spatial attention is manipulated, fMRI-based CRFs undergo an additive shift and thus changes in sensory gain cannot predict behavior and efficient read-out must be invoked (right panels in Fig. 4) (Hara and Gardner, 2014; Pestilli and others 2011). Similar to fMRI, spatial attention also induces a baseline increase in VSDI data obtained as a function of position along the surface of V1 (Fig. 6; Chen and Seidemann 2012). Interestingly, attention-induced changes in behavior that were related to manipulations of focused versus divided spatial attention could not be accounted for by modulations in the VSDI data (Chen and Seidemann 2012). Thus, fMRI and VSDI measures might not be particularly sensitive to attention-induced changes in perceptual sensitivity, and instead might primarily index the overall strength of top-down attentional modulations since the strength of top-down inputs does not vary as a function of stimulus contrast and position along the surface of visual cortex, respectively. If this speculative account is correct, it opens up the exciting possibility that measures such as fMRI and VSDI might be combined with other measures such as EEG and single- and multi-unit recording to simultaneously track changes the magnitude of top-down attentional signals and the impact that these changes have on spiking activity and behavior.

Beyond the domain of EEG, fMRI, and VSDI, Anderson and others (2013) have recently found that although attention generally increases the spiking rate of neurons in V4, it also reduces burstiness and action potential height. These findings pose a challenge for other new imaging methods, such as calcium imaging, which has recently been developed in rodent and nonhuman primate model systems to assay the activity across large populations of neurons (Grienberger and Konnerth 2012; Heider and others 2010). Studies have reported two key observations. First, Ca^{2+} generally increases with increasing stimulus intensity, suggesting that these signals will also increase with attention (Issa and others 2014; Nauhaus and others 2012). However, bursts are also strongly related to Ca^{2+} signals (Bayazitov and others 2013; Coulon and others 2009; Grienberger and others 2014; Peters and others 2014). Therefore, this presents a potential quandary: if attention increases gain, but decreases burstiness, then how will that affect the overall magnitude of Ca^{2+} signals? Furthering our understanding of this relatively new measurement technique, along with developing formal models to link Ca^{2+} modulations with spiking activity will be needed to link these two measurement techniques and to exploit the strengths of each method to further our understanding of attentional modulations in visual cortex. Employing new neuroimaging techniques also raises challenges about understanding nonlinearities between measures. For instance, recent studies have documented a nonlinear relationship between electrophysiology and population-level measures like VSDI (Chen and others 2012) and calcium imaging (Nauhaus and others 2012). However, it is still unknown how these measures relate to perceptual sensitivity because many of these studies were performed in nonbehaving animals. Therefore, major hurdles must be overcome to effectively combine information from multimodal imaging methods to behavior, and this will not only involve developing integrative computational frameworks to relate single measures to behavior but also developing formal frameworks to relate different measures to each other.

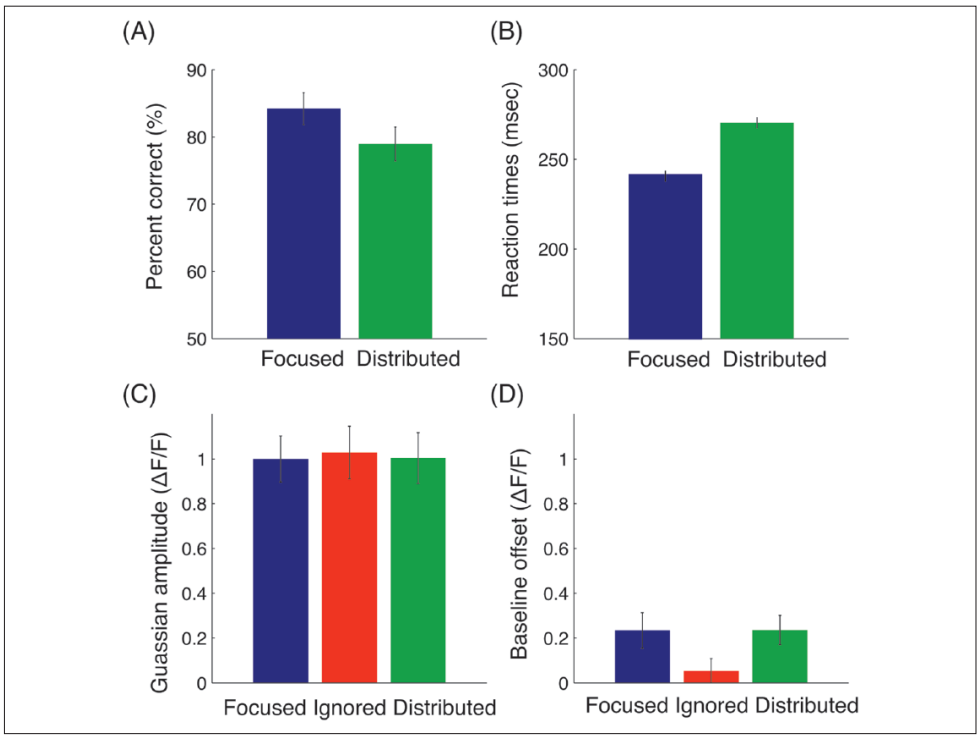

Figure 6. Attention effects on voltage-sensitive dye imaging in monkeys (VSDI; Chen and Seidemann 2012). (A-B) Focused attention enhances subjects' performance in a target detection task: accuracy increases and reaction times decrease for focused attention, compared to distributed attention conditions. (C) There are no changes in the Gaussian amplitude of VSDI signals across all attention conditions. (D) The baseline of the VSDI signals increases for attended, compared to ignored stimuli, and there is no difference in the baseline parameter between the focused and distributed attention conditions, even though significant behavioral differences were observed across these two conditions (A-B). All figures replotted based on original data for color consistency (with permission of authors).

Conclusions

Over the past three decades, more than 3000 studies have investigated the empirical link between selective attention and changes in behavioral performance (reviewed in Carrasco 2011). Studies employing a variety of techniques (monkey electrophysiology, human EEG, fMRI, and VSDI to name a few) seem to support qualitatively distinct linking hypotheses. At first glance, this might be seen as a cause for pessimism about how much progress we can make given available techniques, particularly if we also factor in differences in species, training regimes, and experimental paradigms that all might contribute to data supporting different linking hypotheses. However, these seemingly inconsistent findings can also be viewed under a much more optimistic light—the very fact that different measures produce distinct modulations and support different linking hypotheses suggests that each approach can provide complementary information to better inform theoretical frameworks.

However, realizing the potential afforded by combining information across multiple measurement modalities presents many clear challenges. First, researchers need to be increasingly transparent about the limitations of measurements they use, and any assumptions that link those measurements to both neural processes and to behavior should be explicitly stated and formalized to the fullest extent possible. For example, explicit neurovascular coupling models (Buxton and others 1998; Friston and others 2000) can be used to link neural activity with the fMRI response, providing a framework for integrating studies in nonhuman model systems with measures such as fMRI

that can assay larger neural populations in humans. While no model that bridges such disparate levels is perfect, formalizing this relationship is nevertheless important because it will at least make all the assumptions explicit and thus foster attempts to falsify and subsequently improve specific components of the model (and this logic goes for linking hypotheses in all measurement modalities). Second, a potentially more important and practical challenge is that our grants, promotions, and livelihood depend on publishing, and this is most efficiently accomplished by downplaying methodological differences and by making the most of the specific tools and model systems that we have invested years in mastering. This working model is not particularly conducive to collaborative, cross-disciplinary work, and raises the concern that we will continue to amass an ever larger body of data with little ability to integrate across scales of analysis in order to make progress toward understating how complex patterns of neural activity give rise to equally complex patterns of human behavior.

Acknowledgments

We thank Kexin Cha for help producing figures; Thomas Sprague, Justin Gardner, and Franco Pestilli for useful conversions; and John Reynolds, Jude Mitchell, John Maunsell, Joonyeol Lee, Franco Pestilli, Justin Gardner, Marisa Carrasco, David Heeger, Eyal Seidemann, and Yuzhi Chen for providing materials for data figures.

Declaration of Conflicting Interests

The author(s) declared no potential conflicts of interest with respect to the research, authorship, and/or publication of this article.

Funding

The author(s) disclosed receipt of the following financial support for the research, authorship, and/or publication of this article: Supported by NIH-092345 to JTS, a James S. McDonnell Foundation Scholar Award to JTS, and by an HHMI International Fellowship to SI.

References

Abbott LF, Dayan P. 1999. The effect of correlated variability on the accuracy of a population code. Neural Comput 11(1):91–101.

Anderson EB, Mitchell JF, Reynolds JH. 2013. Attention-dependent reductions in burstiness and action-potential height in macaque area V4. Nat Neurosci 16(8):1125–31.

Anton-Erxleben K, Carrasco M. 2013. Attentional enhancement of spatial resolution: linking behavioral and neurophysiological evidence. Nat Rev Neurosci 14(3):188–200.

Bayazitov IT, Westmoreland JJ, Zakharenko SS. 2013. Forward suppression in the auditory cortex is caused by the Cav3.1 calcium channel-mediated switch from bursting to tonic firing at thalamocortical projections. J Neurosci 33(48):18940–50.

Botha H, Carr J. 2012. Attention and visual dysfunction in Parkinson's disease. Parkinsonism Relat Disord 18(6): 742–7.

Boynton GM, Demb JB, Glover GH, Heeger DJ. 1999. Neuronal basis of contrast discrimination. Vision Res 39:257–69.

Buracas GT, Boynton GM. 2007. The effect of spatial attention on contrast response functions in human visual cortex. J Neurosci 27:93–7.

Buxton RB, Wong EC, Frank LR 1998. Dynamics of blood flow and oxygenation changes during brain activation: the balloon model. Magn Reson Med. 39(6):855–64.

Campbell FW, Kulikowski JJ. 1972. The visual evoked potential as a function of contrast of a grating pattern. J Physiol 222:345–56.

Cardoso MM, Sirotin YB, Lima B, Glushenkova E, Das A. 2012. The neuroimaging signal is a linear sum of neurally distinct stimulus- and task-related components. Nat Neurosci 15:1298–306.

Carrasco M. 2011. Visual attention: the past 25 years. Vis Res 51:1484–525.

Carrasco M, Ling S, Read S. 2004. Attention alters appearance. Nat Neurosci 7:308–13.

Chen Y, Palmer CR, Seidemann E. 2012. The relationship between voltage-sensitive dye imaging signals and spiking activity of neural populations in primate V1. J Neurophysiol 107(12):3281–95.

Chen Y, Seidemann E. 2012. Attentional modulations related to spatial gating but not to allocation of limited resources in primate V1. Neuron 74:557–66.

Cohen MR, Maunsell JH. 2009. Attention improves performance primarily by reducing interneuronal correlations. Nat Neurosci 12:1594–600.

Coulon P, Herr D, Kanyshkova T, Meuth P, Budde T, Pape HC. 2009. Burst discharges in neurons of the thalamic reticular nucleus are shaped by calcium-induced calcium release. Cell Calcium 46(5–6):333–46.

Cutrone EK, Heeger DJ, Carrasco M. 2014. Attention enhances contrast appearance via increased input baseline of neural responses. J Vis 14(14):16.

Di Russo F, Spinelli D, Morrone MC. 2001. Automatic gain control contrast mechanisms are modulated by attention in humans: evidence from visual evoked potentials. Vis Res 41:2435–47.

Eckstein MP, Thomas JP, Palmer J, Shimozaki SS. 2000. A signal detection model predicts the effects of set size on visual search accuracy for feature, conjunction, triple conjunction, and disjunction displays. Percept Psychophys 62(3):425–51.

Friston KJ, Mechelli A, Turner R, Price CJ. 2000. Nonlinear responses in fMRI: the Balloon model, Volterra kernels, and other hemodynamics. Neuroimage 12(4):466–77.

Grienberger C, Chen X, Konnerth A. 2014. NMDA receptor-dependent multidendrite Ca(2+) spikes required for hippocampal burst firing in vivo. Neuron 81(6):1274–81.

Grienberger C, Konnerth A. 2012. Imaging calcium in neurons. Neuron 73(5): 862-885.

Hara Y, Gardner JL. 2014. Encoding of graded changes in spatial specificity of prior cues in human visual cortex. J Neurophysiol 112(11):2834–49.

Hara Y, Pestilli F, Gardner JL. 2014. Differing effects of attention in single-units and populations are well predicted by heterogeneous tuning and the normalization model of attention. Front Comput Neurosci 8:12.

Heider B, Nathanson JL, Isacoff EY, Callaway EM, Siegel RM. 2010. Two-photon imaging of calcium in virally transfected striate cortical neurons of behaving monkeys. PLoS One 5(11):e13829.

Heinrichs RW, Zakzanis KK. 1998. Neurocognitive deficits in schizophrenia: a quantitative review of the evidence. Neuropsychology 12(3):426–45.

Herrero JL, Gieselmann MA, Sanayei M, Thiele A. 2013. Attention-induced variance and noise correlation reduction in macaque V1 is mediated by NMDA receptors. Neuron 78:729–39.

Herrmann K, Montaser-Kouhsari L, Carrasco M, Heeger DJ. 2010. When size matters: attention affects performance by contrast or response gain. Nat Neurosci 13:1554–9.

Hillyard SA, Vogel EK, Luck SJ. 1998. Sensory gain control (amplification) as a mechanism of selective attention: electrophysiological and neuroimaging evidence. Philos Trans R Soc Lond B Biol Sci 353:1257–70.

Issa JB, Haeffele BD, Agarwal A, Bergles DE, Young ED, Yue DT. 2014. Multiscale optical Ca^{2+} imaging of tonal organization in mouse auditory cortex. Neuron 83(4):944–59.

Itthipuripat S, Ester EF, Deering S, Serences JT. 2014a. Sensory gain outperforms efficient readout mechanisms in predicting attention-related improvements in behavior. J Neurosci 34(40):13384–98.

Itthipuripat S, Garcia JO, Rungratsameetaweemana N, Sprague TC, Serences JT. 2014b. Changing the spatial scope of attention alters patterns of neural gain in human cortex. J Neurosci 34:112–23.

Kastner S, Pinsk MA, De Weerd P, Desimone R, Ungerleider LG. 1999. Increased activity in human visual cortex during directed attention in the absence of visual stimulation. Neuron 22:751–61.

Kim YJ, Grabowecky M, Paller KA, Muthu K, Suzuki S. 2007. Attention induces synchronization-based response gain in steady-state visual evoked potentials. Nat Neurosci 10:117–25.

Krauzlis RJ, Bollimunta A, Arcizet F, Wang L. 2014. Attention as an effect not a cause. Trends Cogn Sci 18:457–64.

Lauritzen TZ, Ales J, Wade AR. 2010. The effects of visuospatial attention measured across visual cortex using source-imaged, steady-state EEG. J Vis 10(14):1–17.

Lee J, Maunsell JH. 2009. A normalization model of attentional modulation of single unit responses. PLoS One 4:e4651.

Lee J, Maunsell JH. 2010. The effect of attention on neuronal responses to high and low contrast stimuli. J Neurophysiol 104:960–71.

Logothetis NK. 2002. The neural basis of the blood-oxygen-level-dependent functional magnetic resonance imaging signal. Philos Trans R Soc Lond B Biol Sci 357:1003–37.

Logothetis NK. 2008. What we can do and what we cannot do with fMRI. Nature 453:869–78.

Logothetis NK, Wandell BA. 2004. Interpreting the BOLD signal. Annu Rev Physiol 66:735–69.

Martínez-Trujillo J, Treue S. 2002. Attentional modulation strength in cortical area MT depends on stimulus contrast. Neuron 35:365–70.

Mitchell JF, Sundberg KA, Reynolds JH. 2007. Differential attention-dependent response modulation across cell classes in macaque visual area V4. Neuron 55:131–41.

Mitchell JF, Sundberg KA, Reynolds JH. 2009. Spatial attention decorrelates intrinsic activity fluctuations in macaque area V4. Neuron 63:879–88.

Murray SO. 2008. The effects of spatial attention in early human visual cortex are stimulus independent. J Vis 8(10):2.1–2.11.

Niebergall R, Khayat PS, Treue S, Martinez-Trujillo JC. 2011. Expansion of MT neurons excitatory receptive fields during covert attentive tracking. J Neurosci 31:15499–510.

Nauhaus I, Nielsen KJ, Callaway EM. 2012. Nonlinearity of two-photon Ca^{2+} imaging yields distorted measurements of tuning for V1 neuronal populations. J Neurophysiol 107(3):923–36.

Palmer J, Verghese P, Pavel M. 2000. The psychophysics of visual search. Vis Res 40:1227–68.

Pelli DG. 1985. Uncertainty explains many aspects of visual contrast detection and discrimination. J Opt Soc Am 2:1508–32.

Pestilli F, Carrasco M, Heeger DJ, Gardner JL. 2011. Attentional enhancement via selection and pooling of early sensory responses in human visual cortex. Neuron 72:832–46.

Peters AJ, Chen SX, Komiyama T. 2014. Emergence of reproducible spatiotemporal activity during motor learning. Nature. 510(7504):263–7.

Ress D, Backus BT, Heeger DJ. 2000. Activity in primary visual cortex predicts performance in a visual detection task. Nat Neurosci 3:940–5.

Ress D, Heeger DJ. 2003. Neuronal correlates of perception in early visual cortex. Nat Neurosci 6(4): 414-20.

Reynolds JH, Heeger DJ. 2009. The normalization model of attention. Neuron 61:168–85.

Reynolds JH, Pasternak T, Desimone R. 2000. Attention increases sensitivity of V4 neurons. Neuron 26:703–14.

Ruff DA, Cohen MR. 2014. Attention can either increase or decrease spike count correlations in visual cortex. Nat Neurosci 17(11):1591–7.

Sejnowski TJ. 1991. Neuroscience. Back together again. Nature 352(6337):669–70.

Sejnowski TJ, Churchland PS, Movshon JA. 2014. Putting big data to good use in neuroscience. Nat Neurosci 17(11):1440–1.

Serences JT, Yantis S, Culberson A, Awh E. 2004. Preparatory activity in visual cortex indexes distractor suppression during covert spatial orienting. J Neurophysiol 92:3538–45.

Shaw ML. 1984. Division of attention among spatial locations: a fundamental difference between detection of letters and detection of luminance increments. In: Bouma H, Bouwhais DG, editors. Attention & performance X. Hillsdale, NJ: Erlbaum. p. 109–121.

Sirotin YB, Das A. 2009. Anticipatory haemodynamic signals in sensory cortex not predicted by local neuronal activity. Nature 457:475–9.

Sprague TC, Saproo S, Serences JT. 2015 Visual attention mitigates information loss in small- and large-scale neural codes. Trends Cogn Sci 19(4):215–26.

Stefanatos GA, Baron IS. 2007. Attention-deficit/hyperactivity disorder: a neuropsychological perspective towards DSM-V. Neuropsychol Rev 17(1):5–38.

Störmer VS, McDonald JJ, Hillyard SA. 2009. Cross-modal cueing of attention alters appearance and early cortical processing of visual stimuli. Proc Natl Acad Sci U S A 106:22456–61.

Sylvester CM, Shulman GL, Jack AI, Corbetta M. 2009. Anticipatory and stimulus-evoked blood oxygenation level-dependent modulations related to spatial attention reflect a common additive signal. J Neurosci 29:10671–82.

Tanner WP, Jr, Swets JA. 1954. A decision-making theory of visual detection. Psychol Rev 61(6):401–9.

Viswanathan A, Freeman RD. 2007. Neurometabolic coupling in cerebral cortex reflects synaptic more than spiking activity. Nat Neurosci 10:1308–12.

Wang J, Wade AR. 2011. Differential attentional modulation of cortical responses to S-cone and luminance stimuli. J Vis 11(6):1–15.

Williford T, Maunsell JH. 2006. Effects of spatial attention on contrast response functions in macaque area V4. J Neurophysiol 96:40–54.

Whittingstall K, Logothetis NK. 2009. Frequency-band coupling in surface EEG reflects spiking activity in monkey visual cortex. Neuron 64:281–9.

Chapter 1, in full, is a reprint of the material as it appears in a review entitled "Integrating levels of analysis in systems and cognitive neurosciences: selective attention as a case study" published in The Neuroscientist 2015. Itthipuripat, S.; Serences, John T., SAGE Publications, 2015. The dissertation author was the primary author of the manuscript. Supported by NIH-092345 and a James S. McDonnell Foundation Scholar Award to J.T.S., and by an HHMI International Fellowship to SI. We thank Kexin Cha for help producing figures; Thomas Sprague, Justin Gardner, and Franco Pestilli for useful conversions; and John Reynolds, Jude Mitchell, John Maunsell, Joonyeol Lee, Franco Pestilli, Justin Gardner, Marisa Carrasco, David Heeger, Eyal Seidemann, and Yuzhi Chen for providing materials for data figures.

Chapter 2:

Temporal dynamics of

divided spatial attention

Temporal dynamics of divided spatial attention

Sirawaj Itthipuripat,[1] Javier O. Garcia,[2] and John T. Serences[1,2]

[1]*Neurosciences Graduate Program, University of California, San Diego, La Jolla, California; and* [2]*Department of Psychology, University of California, San Diego, La Jolla, California*

Submitted 4 December 2012; accepted in final form 4 February 2013

Itthipuripat S, Garcia JO, Serences JT. Temporal dynamics of divided spatial attention. *J Neurophysiol* 109: 2364–2373, 2013. First published February 6, 2013; doi:10.1152/jn.01051.2012.—In naturalistic settings, observers often have to monitor multiple objects dispersed throughout the visual scene. However, the degree to which spatial attention can be divided across spatially noncontiguous objects has long been debated, particularly when those objects are in close proximity. Moreover, the temporal dynamics of divided attention are unclear: is the process of dividing spatial attention gradual and continuous, or does it onset in a discrete manner? To address these issues, we recorded steady-state visual evoked potentials (SSVEPs) as subjects covertly monitored two flickering targets while ignoring an intervening distractor that flickered at a different frequency. All three stimuli were clustered within either the lower left or the lower right quadrant, and our dependent measure was SSVEP power at the target and distractor frequencies measured over time. In two experiments, we observed a temporally discrete increase in power for target- vs. distractor-evoked SSVEPs extending from ~350 to 150 ms prior to correct (but not incorrect) responses. The divergence in SSVEP power immediately prior to a correct response suggests that spatial attention can be divided across noncontiguous locations, even when the targets are closely spaced within a single quadrant. In addition, the division of spatial attention appears to be relatively discrete, as opposed to slow and continuous. Finally, the predictive relationship between SSVEP power and behavior demonstrates that these neurophysiological measures of divided attention are meaningfully related to cognitive function.

attention; decision making; electroencephalography; steady-state visual evoked potentials

IN EVERYDAY PERCEPTION, organisms must often monitor multiple noncontiguous objects that are arrayed across the visual field. Early models proposed that spatial attention operates as a unitary "spotlight" that only covers one circumscribed region of the visual field and may switch rapidly among multiple relevant objects (Posner et al. 1980). Later models incorporated the notion of a variable-sized spotlight ("zoom lens") that can be reshaped on the basis of perceptual demands (Barriopedro and Botella 1998; Erkisen and St. James 1986; Eriksen and Yeh 1985; Heinze et al. 1994; McCormick and Jolicoeur 1994; Müller et al. 2003b). In contrast to these earlier models, "flexible allocation" models postulate that spatial attention can be allocated to noncontiguous regions of space (Awh and Pashler 2000; Baldauf and Deubel 2008; Bichot et al. 1999; Carlson et al. 2007; Castiello and Umiltà 1992; Cavanagh and Alvarez 2005; Dubois and Hamker 2009; Gobell et al. 2004; Godijn and Theeuwes 2003; Hahn and Kramer 1998; Howe et al. 2011; Kraft et al. 2005; Kramer and Hahn 1995; Malinowski et al. 2007; McMains and Somers 2004, 2005; Müller et al. 2003a; Niebergall et al. 2010, 2011). However, the extent to which attention can be divided across multiple locations is still controversial (Cave et al. 2010; Jans et al. 2010), and here we investigated three main theoretical issues related to this debate.

First, the extent to which attention can be divided between objects that are in close proximity is unclear, particularly when those items fall within the same hemifield/quadrant of space (Maertens and Pollmann 2005; Malinowski et al. 2007; McMains and Somers 2004; Pollmann et al. 2003; Sereno and Kosslyn 1991). Second, few studies have evaluated the temporal dynamics of divided spatial attention, so it is unclear whether the division of spatial attention arises slowly and gradually over time, or whether attention can be divided in a discrete manner analogous to a unitary spotlight that splits into multiple foci. Finally, predictive relationships between neurophysiological measures of divided spatial attention and behavior have not been clearly established.

In this study, we evaluated these issues by monitoring neural activity associated with attended targets and ignored distractors using steady-state visual evoked potentials (SSVEPs). This method provides a temporally continuous measure of electrophysiological responses that oscillate at the same temporal frequency as a visual stimulus (Regan 1989), and is thus useful for investigating the temporal dynamics of attentional phenomena (e.g., Andersen and Müller 2010; Müller et al. 1998). In two experiments, subjects performed a multiple-object discrimination task in which two visual targets and an intervening distractor were presented in either the lower left or the lower right quadrant (Fig. 1). The targets and the distractor were presented at different frequencies to elicit separable SSVEPs. In addition, we calibrated task difficulty for each subject by adjusting the contrast of the targets to yield ~66% correct responses. By setting accuracy at this below-ceiling level, we sought to ensure that we had enough power to compare stimulus- and response-locked SSVEP responses on correct and incorrect trials.

Using this approach, we did not find robust evidence that differences in stimulus-locked target and distractor SSVEP power predicted behavioral performance. However, when SSVEP power was time-locked to the behavioral response, we observed an abrupt divergence of target- and distractor-evoked SSVEP power immediately preceding a correct behavioral response. These results suggest that spatial attention can be divided between objects in the same visual quadrant, that this division happens in a relatively discrete manner, and that the degree of segregation between target- and distractor-evoked responses predicts behavioral performance.

Address for reprint requests and other correspondence: S. Itthipuripat, Neurosciences Graduate Program, Univ. of California, San Diego, La Jolla, CA 92093 (e-mail: Itthipuripat.Sirawaj@gmail.com).

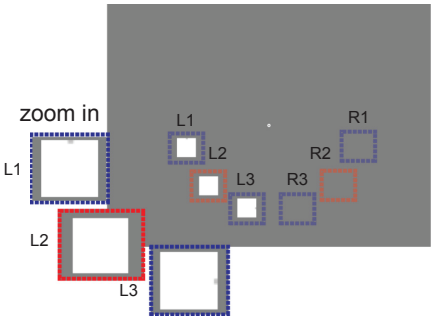

Fig. 1. Depiction of the stimulus display. On a given trial, subjects maintained central fixation and viewed 3 stimuli presented in either the lower left or the lower right quadrant. Their task was to make a discrimination on the upper and the lower stimuli (either R1 and R3 or L1 and L3; see text for details) while ignoring the intervening distractor (either R2 or L2). A trial in which the stimuli were presented in the lower right quadrant is shown. The dashed lines surrounding each potential stimulus location were not visible in the actual experiment.

MATERIALS AND METHODS

Subjects. Forty-eight neurologically healthy volunteers with normal or corrected-to-normal vision were recruited from the University of California, San Diego (UCSD). All participants provided written informed consent for this study, which was approved by the human subjects Institutional Review Board at UCSD. Eleven subjects (4 females, mean age 22 yr) participated in SSVEP *experiment 1* (E1), 15 subjects (9 females, mean age 21 yr) participated in SSVEP E2, 10 subjects (7 females, mean age 23 yr) participated in behavioral control *experiment 1* (CE1), and 13 subjects (7 females, mean age 21 yr) participated in behavioral CE2. Data from one subject in E2 were excluded from analysis due to excessive eye movement artifacts (see below). All subjects received either class credit or monetary compensation for participation ($15/h for E1 and E2 and $10/h for CE1 and CE2).

Stimuli and experimental design. The experiment was carried out using a personal computer running Windows XP. Stimulus presentation was controlled using MATLAB (The MathWorks, Natick, MA) with the Psychophysics Toolbox (version 3; Brainard 1997; Pelli 1997), and all stimuli were rendered on a 20-in. CRT monitor (HP P1203; Hewlett-Packard, Palo Alto, CA) running at 75 Hz. Subjects were seated 60 cm from the computer screen and instructed to fixate at the center of the screen for the duration of each trial. Stimulus timing was directly measured via fiber-optic cables that were linked to photocells and attached to the stimulus monitor. The gain and sensitivity of this custom-built fiber-optic photocell system (Javi's Phototransmogrifier 2000; Electronic Development and Repair Facility, Department of Physics, UCSD) was adjusted to give accurate and fast sampling of stimulus parameters (i.e., precise timing of the flickering stimuli), and the output was fed directly into the electroencephalogram (EEG) data files for later use during data analysis.

An example of the stimulus presentation paradigm is illustrated in Fig. 1. Before the start of each trial, a central fixation point was presented for 700 ms, followed by the onset of three white squares (72 cd/m^2) that were presented at an isoeccentric distance from fixation (9.5° visual angle) in either the lower left or the lower right quadrant (positions in the lower left and lower right quadrants, arranged from upper to lower eccentric locations, are hereby referred to as L1, L2, L3 and R1, R2, R3, respectively; see Fig. 1). The background was medium gray (mean luminance 21 cd/m^2). Each square stimulus subtended 2.4° × 2.4° visual angle with equal spacing between each square (3.8° visual angle between the centers of adjacent squares). The two outer squares were always to be attended (L1/L3 or R1/R3), and each square contained a small light gray rectangle-shaped mark (0.1° × 0.2° visual angle; 0.035% of the area of each square stimulus) on one of its edges. The contrast between the attended stimuli and the small markings was adjusted across a range from 10 to 30% depending on subjects' performance on the block-by-block basis (see details below). The marked location on the two attended stimuli (L1/L3 or R1/R3) could be the same, offset clockwise or counterclockwise by 90°, or offset by 180°; each of these target configurations was presented with equal probability. The middle square (L2 or R2) was located between the two targets and served as a distractor that contained no additional markings. During the experiment, subjects were asked to respond to the target configuration by pressing one of three buttons on a keyboard with their right index, middle, or ring finger indicating if the marked locations targets were in the same orientation, offset by ±90°, or offset by 180° (yielding a 3-alternative forced-choice design, or 3AFC). The small and low contrast markings on the attended stimuli were designed to make the task very difficult and to encourage subjects to continuously attend to both target objects for an extended period of time.

In E1, we separately assessed target- and distractor-related SSVEPs by flickering the two targets at the same frequency while the middle distractor was flickered at a different frequency (the targets and distractor were flickered at either 6.9 or 10.4 Hz, counterbalanced within subjects across repeated testing blocks). To discourage the possibility that divided attention was supported by grouping based on target frequency, and to ensure that our results were not specific to our exact choice of stimulus frequencies in E1 (6.9 and 10.4 Hz), we conducted E2 using a similar design except that all three squares were flickered at different frequencies (15, 18.76, and 25.02 Hz). The six possible frequency combinations were counterbalanced within observer across blocks of trials. In both experiments, the stimulus array was presented for 3,200 ms on each trial with an intertrial interval of 1,500 ms.

Our main focus was to compare responses on correct and incorrect trials, as opposed to comparing responses to each stimulus when it was attended versus ignored. Although this design deviates from most previous efforts, it allowed us to link EEG response modulation to behavioral performance while still maintaining perfectly matched sensory stimulation across conditions (since the stimuli were identical on correct and incorrect trials). To ensure that enough trials were acquired to support a comparison of SSVEP power on correct and incorrect trials, the luminance of the small square markings on each target stimulus was adjusted on a block-by-block basis to maintain performance at ~66% correct (which is 2 times chance given the 3AFC design). Subjects were instructed to respond as quickly and accurately as possible and were free to respond before the termination of the stimulus array.

Before each recording session, subjects practiced for ~20 min to gain familiarity with the task and to calibrate initial difficulty thresholds. Each recording session consisted of 10 blocks of 60 trials and contained an equal number of stimulus arrays presented in the lower left and right quadrants (in a pseudorandomly selected order). Each block lasted ~5 min, resulting in a 1.5-h-long experiment session, including EEG preparation and short breaks in between each block.

In addition, we also ran two additional behavioral control experiments (CE1 and CE2) to evaluate the efficacy of the intermediate distractor. CE1 was identical to E1 and CE2 was identical to E2, except that only half of the trials contained the intermediate distractor and the other half did not.

EEG recording, preprocessing, and SSVEP analysis. EEG data were recorded using a 128-channel Geodesic Sensor Net coupled with a NetAmps 200 amplifier [Electrical Geodesics Inc. (EGI), Eugene, OR]. EEG data were sampled at 1,000 Hz and referenced to the central channel. Electrode impedances were kept below 50 kΩ, which is standard with high input impedance amplifiers like the EGI system. Blinks and vertical eye movements were monitored by four built-in

electrodes placed above and below the left and right eyes. Horizontal eye movements were monitored by two built-in electrodes placed at the outer canthi of the eyes. Blink suppression and fixation control were verbally encouraged throughout the experiment.

We used customized MATLAB scripts for EEG preprocessing and SSVEP analysis. First, we applied a high-pass Butterworth filter with 2-dB attenuation at 2 Hz to remove slow drifts and a bandstop Butterworth filter with 30-dB attenuation between 58 and 62 Hz to attenuate line noise. Second, the continuous EEG recordings from each subject were segmented into single-trial epochs extending from 1,000 ms before to 3,500 ms after stimulus onset. Individual trials that exhibited prominent blink, electro-oculogram, or electromyogram artifacts were discarded using threshold rejection (more than ± 100 μV deviation from the mean) and visual inspection, which resulted in the removal of $<15\%$ of trials across subjects [with the exception of the single subject in E2 that was discarded from further analysis due to ~45% rejected trials based on these criteria]. Principal components were then computed and selected for removal on the basis of visual analysis to attenuate any residual artifacts. Third, each of the trials was cropped to an integer number of cycles using the photocell traces that directly measured stimulus onset timing during each trial. Fourier coefficients were then computed on the epoched data from each trial using the fast-Fourier transform algorithm implemented in MATLAB. Power across the entire trial interval at each target and distractor frequency was calculated as the squared real component of the Fourier coefficients.

The power of the SSVEP response over the entire trial at each target- and distractor-specific frequency was then binned on the basis of spatial position (left or right) and the subject's performance (correct response or incorrect response; all trials in which a response was omitted were excluded from the SSVEP analysis, see RESULTS). For the main analysis, we selected three EEG channels in the occipital-parietal area that exhibited the highest SSVEP power as electrodes of interest (EOIs); this selection process was carried out separately for each stimulus location and frequency assignment. Separate electrodes were used in each condition because of expected differences in distribution of SSVEP power across the scalp as a function of target position and frequency. For example, Fig. 2 illustrates the topographical maps of averaged SSVEP power collapsed across all frequency assignments in E1 (*top*) and in E2 (*bottom*). SSVEP power was standardized across channels so that the positive and negative values indicate responses above and below the mean value, respectively (in units of z scores). Note that the EOIs for both target- and distractor-evoked SSVEPs were clustered in the occipital-parietal area contralateral to the locus of visual stimulation, consistent with the known contralateral mapping of external spatial locations to internal cortical representations. To evaluate the reliability and the specificity of power at each stimulus presentation frequency, we compared the magnitude of the SSVEP response across the entire trial divided by the power in four surrounding frequency bins. This produces a measure of the signal-to-noise (SNR) ratio of the response at the specific flicker frequency of each stimulus (see e.g., Kim and Verghese 2012; Sutoyo and Srinivasan 2006; Srinivasan et al. 2006). Figure 3 illustrates these SNR measures at the flicker frequencies of 6.9 (*A*) and 10.4 Hz (*B*) in E1 and at the flicker frequencies of 15 (*C*), 18.76 (*D*), and 25 Hz (*E*) in E2. Across all flicker frequencies, there is a clear and sharply tuned increase in power.

Finally, we calculated the power at each stimulus frequency across time from each set of EOIs using an analytic Gabor basis function (Gaussian-weighted complex-valued sinusoid; see Bruns 2004; Canolty et al. 2007) with a fractional bandwidth of 0.5 Hz and a time-domain standard deviation that varied with the frequency of the stimulus (36 and 54 ms for the 10.4- and 6.9-Hz stimuli in E1, and 15, 20, and 25 ms for the 25-, 18.76-, and 15-Hz stimuli in E2; Canolty et al. 2007). The resulting SSVEP power time courses were then averaged at each time point across the three electrodes of interest. Normalization was performed by dividing the power at each time point by the mean power from 500 to 0 ms before stimulus onset, and then this baseline was subtracted. We then collapsed the data across all flicker frequencies assigned to like conditions and across left and right stimulation epochs. The target and distractor responses for correct and incorrect trials were then time-locked to either stimulus onset or response onset, and averaged across all subjects.

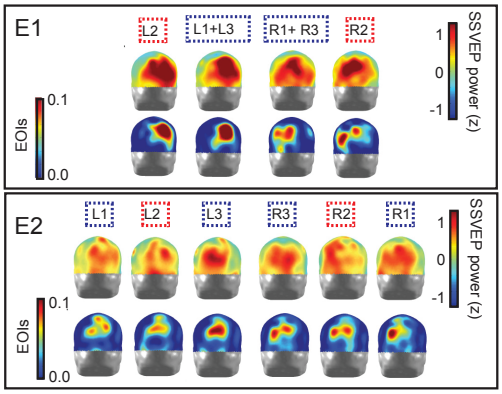

Fig. 2. Posterior-occipital view of topographical maps depicting steady-state visual evoked potentials (SSVEP) power averaged across the 3.2-s stimulus duration (z scores; *top* rows) and electrode-of-interest (EOI) probability maps (*bottom* rows; color bars indicate the probability with which each electrode was included in an EOI across subjects), corresponding to each of the possible target (blue dotted frame) and distractor locations (red dotted frame) in *experiment 1* (E1, $n = 11$; *top*) and *experiment 2* (E2, $n = 14$; *bottom*). Note that in E1, the 2 targets flickered at the same frequency so that only 2 topographical maps were produced, 1 for trials in the lower left quadrant and 1 for trials in the lower right quadrant. In contrast, the 2 targets in E2 flickered at different frequencies, yielding 6 distinct topographical maps corresponding to the lower left and lower right targets. Also, note that SSVEP power associated with left targets was most prominent over right occipital/parietal cortex, and SSVEP power associated with right targets was most pronounced over left visual cortex. This pattern is expected based on the contralateral mapping of external visual space to internals cortical representations.

Statistical analysis. Average accuracy was calculated separately for stimulus arrays presented in the left and right visual fields and also for each combination of target and distractor frequency assignments (2 combinations in E1 and 6 combinations in E2). Response times (RTs) were analyzed in a corresponding manner separately on correct and incorrect trials. In E1, two-way repeated-measures analysis of variance (ANOVA) tests were used to evaluate accuracy and RT data, with separate factors for stimulus location (left, right) and target frequency (6.9 Hz, 10.4 Hz). In E2, a similar statistical approach was performed, but there were six levels of the target frequency factor.

False discovery rate (FDR)-corrected post hoc t-tests were also performed to further examine any significant effects revealed by the repeated-measures ANOVAs. For the analysis of stimulus-locked SSVEP power and response-locked SSVEP power, we first performed repeated-measures t-tests to test for differences between target- and distractor-evoked responses at each time point on correct and incorrect trials. To correct for family-wise error rates, we then calculated the P values associated with the t scores for each time point. We sorted the P values in ascending order ($P_1, P_2, P_3, \ldots, P_k, \ldots, P_M$) and determined a threshold according to the following: $P_k > (K \cdot \alpha)/M$, where P_k is the FDR-corrected α-value ($P < 0.05$), K is the rank of the P value corresponding to the threshold, α is 0.05, and M is the total number of comparisons. All significant effects were defined as having a P value <0.05 after FDR correction. In addition, repeated-measures ANOVAs were performed on SSVEP power averaged across time windows identified as being significant based on the t-tests to evaluate

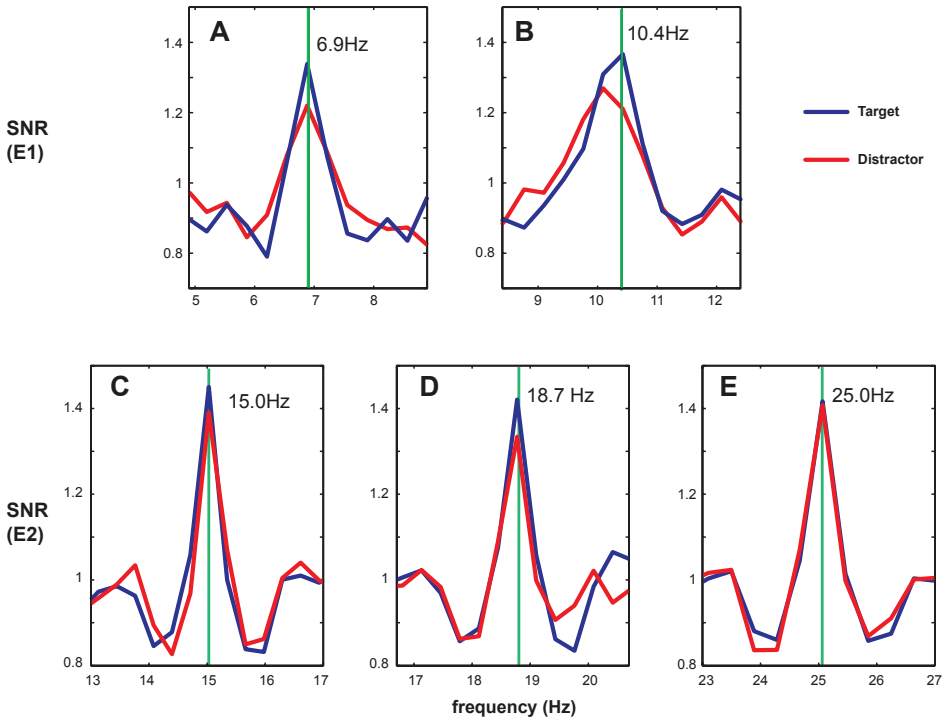

Fig. 3. Signal-to-noise ratio (SNR) at different frequencies, computed across the entire trial. The sharp peaks at each stimulation frequency demonstrate the specificity of the SSVEPs at 6.9 (*A*) and 10.4 Hz (*B*) in E1 and at 15.0 (*C*), 18.7 (*D*), and 25.0 Hz (*E*) in E2. SNR was calculated by dividing power at central frequency by the power in 4 surrounding frequency bins.

possible interactions between accuracy (correct/incorrect) and stimulus type (target/distractor). FDR correction was also applied to the analysis of behavioral data.

RESULTS

Behavioral results. In E1, the average percent correct, percent incorrect, and percent misses, collapsed across hemifields and flicker frequencies, were 65.4% (SD 8.3%), 25.8% (SD 11.0%), and 8.8% (SD 6.7%), respectively. A two-way repeated-measures ANOVA revealed no effect of stimulus location [$F(1,10) = 2.44, P = 0.15$], target frequency [$F(1,10) = 0.004$, $P = 0.95$], and no interaction between these factors on accuracy [$F(1,10) = 0.12, P = 0.74$]. Average RTs on correct and incorrect trials were 1,980 ms (SD 114.1 ms) and 2,092 ms (SD 171.6 ms), respectively. Two-way repeated measures ANOVAs revealed no main effect of stimulus location or flicker frequency on either correct or incorrect RTs, and no interaction between stimulus location and flicker frequency (all F values ≤ 1.08, all P values ≥ 0.32).

In E2, the average percent correct and percent incorrect, collapsed across hemifields and flicker frequencies, were 68.5% (SD 7.4%) and 31.5% (SD 7.4%), respectively (with no misses). A two-way repeated-measures ANOVA revealed a significant effect of target frequency on accuracy [$F(5, 65) = 11.86, P < 0.001$] but no effect of stimulus location [$F(1, 13) = 0.031, P = 0.826$] and no interaction between target frequency and stimulus location [$F(5, 65) = 1.024, P = 0.41$]. Post hoc *t*-tests revealed that the main effect of frequency resulted from higher performance when stimuli in *positions 1*, *2*, and *3* were flickered at 25, 18.76, and 15 Hz, respectively (compared with the other 5 combinations) and from higher performance when stimuli were flickered at 18.76, 15, and 25 Hz compared with when stimuli were flickered at either 18.76, 25, and 15 Hz or 15, 25, and 18.76 Hz, respectively (all t values >2.43, all P values <0.05, FDR corrected). This slight impairment when the distractor frequency was higher than both target frequencies might be due to the fact that lower frequencies translate into fewer presentation cycles across a fixed stimulus duration. However, this scenario was rare (only 9.5% of all comparisons), and we did not observe this effect in E1. Therefore, it is difficult to determine the ultimate cause of this frequency assignment effect in E2. Average RTs for correct and incorrect trials were 1,818 ms (SD 134 ms) and 1,847 ms (SD 231 ms). Two-way repeated-measures ANOVAs on the RT data revealed no significant effects of either frequency or stimulus location, and no interaction between these factors (this was true for RTs on both correct and incorrect trials, all F values ≤ 1.89, all P values ≥ 0.107).

We also computed *d*=on trials where the small target squares were offset by 0°, 90°, and 180° (where hits were defined as reporting that the offset was *X*° when it was in fact *X*°, and false alarms were defined as reporting that the offset was *X*° when it was either *Y*° or *Z*°). No significant differences in the sensitivity were observed as a function of target offset [*d*=for E1: 1.02 (SD 0.72), 1.13 (SD 0.47), 1.05 (SD 0.66) for 0°, 90°, 180° offsets, respectively, $F(2, 20) = 0.698$, $P = 0.509$; *d*=for E2: 0.97 (SD 0.49), 0.97 (SD 0.32), 0.85 (SD 0.41) for 0°, 90°, 180° offsets, respectively, $F(2, 28) = 2.452$, $P = 0.104$]. However, there was a modest but reliable difference in RTs on correct trials as a function of target offset [for E1: $F(2,20) = 7.169$, $P = 0.004$; for E2: $F(2,28) = 4.181$, $P = 0.029$]. Post hoc *t*-tests revealed that in E1, responses on 0° offset trials [1,921.5 ms (SD 168.3 ms)] were significantly shorter than responses on either 90° [2,009.8 ms (SD 193.8 ms), $t(10) = 3.063$, $P = 0.012$] or 180° trials [2,003.6 ms (SD 1,837 ms), $t(10) = 4.165$, $P = 0.002$]. In E2, there was only a difference between responses on trials with a 0° degree offset [1,783.3 ms (SD 155.1 ms)] and trials with a 180° offset [1,855.6 ms (SD 183.2 ms), $t(13) = 2.640$, $P = 0.02$].

SSVEP results. Figure 4, *top*, shows stimulus-locked SSVEP power across the entire stimulus interval for correct and incorrect trials in E1. Power increased significantly above baseline from ~50 to 3,200 ms poststimulus for both correct and incorrect target- and distractor-evoked SSVEPs [minimum *t*-value across this temporal window: $t(10) > 2.25$, $P < 0.05$]. There were no significant differences in SSVEP power associated with targets and distractors across time on either correct [all $t(10) < 2.01$, not significant (n.s.)] or incorrect trials [all $t(10) < 1.41$, n.s.]. However, both targets had a different flicker frequency than the single distractor, and this sensory difference may have obscured any differences in the overall responses to targets and distractors. In contrast, comparisons between target (or distractor) responses on correct and incorrect trials are controlled for sensory differences. However, there were no power differences in the target-evoked SSVEPs on correct and incorrect trials [all $t(10) < 2.90$, n.s.] or in the distractor-evoked SSVEPs on correct and incorrect trials [all $t(10) < 2.49$, n.s.].

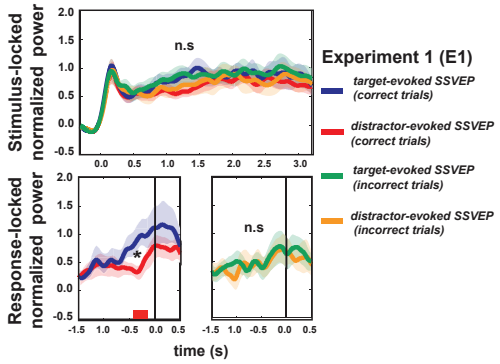

Fig. 4. Normalized power of target- and distractor-evoked SSVEPs on correct and incorrect trials in E1, time-locked to either the stimulus onset (*top*) or the onset of the behavioral response (*bottom*). Note that for response-locked data, responses on correct and incorrect trials are plotted separately for clarity. For all plots, the zero point on the *x*-axis represents the time of either stimulus onset or response onset for stimulus-locked and response-locked data, respectively. Red horizontal bar (*bottom left*) indicates the temporal window over which the target-evoked SSVEP power was significantly greater than the distractor evoked SSVEP power on correct trials [$P < 0.05$, false discovery rate (FDR) corrected]. Shaded areas in all plots represent ±1 SE across subjects; n.s, not significant.

When the normalized power was locked to the response, however, significant differences emerged. On correct trials (Fig. 4, *bottom left*), we found a significant increase in the power of the target-evoked SSVEP compared with the distractor-evoked SSVEP extending from 350 to 150 ms before the response [minimum *t*-value: $t(10) > 3.12$, all *P* values <0.05]. However, no differences in target- and distractor-evoked SSVEP power were observed on incorrect trials [maximum *t*-value: $t(10) < 3.06$, n.s.; Fig. 4, *bottom right*]. A repeated-measures ANOVA with factors for accuracy (correct/incorrect) and stimulus type (target/distractor) revealed no main effect of accuracy [$F(1, 10) = 0.55$, n.s.] but a significant main effect of stimulus type [$F(1, 10) = 6.82$, $P = 0.026$] and a significant interaction between accuracy and stimulus type on SSVEP power averaged across a response window extending from 350 to 150 ms before the behavioral response [$F(1, 10) = 13.39$, $P = 0.004$].

To address the possibility that attention might be efficiently split only in the trials in which subjects identified the targets quickly, we conducted an auxiliary analysis on the SSVEP data in E1, specifically sorting the data into trials with short and long RTs via a median split. Figure 5 shows the stimulus-locked (*left*) and response-locked SSVEP data (*right*) sorted into short RT trials (*top*) and long RT trials (*bottom*). As in the main analysis (Fig. 4), we observed no significant difference between target- and distractor-evoked SSVEP responses on correct trials at any time point [$t(10) < 2.55$, n.s.]. However, response-locked SSVEP responses significantly increased right before a correct response was made, and this was true for trials with short RTs [−350 to −150 ms: $t(10) > 3.17$, $P < 0.05$] and long RTs [−330 to −260 ms: $t(10) > 3.14$, $P < 0.05$]. Importantly, no response-locked differences were found on incorrect trials [$t(10) < 2.31$ for short RTs and $t(10) < 2.08$ for long RTs]. This pattern gave rise to a significant interaction between stimulus type (target/distractor) and accuracy on short RT trials [$F(1, 10) = 5.101$, $P = 0.047$] and a marginally significant interaction on long RT trials [$F(1, 10) = 3.887$, $P = 0.077$].

To evaluate the possibility that the divergence in the SSVEP power associated with targets and distractors on correct trials was driven by motor activity preceding the response, which was presumably focused contralateral to the right hand, we also tested SSVEP power separately when the stimuli were in the left and right visual fields. On correct trials, we found a significant divergence in target- and distractor-evoked SSVEP power for stimuli presented in both the left hemifield [$t(10) = 2.34$, $P = 0.04$, averaged across a window 350 to 150 ms before the response] and the right hemifield [$t(10) = 2.89$, $P = 0.05$, averaged across a window 350 to 150 ms before the response]. The observation of a qualitatively similar effect in both hemifields argues against motor preparation as the main factor in driving the divergence of SSVEP power associated with targets and distractors on correct trials.

Furthermore, to evaluate the possibility that the increased target-evoked power on correct trials was facilitated by group-

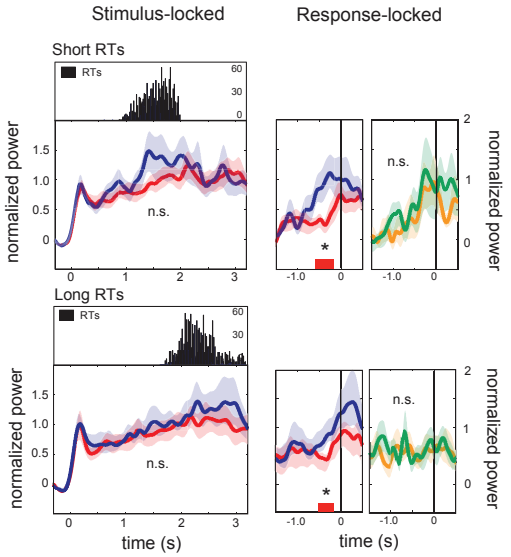

Fig. 5. Stimulus-locked (*left*) and response-locked (*right*) normalized power of target- and distractor-evoked SSVEPs in E1, sorted into trials with short (*top*) and long (*bottom*) response times (RTs). *Insets* above each stimulus-locked plot are the RT histograms (data from all subjects), with the mean trial count on the *y*-axis. In all plots, the zero point on the *x*-axis represents the time of either stimulus onset or response onset for stimulus-locked and response-locked data, respectively. Red horizontal bars in the response-locked plots indicate the temporal window over which the target-evoked SSVEP power was significantly greater than the distractor-evoked SSVEP power on correct trials ($P < 0.05$, FDR corrected). Shaded areas in all plots represent ±1 SE across subjects.

ing the targets on the basis of a common flicker frequency, we used separate flicker frequencies for all three stimuli in E2 (Fig. 6). This experiment also speaks to the "motor preparation" account referred to above, because the flicker rates used in E2 were well above the theta range typically associated with motor preparation (e.g., Luu and Tucker 2001; Makeig et al. 2004). In addition, assigning (and counterbalancing) a unique flicker frequency to each stimulus allowed for a more balanced comparison between the SSVEP responses associated with targets and distractors (compared with E1, where both targets shared a common flicker frequency).

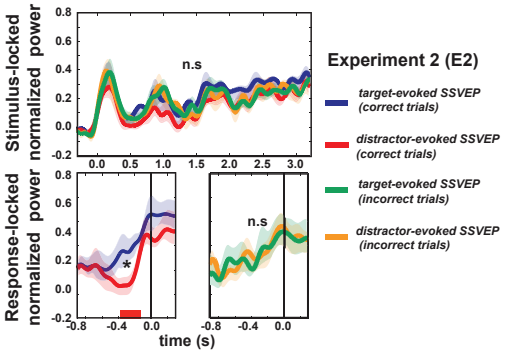

Fig. 6. Normalized power of target- and distractor-evoked SSVEPs on correct and incorrect trials in E2, time-locked to either the stimulus onset (*top*) or the onset of the behavioral response (*bottom*). Note that for response-locked data, responses on correct and incorrect trials are plotted separately for clarity. In all plots, the zero point on the *x*-axis represents the time of either stimulus onset or response onset for stimulus-locked and response-locked data, respectively. Red horizontal bar (*bottom left*) indicates the temporal window over which the target-evoked SSVEP power was significantly greater than the distractor evoked SSVEP power on correct trials ($P < 0.05$, FDR corrected). Shaded areas in all plots represent ±1 SE across subjects.

The SSVEP results in E2 were highly consistent with those in E1 (Fig. 6). For stimulus-locked data (Fig. 6, *top*), power increased significantly above baseline from ~50 to 3,200 ms poststimulus for both target- and distractor evoked SSVEPs [minimum *t*-value: $t(13) > 2.20$, $P < 0.05$]. However, just as in E1, there were no significant differences in SSVEP power between target- and distractor-evoked SSVEPs at any time point for either correct [all $t(13) < 3.30$, n.s.] or incorrect trials [all $t(13) < 3.36$, n.s.] and no significant differences in power across correct and incorrect trials for either target [all $t(13) < 2.60$, n.s.] or distractor-evoked SSVEP [all $t(13) < 2.49$, n.s.].

When the data were aligned to response onset (Fig. 6, *bottom left*), we found a significant increase in the target-related SSVEP compared with the distractor-related SSVEP across a window extending from 350 to 150 ms before the response [collapsed across left and right stimulus presentations: minimum *t*-value: $t(13) > 2.56$; left stimuli only: all $t(13) > 2.49$; right stimuli only: all $t(13) > 2.70$; all P values <0.05]. No power differences were observed on incorrect trials [maximum *t*-value: $t(13) < 2.22$, all n.s.; Fig. 6, *bottom right*]. A repeated-measures ANOVA with factors for accuracy and stimulus type revealed no main effect of accuracy [$F(1, 13) = 3.10$, n.s.] but a significant main effect of stimulus type [$F(1, 13) = 7.32$, $P = 0.018$] and a significant interaction between accuracy and stimulus type on SSVEP power averaged across a window from 350 to 150 ms before the response [$F(1, 13) = 9.744$, $P = 0.008$].

Just as in E1, we also analyzed SSVEPs separately on trials with the fastest and slowest RTs. Figure 7 shows the stimulus-locked (*left*) and response-locked SSVEP data (*right*) sorted into short RT trials (*top*) and long RT trials (*bottom*). When time-locked to stimulus onset, there were no significant differ-

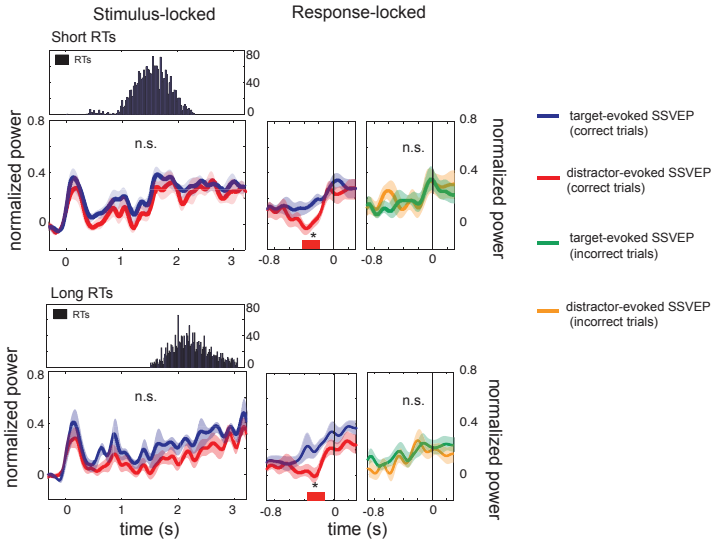

Fig. 7. Stimulus-locked (*left*) and response-locked (*right*) normalized power of target- and distractor-evoked SSVEPs in E2, sorted into trials with short (*top*) and long RTs (*bottom*). *Insets* above each stimulus-locked plot are the RT histograms (data from all subjects), with the mean trial count on the *y*-axis. In all plots, the zero point on the *x*-axis represents the time of either stimulus onset or response onset for stimulus-locked and response-locked data, respectively. Red horizontal bars in the response-locked plots indicate the temporal window over which the target-evoked SSVEP power was significantly greater than the distractor evoked SSVEP power on correct trials ($P < 0.05$, FDR corrected). Shaded areas in all plots represent ±1 SE across subjects.

ences between target- and distractor-evoked SSVEP responses on correct trials [$t(13) < 2.837$, n.s.]. However, the response-locked SSVEPs were significantly different right before a correct response for both short RT [−400 to −200 ms: $t(10) > 3.17$, $P < 0.05$] and long RT trials[−300 to −150 ms: $t(10) > 3.14$, $P < 0.05$]. Importantly, no response-locked differences were found on incorrect trials [$t(10) < 2.31$ for short RTs and $t(10) < 2.08$ for long RTs]. This pattern gave rise to a significant interaction between stimulus type (target/distractor) and accuracy on short RT trials [$F(1, 13) = 6.036$, $P = 0.029$] and on long RT trials [$F(1, 13) = 11.464$, $P = 0.005$].

Finally, we performed two control experiments (CE1 and CE2) to determine if the interleaved distractors used in E1 and E2 actually interfered with target processing. We found that in both control studies, subjects were significantly slower when an intervening distractor was presented compared with when no distractor was present [CE1: mean RT with a distractor = 1,674 ms, mean RT without a distractor = 1598 ms, $t(9) = 3.606$, $P = 0.0057$; CE2: mean RT with a distractor = 1,697 ms, mean RT without a distractor = 1,611 ms, $t(12) = 7.086$, $P < 0.0001$]. Subjects were also less accurate when a distractor was present versus absent [CE1: %correct with a distractor = 69.6%, %correct without a distractor = 72.83%, $t(9) = 2.457$, $P = 0.036$; CE2: %correct with a distractor = 71.88%, %correct without a distractor = 74.62%, $t(12) = 2.317$, $P = 0.039$]. Together, these two control experiments suggest that the intervening distractors did compete with target processing and thus are likely to encourage split attention foci.

DISCUSSION

To study the temporal dynamics of divided attention, we employed a multiple-object discrimination task, where two visual targets and an intervening distractor were presented in a single quadrant at different flicker frequencies. An analysis of SSVEPs was used to continuously monitor the responses associated with each stimulus. In both experiments, we failed to observe a difference between target- and distractor-evoked responses when the normalized SSVEP power was time-locked to the onset of the stimulus. Such effects may have been obscured in E1, because a direct comparison between target and distractor evoked responses may have been confounded due to the common flicker frequency of the target stimuli. However, a comparison of target and distractor evoked responses on correct and incorrect trials, which controls for this sensory difference, also revealed no stimulus-locked effects. Moreover, each stimulus in E2 had a unique frequency, and similar null results were observed. That said, we did not measure responses to the targets and distractors when they were attended and when they were unattended, so this null result should be interpreted with caution. In contrast, however, when the data were locked to the onset of the behavioral response, target-evoked SSVEP power was selectively larger compared with distractor-evoked SSVEP power approximately 150–350 ms before correct (but not incorrect) responses. Taken together, this evidence suggests that *1*) attention can be divided across noncontiguous regions of space even when the stimuli are presented in close proximity within the same visual quadrant, *2*) the division of spatial attention can occur in a temporally discrete manner, and *3*) there is a strong predictive relationship between the magnitude of responses tied to spatially distinct stimuli and the success of perceptual decision making.

Over the past several decades, evidence supporting the flexible division of attention has been accumulating based on tasks such as multiple object tracking (reviewed by Cavanagh and Alvarez 2005; Intriligator and Cavanagh 2001; Pylyshyn and Annan 2006; Pylyshyn and Storm 1988). However, studies that have reported neuronal evidence in favor of divided

attention typically employed visual stimuli that were spaced quite far from one another, often crossing the vertical meridian or spanning the entire visual field (e.g., McMains and Somers 2004, 2005; Müller et al. 2003a). In one notable exception, McMains and Somers (2004) found evidence for divided attention between two locations in a single quadrant. However, in their study, one target stimulus was always located at fixation and the other target was located peripherally. Therefore, the extent to which attention can be efficiently divided between objects that are in close spatial proximity is still unclear, particularly when more than one relevant stimulus falls within the same hemifield/quadrant of space (Maertens and Pollmann 2005; Pollmann et al. 2003; Sereno and Kosslyn 1991). More recently, Malinowski et al. (2007) also tested whether attention could be divided into multiple spotlights when the stimuli were spaced closely together (i.e., within the same hemifield) using an SSVEP design. In contrast to the present study, they did not find consistent evidence for divided attention. Instead, they observed divided attention effects only when subjects attended to stimuli in the upper left but not in the lower left quadrant. The authors suggested that these mixed results may have been caused by the higher perceived saliency of the intermediate distractor in the lower quadrant. However, computing the average SSVEP power over the entire stimulus period (~2–3 s) [as done by Malinowski et al. (2007)] may have reduced their ability to detect evidence for divided attention, particularly if the effect has a discrete onset that immediately precedes the behavioral response as in the current study.

Consistent with some aspects of Malinowski et al. (2007), our stimulus-locked analysis yielded no significant power difference between target- and distractor-evoked SSVEPs. At first glance, the results from this stimulus-locked analysis are consistent with spotlight models in which attention is always unitary (Posner et al. 1980) or zoomed/reshaped based on task demands (Barriopedro and Botella 1998; Erkisen and St. James 1986; Eriksen and Yeh 1985; Heinze et al. 1994; McCormick and Jolicoeur 1994; Müller et al. 2003b). However, our data argue against this account on the basis of two key pieces of evidence. First, the unitary spotlight models predict that the overall level of stimulus-locked SSVEP power should predict discrimination success. Instead, we observed that overall stimulus-locked SSVEP power did not predict successful performance on the discrimination task. Second, a unitary spotlight model cannot account for a response-locked increase in SSVEP power that immediately precedes successful discriminations, an observation that strongly favors the divided attention hypothesis (Awh and Pashler 2000; Baldauf and Deubel 2008; Bichot et al. 1999; Carlson et al. 2007; Castiello and Umiltà 1992; Cavanagh and Alvarez 2005; Dubois et al. 2009; Gobell et al. 2004; Godijn and Theeuwes 2003; Hahn and Kramer 1998; Howe et al. 2011; Kraft et al. 2005; Kramer and Hahn 1995; Malinowski et al. 2007; McMains and Somers 2004, 2005; Müller et al. 2003a, 2003b; Niebergall et al. 2010, 2011). This response-locked increase in power that predicted successful performance was replicated in two experiments, and the temporal window of the divergence between target- and distractor-evoked SSVEP power was consistently found to occur ~350 to 150 ms preceding correct responses. The significant main effect of stimulus type (target vs. distractor) and interaction between stimulus type and accuracy on SSVEP power averaged across a 350- to 150-ms window prior to the response further suggests that successful discrimination was achieved by a temporally discrete segregation of neuronal responses tied to targets and distractors, respectively.

Although we cannot directly assess the degree to which our results were driven by active neuronal suppression, our findings complement recent single-unit electrophysiological data recorded from the middle temporal visual area (MT) of macaques. The monkeys were trained to attend to two translating objects while ignoring an intermediate distractor located inside the receptive field of the neuron that was being monitored (Niebergall et al. 2011). Niebergall et al. (2011) found that when the monkey attended to the two translating objects, neuronal responses associated to the distractor were either suppressed or remained unaltered, providing strong evidence in support of divided spatial attention. Taking these findings together with the present observations, it is possible that the division of spatial attention is achieved not only by enhancing responses to attended targets but also by actively suppressing responses to ignored distractors. Future research in humans using SSVEP could further explore this issue by using paradigms in which a clear baseline SSVEP response is maintained throughout a block of trials, thereby providing a benchmark for evaluating relative degrees of enhancement and suppression (see e.g., Andersen and Müller 2010 for an example of this approach).

Since the difference between target- and distractor-evoked SSVEP power was observed only when the data were locked to behavioral responses, it is possible that this difference simply reflects a broadband increase in power related to the preparation of a motor response. However, this is unlikely because we obtained sharply tuned SSVEP signals peaking only at the stimulus frequencies in both E1 and E2 (Fig. 3). Furthermore, there are several other factors that argue against a broadband frequency modulation. First, if the effect reflects a broadband increase in power related to response preparation, there should have been an additive effect for both target- and distract-evoked SSVEP responses. Instead, we observed a significant divergence of target- and distractor-evoked SSVEP responses, which rules out a broadband source of our main effect of interest. Second, the observed divergence in power on correct and incorrect trials was consistent across the two experiments even though stimulus frequencies ranged widely, from 6.9 to 25 Hz. Thus the effect is unlikely to be specific to any intrinsic oscillation related to response preparation.

Among past psychophysical studies that reported evidence in support of divided attention, some assumed that attention can be split into multiple spotlights only in a rapid and discrete manner and thus limited their cue-to-stimulus intervals (CSIs) to <200 ms (e.g., Baldauf and Deubel 2008; Bichot et al. 1999; Kramer and Hahn 1995). On the other hand, others assumed that the division of attention can be sustained over a longer period of time and thus employed longer CSIs (~500 ms to 10 s; e.g., Awh and Pashler 2000; Gobell et al. 2004; Kraft et al. 2005). To more directly address this issue, Dubois et al. (2009) conducted a psychophysical experiment in which CSIs were varied and found that divided attention could occur only over very short timescales (CSIs less than ~200 ms). In contrast, Müller et al. (2003a) observed divided attention effects on SSVEP responses averaged over the entire stimulus interval (~2–3 s) and thus proposed that divided spatial attention could

be sustained over several seconds. However, an effect that is based on the averaged SSVEP power over a long temporal window could be driven either by a truly sustained process or by a temporally discrete process that has a large impact on the overall average power of the SSVEP response. In the present study, we examined changes of target- and distractor-evoked SSVEP power across time to characterize the temporal properties of divided attention, and the data support a temporally discrete splitting process that occurs immediately preceding correct responses and is sustained for only several hundred milliseconds (which is broadly consistent with the temporal estimates based on the behavioral data reported by Dubois et al. 2009). Nevertheless, our conclusion that attention can be divided in a temporally discrete manner must be qualified as our stimuli were close together and always presented in the same visual quadrant. It is possible, for example, that sustained divided attention might be more feasible when the targets are in different hemifields (Maertens and Pollmann 2005; Pollmann et al. 2003; Sereno and Kosslyn 1991), and it is also possible that cross-hemispheric division might operate on a more graded timescale due to anatomic constraints governing cross-hemispheric communication (e.g., McMains and Somers 2004, 2005; Müller et al. 2003). Thus future studies are needed to further explore the relationship between the time course of divided attention and the spatial properties of the visual display.

Finally, given that the focus of spatial attention can be alternated rapidly, it is possible that subjects were switching between the two target stimuli as opposed to continuously dividing attention. In the present studies, we observed a divergence in SSVEP power right before a correct response across a relatively brief temporal window that lasted for ~200 ms. Although estimates of switching time vary considerably across studies, if the lower limit of 100 ms proposed by Jans et al. (2010) is adopted, then subjects in our task may in fact have been switching attention rapidly between the two target stimuli (and this would also pose a challenge for many previous studies as well; e.g., Baldauf et al. 2006; Gobell et al. 2004; McMains and Somers 2004, 2005; Müller et al. 2003a). However, the lower bound of 100 ms is based on studies that could not rule out parallel encoding accounts, so this may be an underestimate of the actual switch time (e.g., Czerwinski et al. 1992; Kramer and Hahn 1995). On the other hand, if a more conservative estimate of switching time in the range of 200–250 ms (or more) is adopted (e.g., Duncan et al. 1994; Kröse and Julesz 1989; Weichselgartner and Sperling 1987), then it is less likely that a rapid-switching account can explain the present data or the results reported by others. That said, the temporal scale at which attention can be switched is still an issue of debate, and it is difficult to conclusively rule out all forms of this account. However, even in light of this ambiguity, the present data provide a high temporal resolution metric that we think plausibly reflects the division of attention immediately preceding a successful perceptual discrimination.

In summary, our data suggest that dividing attention across noncontiguous locations is possible even when the stimuli are in close proximity and located within the same visual quadrant. Moreover, the multifocal division of attention within a quadrant onsets in a discrete manner and is primarily time-locked to the onset of a correct behavioral response. Thus these data suggest a tight temporal relationship between the transient division of spatial attention and successful perceptual decision making.

ACKNOWLEDGMENTS

We thank Candace Linscheid, Tony Abuyo, and Danna Lee for help with data collection.

GRANTS

This study was funded by National Institute of Mental Health (NIMH) Grant R01-MH092345 (to J. T. Serences). J. O. Garcia was supported by NIMH Grant R01-MH68004 (to R. Srinivasan).

DISCLOSURES

The authors declare no competing financial interests.

AUTHOR CONTRIBUTIONS

S.I. and J.T.S. conception and design of research; S.I. performed experiments; S.I. and J.O.G. analyzed data; S.I., J.O.G., and J.T.S. interpreted results of experiments; S.I. prepared figures; S.I. and J.T.S. drafted manuscript; S.I., J.O.G., and J.T.S. edited and revised manuscript; S.I. and J.T.S. approved final version of manuscript.

REFERENCES

Andersen SK, Müller MM. Behavioral performance follows the time course of neural facilitation, and suppression during cued shifts of feature-selective attention. *Proc Natl Acad Sci USA* 107: 13878–13882, 2010.

Awh E, Pashler H. Evidence for split attentional foci. *J Exp Psychol Hum Percept Perform* 26: 834–846, 2000.

Baldauf D, Deubel H. Visual attention during the preparation of bimanual movements. *Vision Res* 48: 549–563, 2008.

Baldauf D, Wolf M, Deubel H. Deployment of visual attention before sequences of goal-directed hand movements. *Vision Res* 46: 4355–4374, 2006.

Barriopedro MI, Botella J. New evidence for the zoom lens model using the RSVP technique. *Percept Psychophys* 60: 1406–1414, 1998.

Bichot NP, Cave KR, Pashler H. Visual selection mediated by location: feature-based selection of noncontiguous locations. *Percept Psychophys* 61: 403–423, 1999.

Brainard DH. The Psychophysics Toolbox. *Spat Vis* 10: 433–436, 1997.

Bruns A. Fourier-, Hilbert-, and wavelet-based signal analysis: are they really different approaches? *J Neurosci Methods* 137: 321–332, 2004.

Canolty RT, Soltani M, Dalal SS, Edwards E, Dronkers NF, Nagarajan SS, Kirsch HE, Barboro NM, Knight RT. Spatiotemporal dynamics of word processing in the human brain. *Front Neurosci* 1: 185–196, 2007.

Carlson T, VanRullen R, Hogendoorn H, Verstraten F, Cavanagh P. Distinguishing models of multifocal attention: it's a matter of time. *J Vis* 7: 641, 2007.

Castiello U, Umiltà C. Splitting focal attention. *J Exp Psychol Hum Percept Perform* 18: 837–848, 1992.

Cavanagh P, Alvarez GA. Tracking multiple targets with multifocal attention. *Trends Cogn Sci* 9: 349–354, 2005.

Cave KR, Bush WS, Taylor TG. Split attention as part of a flexible attentional system for complex scenes: comment on Jans, Peters, and De Weerd. *Psychol Rev* 117: 685–696, 2010.

Czerwinski M, Lightfoot N, Shiffrin RM. Automatization and training in visual search. *Am J Psychol* 105: 271–315, 1992.

Dubois J, Hamker FH. Attentional selection of noncontiguous locations: the spotlight is only transiently "split". *J Vis* 9: 1–11, 2009.

Duncan J, Ward R, Shapiro KL. Direct measurement of attentional dwell time in human vision. *Nature* 369: 313–315, 1994.

Eriksen CW, St. James JD. Visual attention within and around the field of focal attention: a zoom lens model. *Percept Psychophys* 40: 225–240, 1986.

Eriksen CW, Yeh YY. Allocation of attention in the visual field. *J Exp Psychol Hum Percept Perform* 11: 583–597, 1985.

Gobell JL, Tseng C, Sperling G. The spatial distribution of visual attention. *Vision Res* 44: 1273–1296, 2004.

Godijn R, Theeuwes J. Parallel allocation of attention prior to the execution of saccade sequences. *J Exp Psychol Hum Percept Perform* 29: 882–896, 2003.

Hahn S, Kramer AF. Further evidence for the division of attention between noncontiguous locations. *Vis Cogn* 5: 217–256, 1998.

Heinze HJ, Luck SJ, Münte TF, Gös A, Mangun GR, Hillyard SA. Attention to adjacent and separate positions in space: an electrophysiological analysis. *Percept Psychophys* 56: 42–52, 1994.

Howe PD, Drew T, Pinto Y, Horowitz TS. Remapping attention in multiple object tracking. *Vision Res* 51: 489–495, 2011.

Intriligator J, Cavanagh P. The spatial resolution of visual attention. *Cogn Psychol* 43: 171–216, 2001.

Jans B, Peters JC, De Weerd P. Visual spatial attention to multiple locations at once: the jury is still out. *Psychol Rev* 117: 637–684, 2010.

Kim YJ, Verghese P. The selectivity of task-dependent attention varies with surrounding context. *J Neurosci* 32: 12180–12191, 2012.

Kraft A, Müller NG, Hagendorf H, Schira MM, Dick S, Fendrich RM, Brandt SA. Interactions between task difficulty and hemispheric distribution of attended locations: implications for the splitting attention debate. *Cogn Brain Res* 24: 19–32, 2005.

Kramer AF, Hahn S. Splitting the beam: distribution of attention over noncontiguous regions of the visual field. *Psychol Sci* 6: 381–386, 1995.

Kröse BJ, Julesz B. The control and speed of shifts of attention. *Vision Res* 29: 1607–1619, 1989.

Luu P, Tucker DM. Regulating action: alternating activation of midline frontal, and motor networks. *Clin Neurophysiol* 112: 1295–1306, 2001.

Maertens M, Pollmann S. Interhemispheric resource sharing: decreasing benefits with increasing processing efficiency. *Brain Cogn* 58: 183–192, 2005.

Makeig S, Delorme A, Westerfield M, Jung TP, Townsend J, Courchesne E, Sejnowski TJ. Electroencephalographic brain dynamics following manually responded visual targets. *PLoS Biol* 2: 176, 2004.

Malinowski P, Fuchs S, Müller MM. Sustained division of spatial attention to multiple locations within one hemifield. *Neurosci Lett* 414: 65–70, 2007.

McCormick PA, Jolicoeur P. Manipulating the shape of distance effects in visual curve tracing: further evidence for the zoom lens model. *Can J Exp Psychol* 48: 1–24, 1994.

McMains SA, Somers DC. Multiple spotlights of attentional selection in human visual cortex. *Neuron* 42: 677–686, 2004.

McMains SA, Somers DC. Processing efficiency of divided spatial attention mechanisms in human visual cortex. *J Neurosci* 25: 9444–9448, 2005.

Müller MM, Malinowski P, Gruber T, Hillyard SA. Sustained division of the attentional spotlight. *Nature* 424: 309–312, 2003a.

Müller MM, Teder-Sälejärvi W, Hillyard SA. The time course of cortical facilitation during cued shifts of spatial attention. *Nat Neurosci* 1: 631–634, 1998.

Müller NG, Bartelt OA, Donner TH, Villringer A, Brandt SA. A physiological correlate of the "zoom lens" of visual attention. *J Neurosci* 23: 3561–3565, 2003b.

Niebergall R, Huang L, Martinez-Trujillo JC. Similar perceptual costs for dividing attention between retina- and space-centered targets in humans. *J Vis* 10: 1–14, 2010.

Niebergall R, Khayat PS, Treue S, Martinez-Trujillo JC. Multifocal attention filters targets from distracters within and beyond primate MT neurons' receptive field boundaries. *Neuron* 72: 1067–1079, 2011.

Pelli DG. The VideoToolbox software for visual psychophysics: transforming numbers into movies. *Spat Vis* 10: 437–442, 1997.

Pollmann S, Zaidel E, von Cramon DY. The neural basis of the bilateral distribution advantage. *Exp Brain Res* 153: 322–333, 2003.

Posner MI, Snyder CR, Davidson BJ. Attention and the detection of signals. *J Exp Psychol Hum Percept Perform* 109: 160–174, 1980.

Pylyshyn ZW, Annan V Jr. Dynamics of target selection of multiple object tracking (MOT). *Spat Vis* 19: 485–504, 2006.

Pylyshyn ZW, Storm WS. Tracking multiple independent targets: evidence for a parallel tracking mechanism. *Spat Vis* 3: 179–197, 1988.

Regan D. *Human brain electrophysiology: evoked potentials and evoked magnetic fields in science and medicine*. *New* York: McGraw-Hill, 1989.

Sereno AB, Kosslyn SM. Discrimination within, and between hemifields: a new constraint on theories of attention. *Neuropsychologia* 29: 659–675, 1991.

Srinivasan R, Bibi FA, Nunez PL. Steady-state visual evoked potentials: distributed local sources and wave-like dynamics are sensitive to flicker frequency. *Brain Topogr* 18: 167–187, 2006.

Sutoyo D, Srinivasan R. Nonlinear SSVEP responses are sensitive to the perceptual binding of visual hemifields during conventional 'eye' rivalry and interocular 'percept' rivalry. *Brain Res* 1251: 245–255, 2009.

Weichselgartner E, Sperling G. Dynamics of automatic and controlled visual attention. *Science* 238: 778–780, 1987.

Chapter 2, in full, is a reprint of the material as it appears in an article entitled "Temporal dynamics of divided spatial attention" published in Journal of Neurophysiology 2013. Itthipuripat, S.; Garcia, Javier O.; Serences, John T., American Physiological Society, 2013. The dissertation author was the primary author of the manuscript. Supported by National Institute of Mental Health (NIMH) Grant R01-MH092345 to J.S.T. and by NIMH Grant R01-MH68004 G.J.O. We thank Candace Linscheid, Tony Abuyo, and Danna Lee for help with data collection.

Chapter 3:

Changing the spatial scope of attention alters patterns of neural gain in human cortex

Behavioral/Cognitive

Changing the Spatial Scope of Attention Alters Patterns of Neural Gain in Human Cortex

Sirawaj Itthipuripat,[1] Javier O. Garcia,[2] Nuttida Rungratsameetaweemana,[3,4] Thomas C. Sprague,[1] and John T. Serences[1,2]

[1]Neurosciences Graduate Program and [2]Department of Psychology, University of California, San Diego, La Jolla, California 92093-0109, and Departments of [3]Psychology and [4]Mathematics, Middlebury College, Middlebury, Vermont 05753

Over the last several decades, spatial attention has been shown to influence the activity of neurons in visual cortex in various ways. These conflicting observations have inspired competing models to account for the influence of attention on perception and behavior. Here, we used electroencephalography (EEG) to assess steady-state visual evoked potentials (SSVEP) in human subjects and showed that highly focused spatial attention primarily enhanced neural responses to high-contrast stimuli (response gain), whereas distributed attention primarily enhanced responses to medium-contrast stimuli (contrast gain). Together, these data suggest that different patterns of neural modulation do not reflect fundamentally different neural mechanisms, but instead reflect changes in the spatial extent of attention.

Introduction

Selective attention is the mechanism by which behaviorally relevant sensory inputs are preferentially processed at the expense of distracters. This selective information processing is thought to partially depend on changes in the gain of neurons within striate and extrastriate visual cortices. However, developing a parsimonious model to account for gain modulation has been challenging because different studies have found disparate attention effects on stimulus evoked neural responses (Reynolds et al., 2000; Martínez-Trujillo and Treue, 2002; Williford and Maunsell, 2006; Buracas and Boynton, 2007; Kim et al., 2007; Lee and Maunsell, 2009, 2010a,b).

In a canonical paradigm (Reynolds et al., 2000; Martínez-Trujillo and Treue, 2002), attention is covertly deployed to one of two stimuli, whereas stimulus contrast is systematically varied to generate contrast-response functions (CRFs) based on the activity level of visually responsive neurons. Whereas some studies report that attention primarily enhances already strong responses (response gain; see Fig. 1*A*; Di Russo et al., 2001; Kim et al., 2007; Lee and Maunsell, 2010a), others report that attention enhances only responses to midcontrast stimuli (contrast gain; see Fig. 1*B*; Reynolds et al., 2000; Martínez-Trujillo and Treue, 2002). Finally, other studies report patterns that resemble a combination of different gain modulations (Williford and Maunsell, 2006; Buracas and Boynton, 2007; Murray, 2008; Pestilli et al., 2011).

The normalization model of attention (NMA; Reynolds et al., 1999; Lee and Maunsell, 2009, 2010b; Reynolds and Heeger, 2009) suggests that these inconsistent modulatory patterns might arise via changes in the size of the stimulus and the attention field. The NMA is based on the premise that, in the absence of attention, two factors determine the firing rate of a visually responsive neuron. First, a facilitatory component (stimulus drive) is determined by the contrast of the stimulus placed in the receptive field (RF) of a neuron. Second, a suppressive drive is determined by the summed activity of other neighboring neurons, serving to normalize the overall spike rate of the cell in question via mutual inhibition (Heeger 1992). Attention modulates the pattern of neural activity by altering the balance between these facilitatory and suppressive drives (Reynolds and Heeger, 2009). Thus, a highly focused attention field leads to response gain (see Fig. 1*A*) because attentional gain is applied primarily to the stimulus drive. Conversely, a larger attention field leads to contrast gain because attention increases both the stimulus and the suppressive drives, and this normalizes responses at high contrasts (see Fig. 1*B*).

A previous psychophysical study has reported a pattern of behavioral performance that is consistent with the NMA (Herrmann et al., 2010). However, existing studies have not measured neural CRFs to determine whether manipulating the size of the attention field with respect to a constant stimulus size selectively alters the gain pattern of neural CRFs. Here, we evaluated this relationship in human subjects by measuring steady-state visual evoked potentials (SSVEPs) elicited by attended and ignored flickering visual stimuli.

Materials and Methods

Electroencephalography subjects. We initially recruited eight neurologically healthy human subjects (21–27 years old, four females) with normal

Received Sept. 13, 2013; revised Oct. 30, 2013; accepted Nov. 10, 2013.

Author contributions: S.I., T.C.S., and J.T.S. designed research; S.I. and N.R. performed research; J.O.G. contributed unpublished reagents/analytic tools; S.I., J.O.G., N.R., and T.C.S. analyzed data; S.I., J.O.G., T.C.S., and J.T.S. wrote the paper.

This work was supported by NIH Grant R01-MH092345 (J.T.S.) and a James S. McDonnell Foundation grant (J.T.S.). J.O.G. was supported in part by NIH Grant R01-MH068004 to Ramesh Srinivasan. We thank Kimberly Kaye and Edward F. Ester for help with data collection, Anna Byers and Mary E. Smith for assistance with retinotopic mapping procedures, and John Reynolds, Timothy Q. Gentner, Edward Awh, Jeremy Freeman, and Scott Freeman for useful discussions.

The authors declare no competing financial interests.

Correspondence should be addressed to either Sirawaj Itthipuripat or John T. Serences, Neurosciences Graduate Program, Department of Psychology, University of California, San Diego, La Jolla, California 92093-0109. E-mail: itthipuripat.sirawaj@gmail.com or jserences@ucsd.edu.

or corrected-to-normal vision. The recruitment of eight subjects is within the typical range for studies using similar multisession approaches (Di Russo et al., 2001; Morrone et al., 2002, 2004; Carrasco et al., 2004; Pestilli and Carrasco 2005; Ling and Carrasco 2006; Pestilli et al., 2007, 2009, 2011; Herrmann et al. 2010). All subjects signed an informed consent form approved by the Institutional Review Board at the University of California, San Diego (UCSD) and participated in the study for monetary compensation of $15 per hour. They were behaviorally trained for 1.5 h on the task 1 d before undergoing multiple electroencephalography (EEG) sessions (10–15 sessions, 3840–5760 trials in total). Data from one subject were discarded due to a failure to complete the experimental protocol (the subject withdrew after the first EEG session). Of the other seven subjects, four completed 10 sessions, one completed 11 sessions, one completed 13 sessions, and one completed 15 sessions of EEG recording.

EEG task design. EEG data were recorded while subjects performed an attention task that required the covert allocation of either focused or distributed spatial attention (see Fig. 2*A*, *B*). We monitored SSVEPs elicited by flickering a series of small disks (1.22° radius) concurrently in the lower left and right visual field quadrants at a rate of either 21.25 Hz (25% on–off duty cycle) or 28.33 Hz (33.33% on–off duty cycle), respectively (and vice versa in half of the trials). By flickering the left and right stimulus arrays at different frequencies, we were able to isolate the neural response to stimuli presented in each location via a frequency-domain analysis of the stimulus-locked SSVEP response. These high flicker-frequencies were chosen based on previously established methods (Müller et al., 1998a; Breakspear et al., 2010; Bridwell and Srinivasan, 2012; Garcia et al., 2013; Itthipuripat et al., 2013) in an effort to restrict our measurements to entrained activity in visual cortex. The small disk appeared randomly within a circular area with a radius of 4.90° (marked by an imaginary black ring in Fig. 2*A*, centered 8.58° from a central fixation point, which was located 3.50° above the center of the display). The contrast of the flickering disks was systematically varied across trials over a range extending from 2.5 to 90.0% (Michelson contrast: $100 \times (I_s - I_b)/(I_s + I_b)$, where I_s is the luminance of the gray disk, and I_b is the luminance of the dark gray background fixed at 2.7 cd/m^2).

We manipulated the spatial extent of attention by varying the potential location of an occasional target stimulus that was presented on 25% of the trials. The target was a circular oriented grating with the same mean contrast and the same size as the nontarget disk, and subjects pressed one of two buttons to indicate whether the orientation of the grating was 10° clockwise or 10° counterclockwise relative to vertical. In both the focused and the distributed conditions, nontarget disks were presented in a circle (radius, 4.90°; marked by the black ring in Fig. 2). Within this 4.90° radius circle, the location of each nontarget disk was randomly drawn from a nonuniform distribution, approximating a Gaussian, such that there was a higher probability of the disk appearing near the center of the stimulus window than near the edges. In the focused-attention condition (see Fig. 2*A*, left), targets always appeared within a small circle (marked by the blue dotted ring in the figure; radius, 2.04°). Thus, the region of space in which a target disk could appear (the attention field) was smaller than the size of the stimulus drive in the focused-attention condition. In the distributed-attention condition (see Fig. 2*A*, right), targets could be presented inside a larger circle (marked by the cyan dotted ring in the figure; radius, 6.54°). Thus, the size of the attention field (6.54°) was larger than the size of the stimulus drive (4.90°) in the distributed-attention condition. Critically, the spatial extent of the stimulus drive is fixed across the focused and distributed conditions. Thus we predicted more response gain in the focused-attention condition because the attention field is relatively small compared to the stimulus drive, and more contrast gain in the distributed-attention condition because the attention field is relatively large compared to the stimulus drive (Fig. 1*A*, *B*). Note also that these predictions hold as long as the relative size of the attention field is larger in the distributed-attention condition compared to the focused-attention condition (Fig. 1*C–E* for model simulations as described below, Additional model simulations).

The schematic of the trial structure is shown in Figure 2*B*. Each trial started with a fixation point and a 1 s arrow cue instructing subjects to covertly attend to the left or to the right stimulus, followed by a 50 ms auditory cue (400 or 1500 Hz) instructing the subjects to implement either a focused- or distributed-attention strategy. Two seconds after the arrow cue onset, the small flickering nontarget disks appeared in the lower left and lower right quadrants for 7 s. A second 50 ms auditory cue was then presented after a pseudorandomly selected interval of 3–4 s from the stimulus onset and instructed subjects to either maintain or switch their attentional strategy. The intertrial interval (ITI) was 2 s. All trial types were pseudorandomized so that the occurrence of the target-present trials was unpredictable. To ensure that subjects were actively engaged in the task for the duration of each trial, the grating targets were briefly presented for 11.7 ms in the first half of the trial, in the second half of the trial, or in both intervals with equal probability. In addition, the time at which the target appeared was pseudorandomly selected from a uniform distribution to decrease the predictability of the target onset time. Target stimuli could appear only on the attended side (100% cue validity). This was done to ensure that subjects focused only on the attended location and did not divide their attention across hemifields.

EEG experimental procedures. Stimuli were presented on a PC running Windows XP using MATLAB (MathWorks) and the Psychophysics

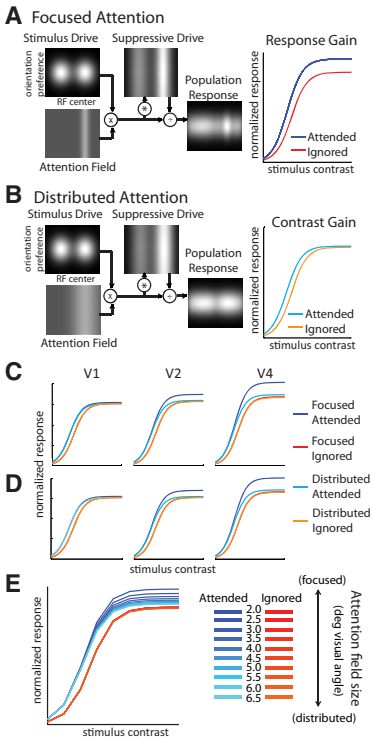

Figure 1. ***A***, The NMA predicts that focused attention leads to response gain, or an upward shift of the CRF. ***B***, On the other hand, distributed attention should lead to contrast gain, or a leftward shift of the CRF. The spatial distribution of the stimulus response and the size of the attention field used here are based on the parameters used in the main EEG experiment. ***C***, ***D***, We also specified the stimulus size and the attention field size in relation to expected RF sizes across striate and extrastriate visual areas (V1, V2, and V4) and found that the NMA generates consistent results across regions. ***E***, The NMA simulation (using the RF parameters from V4) in which the stimulus size is fixed at 4.9° but the size of the attention field varies from 2.0 to 6.5° consecutively in 0.5° steps. The model predicts that as the size of the attention field increases, response gain will decrease and contrast gain will increase in a continuous manner. See model parameters for all figures in Table 1 and simulation procedures in Material and Methods.

Toolbox (version 3.0.8) (Brainard, 1997; Pelli, 1997). Precise stimulus onset times were recorded from the CRT monitor (HP P1203, 85 Hz sh rate) via small fiber-optic cables attached to the screen. The gain sensitivity of the fiber-optic system (custom built by the Electronic lopment and Repair Facility, Department of Physics, University of California, San Diego; schematics available upon request) were adjusted to give accurate and fast sampling to record the precise timing of the flickering stimuli. Participants were seated 70 cm from the monitor in a dark room and used two buttons on a keyboard to make their responses.

Analysis of behavioral data. Only correct button presses occurring between 200 and 1500 ms after the onset of a target were counted as correct. Repeated-measures ANOVAs were used for all behavioral analyses. Note that subjects made no correct responses on trials in which the stimulus contrast was set to 2.5%, as the stimuli were nearly invisible at this level. Thus, the analysis of response time data included only trials from the five higher contrast levels (i.e., from 5–90%). This is reflected in the smaller degrees of freedom [4, 24] in the ANOVA that assessed the effects of contrast on RT.

EEG data acquisition and analysis. EEG data were recorded using a 128-channel Geodesic Sensor Net coupled with a NetAmps 300 amplifier (Electrical Geodesics), sampled at 1000 Hz and referenced to the central channel. Electrode impedances were kept below 50 kΩ, which is standard for this system. Blinks and eye movements were monitored by six built-in electrodes placed above, below, and beside the left and right eyes.

The EEG data were filtered by applying a high-pass Butterworth filter with 2 dB attenuation at 2 Hz and a band-stop Butterworth filter with 30 dB attenuation between 58 and 62 Hz. The EEG data were then segmented into epochs extending from 3000 ms before stimulus onset to 3000 ms after stimulus offset. Trials that exhibited prominent blink, electrooculogram, or electromyogram artifacts were discarded using threshold rejection (more than ± 75 μV deviation from the mean) and visual inspection on trial-by-trial basis, which resulted in the removal of $<$20% of trials across subjects. Principal components were then computed and selected for removal based on visual analysis to attenuate any residual artifacts.

Fourier coefficients were calculated at frequencies of 21.25 and 28.33 Hz (the two stimulus frequencies) and 40 surrounding frequency bins separately for the first half (from 0–3 s after the flicker onset) and the second half of the trial (from 0–3 s after the second auditory cue), and for each spatial cue type (attend left or right), attention condition (focused or distributed), stimulus location (left or right), and stimulus contrast level (six levels). To avoid spectral leakage, we truncated the FFT calculation window to have a length equal to the number of integer stimulus cycles nearest to the 3 s interval. Specifically, for a stimulus flicker of 21.25 Hz, the 3 s interval was truncated to 2.9172 s, giving a central frequency of 21.2547 and a 0.3428 Hz spectral resolution. For the stimulus flicker at 28.33 Hz, the 3 s interval was truncated to 2.9647 s, giving a central frequency of 28.3305 Hz and a 0.3373 Hz spectral resolution. All figures and analyses are based only on the data from nontarget trials on which no false alarm was made. Analyzing only nontarget trials was critical because it prevented confounds related to target detection- and response-related activity, and it also ensured that all sensory aspects of the displays were identical across changes in the size of the attentional field. The signal-to-noise ratio (SNR) of the SSVEP response was calculated on a trial-by-trial basis by dividing the power at the frequency bin centered on the stimulus frequency by the mean power in the two frequency bins 0.69 Hz above and below the center frequency of 21.25 Hz (corresponding to two bins on either side of the center frequency) and 0.68 Hz above and below the center frequency of 28.33 Hz. This SNR metric has been used in previous SSVEP studies (Bridwell and Srinivasan, 2012; Kim and Verghese, 2012; Bridwell et al., 2013; Garcia et al., 2013), and we focused on analyzing the SNR rather than the raw power/amplitude of the SSVEP to ensure that the modulations of the SSVEP were not confounded by any changes in broadband power at β frequencies.

The five electrodes in each subject with the highest median SNR computed across all stimulus contrast levels and attentional conditions at each stimulus frequency and each stimulus location were then defined as electrodes of interest [EOIs; see Fig. 3*A*, bottom; see similar methods in the studies by Itthipuripat et al. (2013) and Müller et al. (2003)]. The EOI approach strengthens the power of our analysis due to a slight variation of SSVEP topography across subjects. Also, the selection of EOIs based on data collapsed across focused- and distributed-attention conditions and across all contrast levels avoids biasing our analysis to favor either one of the alternative patterns of gain (i.e., response or contrast gain). The median SNR in each set of EOIs was then computed for each stimulus contrast level to construct contrast response functions separately for attended and ignored stimuli in the focused and distributed conditions (see Fig. 4).

To quantitatively examine the pattern of gain (either response or contrast gain) separately for the focused and distributed conditions, the grand-averaged SSVEP contrast response functions obtained across all subjects were fit with a Naka–Rushton equation (Geisler and Albrecht, 1997):

$$R(c) = a(c^n/[c^n + C_{50}^n]) + b \quad (1)$$

where R is the magnitude of the SSVEP response as a function of contrast (c), a is a response amplitude parameter (multiplicative gain factor), C_{50} is the semisaturation constant (the contrast value at half the maximum response), n is an exponent that determines the slope of the contrast response function, and b is the baseline response level. In this analysis, b was defined as the lowest SNR of each data set, and n was fixed at 2 (see Herrmann et al., 2010; Carandini and Heeger, 2011). Then, a and C_{50} were estimated using MATLAB's fminsearch function. The fitting procedure was constrained under the assumption that the CRF reaches asymptote before or at the maximal contrast. This constraint was implemented to ensure that the amplitude parameter did not exceed the maximum SSVEP response and the semisaturation constant did not vary outside the range of contrast values that were used in the present experiment (1–90% contrast).

A bootstrapping procedure was then performed to assess significant differences between conditions and to establish 95% confidence intervals on the best fitting model parameters (see Fig. 4*C*,*E*,*G*). First, we resampled EEG trials with replacement for each individual subject. Next, we averaged the resampled trials across subjects to generate a CRF for each experimental condition, and then we fit the averaged CRFs to generate an estimate of a and C_{50}. This resampling and fitting procedure was then repeated 10,000 times to create bootstrapped distributions from which confidence intervals associated with each parameter (a and C_{50}) were computed. To evaluate the interaction between attention field size (focused/distributed) and the locus of attention (attended/ignored) on the model parameters, we compiled bootstrapped distributions of the differences between the estimated fit parameters in the focused-attention condition and the distributed-attention condition, i.e., (focused: attended $-$ ignored) $-$ (distributed: attended $-$ ignored), and computed the percentage of values in the tail of this distribution that were greater or less than zero. Then, post hoc comparisons were performed to test for additional differences between pairs of conditions by evaluating bootstrapped distributions of differences and then computing the percentage of the values in the tails of these distributions that were greater or less than zero. We used two-tailed statistical tests to be conservative and because the NMA does not make specific predictions about the influence of attention field size on CRFs associated with ignored stimuli (Reynolds and Heeger, 2009). All p values associated with post hoc comparisons were Bonferroni corrected, resulting in a corrected threshold for eight comparisons of $\alpha < 0.0063$ (two tailed).

fMRI subjects. fMRI data were obtained from five neurologically healthy human subjects (21–31 years old, three females), three of whom participated in the main EEG experiments. All subjects signed an informed consent form approved by the Institutional Review Board at UCSD and participated in the study for monetary compensation of $20 per hour. Each subject participated in a 2 h scanning session to acquire fMRI for the experimental task, high-resolution anatomical images, and functional localizer scans. Retinotopic mapping for all subjects was carried out in a separate session using standard procedures (Engel et al. 1994; Sereno et al., 1995).

fMRI task design. We conducted this control fMRI experiment to independently verify that the manipulation of attentional field size success-

fully modulated the spatial extent of activation in early visual areas. The protocol and stimulus parameters of the fMRI version of the experiment were similar to the main EEG experiment (see above, EEG task design), except that the auditory cue was replaced by a colored arrow cue (red or blue), there was only one attention strategy used on each trial, and the stimulus flicker frequency was either 20 or 30 Hz (which was limited by the 60 Hz refresh rate of the projector and varied only slightly from the 21.25 and 28.33 Hz flicker rates used in the EEG study). Stimuli were front-projected on a screen (90 cm width), located 380 cm from the subject's eyes. The stimulus contrast was fixed at 20.3%, the contrast level at which SSVEP responses reached about half of their maximal response. The gray nontarget stimulus disk (radius, 0.60°) was flickered in an area with a radius of 2.00°. The spatial extent of the target stimulus in the focused-attention condition and the distributed-attention conditions were 0.93° and 2.65° in radius, respectively. Note that the stimulus parameters used in the fMRI study are smaller than those in the EEG study, which was caused by a limited visible screen area due to the narrow scanner bore. However, the respective ratio of the stimulus parameters across conditions are closely matched to those used in the EEG study.

Each trial started with an arrow cue pointing to the left or the right side of the visual field (duration, 2 s), instructing subjects to covertly shift their attention to the left or the right (with equal probability). Subjects applied the focused- and distributed-attention strategies when the arrow cue was red and blue, respectively. The flickering nontarget disks then appeared in the left and right lower visual fields at 20 and 30 Hz, respectively (and vice versa on one-half of the trials) for 3 s, followed by a passive-fixation ITI of 3 s. Each run contained 12 focused-attention nontarget trials, 12 distributed-attention nontarget trials, 4 focused-attention target trials, 4 distributed-attention target trials, and 5 null trials (null trial duration, 8 s of passive fixation) in pseudorandomized order. Each subject completed 9–10 runs of the main fMRI experiment.

fMRI functional localizer task. Subjects also performed two runs of a functional localizer task to identify voxels that were visually responsive to the portion of the visual field subtended by the maximum area over which a target stimulus could be presented during the distributed-attention condition in the fMRI main task (radius, 2.65°). Note that the size of the localizer stimulus is larger than the region over which the flickering nontarget disks were presented (i.e., the stimulus drive had a radius, 2.00°; see respective ratio in Fig. 2*A*). Subjects maintained fixation while covertly attending to a single flickering circular checkerboard with 100% contrast that was alternately presented in the left and right stimulus locations for 12 s/trial. Subjects responded with a button press when they perceived a brief and small contrast change in the checkerboard; contrast detection targets could appear between one and three times per 10 s trial.

fMRI retinotopic mapping procedure. Striate and extrastriate visual areas (V1, V2v, V3v, V2d, V3d) were defined by standard retinotopic mapping procedures (using a rotating counterphase flickering checkerboard), and the data were projected onto a computationally inflated gray/white matter boundary surface reconstruction for visualization (Engel et al. 1994; Sereno et al., 1995).

fMRI data acquisition, preprocessing, and analysis. All subjects were scanned on a 3T GE MR750 scanner at the Center for Functional magnetic Resonance Imaging at UCSD. Functional images were collected using a gradient EPI pulse sequence and a 32-channel head coil (Nova Medical), except one subject with whom an 8-channel head coil was used. Functional acquisition parameters were otherwise identical (19.2 × 19.2 cm FOV, 64 × 64 matrix size, 35 3-mm-thick slices with 0 mm gap, TR = 2000 ms, TE = 30 ms, 90° flip angle), yielding a voxel size of 3 × 3 × 3 mm. We acquired axial slices that covered the entire occipital cortex. In addition, we obtained a high-resolution anatomical scan (fast spoiled gradient-recalled-echo T1-weighted sequence, TR = 11 ms, TE = 3.3 ms, TI = 1100 ms, 172 slices, 18° flip angle, 1 mm^3 resolution). EPI images were first unwarped using the FMRIB Software Library (Oxford, UK). Then, BrainVoyager 2.3 (Brain Innovations) was used to perform slice-time correction, 3D motion correction, temporal high-pass filtering (three cycles per run), and transformation into Talairach space.

In the main analysis, we first used a general linear model (GLM) to identify voxels that showed a significant response to contralateral versus ipsilateral epochs of visual stimulation during the independent functional localizer task [single-voxel false discovery rate (FDR)-corrected threshold, $p < 0.05$]; voxels showing a significant response in each were then retained for further analysis in the main experimental Next, we ran a GLM with eight regressors (focused attention left, foc attention right, distributed attention left, distributed attention righ., ., cused attention left target trial, focused attention right target trial, distributed attention left target trial, and distributed attention right target trial) on each retained voxel in each visual area. Note that in the main fMRI task, we only analyzed the nontarget trials to keep the stimulus drive fixed across the focused and distributed conditions and to prevent possible confounds from target-evoked sensory responses, decision processes, and/or motor-related processes. Each regressor was constructed by convolving a boxcar model of the stimulus sequence with the standard difference-of-two-gamma function hemodynamic response function model implemented in Brain Voyager. We then preformed *t* tests on the resulting beta weights to assess the proportion of voxels in each visual area that showed a significant response on trials where attention was directed to the contralateral visual field. A sign test was then performed to determine whether the number of visual areas in which more voxels were significantly active in the distributed condition (compared to the focused condition) was different from the number of areas expected by chance. Since these areas are retinotopically mapped, a higher proportion of significant voxels in one condition compared to another should translate into a larger spatial extent of activation, allowing us to infer changes in the relative size of the attention field. To ensure that the results were not biased by the exact choice of a single-voxel statistical threshold, we used three *p* values, $p < 0.10$, $p < 0.05$, and $p < 0.01$, all FDR corrected. We also repeated this analysis across a large range of statistical thresholds (a range of *t* values from −1 to 10; see Fig. 5*B*). At each point in these cumulative plots, we computed the percentage of voxels within each unilateral ROI (30 ROIs total) with *t* values exceeding each *t* threshold. At each *t* threshold, we then compared whether more ROIs had more voxels active during the distributed-attention condition compared to the focused-attention condition than would be expected by chance using a sign test, correcting for multiple comparisons using FDR ($p < 0.05$).

Finally, we examined the response in all voxels within each localizer-defined ROI to determine whether the least active voxels in the focused-attention condition became more active in the distributed-attention condition. We sorted voxels from each ROI into 20 evenly spaced bins based on the β coefficient corresponding to the focused-attention condition. Next, we computed the average response across all voxels within each of the 20 bins on both focused- and distributed-attention trials. We then evaluated, for each bin, whether average betas increased in more ROIs than would be expected by chance using a sign test (corrected for multiple comparisons at an FDR threshold of $p < 0.05$).

Additional model simulations. Since EEG measurements are presumably influenced by distributed activity across visual areas with different RF sizes, we modified the NMA as written by Reynolds and Heeger (2009) to use the exact stimulus/task parameters used in the EEG study (for model parameters, see Table 1) and constrained the simulation of RF sizes in each modeled visual area based on estimates from monkey neurophysiology (Gattass et al., 1981, 1988; Freeman and Simoncelli, 2011). The stimulus is assumed to have a Gaussian shape. This is consistent with the fact that the potential location of the small nontarget disk is randomly drawn from a nonuniform distribution, with higher probability associated with the disk appearing near the center of the stimulus window than near the edges, similar to a Gaussian. The attention field, excitatory field, and suppressive field are also assumed to have Gaussian shape similar to the original NMA (Reynolds and Heeger, 2009). Given the eccentricity of our stimuli in the EEG experiment (8.58°), the RF sizes were fixed at V1 = 1.46°, V2 = 4.33°, and V4 = 6.86° (Gattass et al., 1981, 1988; Freeman and Simoncelli, 2011). In the RF-size-constrained model, the size of the excitatory field was set equal to the estimated RF size of neurons in each region. The bandwidth of the suppressive field is set to be two times larger than the stimulation field (Cavanaugh et al., 2002); thus the size of the suppressive field is linearly scaled with the RF size. We convolved the excitatory field with the stimulus (E) and applied the attentional field (A) via multiplication to estimate the stimulus drive as enhanced by attention (AE). Then, we convolved the suppressive field

Table 1. Model parameters used in Figure 1*A–E*

			Attention field size (in degrees)		Receptive field size (in degrees)			Suppressive field size (in degrees)		
	label	Stimulus size (in degrees)	Focused	Distributed	V1	V2	V4	V1	V2	V4
..		4.90	2.04				6.86			13.72
B		4.90		6.54			6.86			13.72
C		4.90	2.04	6.54	1.46	4.33	6.86	4.94	8.66	13.72
D		1.20	2.04	6.54	1.46	4.33	6.86	4.94	8.66	13.72
E		4.90	2.0 to 6.5 in 0.5 steps				6.86			13.72

with *AE* (the stimulus drive that is already enhanced by attention) to generate the suppressive drive (*S*). Finally, we divided *AE* by *S* to generate a predicted population response. The model predicts similar patterns of gain modulation across all simulated visual areas (Fig. 1*C*). Specifically, in the focused-attention condition, there is clear response gain pattern (i.e., attention enhances already strong responses). These enhanced responses are normalized when the attention field becomes larger, resulting in a pattern resembling contrast gain in the distributed-attention condition. The observation of similar effects in all areas is particularly relevant as our scalp recorded SSVEP signals likely reflect the combined activity across several early visual areas in occipital cortex.

Although the SSVEP signals that we measure reflect oscillatory activity evoked by stimuli spanning the entire stimulus drive (4.9°), we also considered a model in which the stimulus drive consisted of a single presentation of a 1.2° nontarget disk (Fig. 1*D*). Under these conditions, the NMA still predicts the same general shift from relatively more response gain to relatively more contrast gain as the size of the attention field increases. Note that the simulation parameters in Figure 1*D* are the same as *C*, except that the stimulus is 1.2° in radius and has a square-wave shape (consistent with the shape of the small disk used in the EEG experiment). We also ran the stimulation (using the parameters from V4) in which the stimulus size is fixed at 4.9° but the size of the attention field varies from 2.0° to 6.5° consecutively in 0.5° steps (Fig. 1*E*). The model simulation predicts that as the size of the attention field increases, response gain will decrease and contrast gain will increase in a continuous manner. This highlights the importance of the relative size between the attention field and stimulus drive, and a shift from response to contrast gain should be observed as long as the size of the attention field increases and the stimulus drive remains constant.

Results

Behavioral results

Subjects' accuracy during the EEG experiment significantly improved (Fig. 2*C*, left; $F_{(5,30)} = 128.547$, $p < 0.001$), and reaction times (RTs) on correct trials significantly decreased as a function of stimulus contrast (Fig. 2*C*, right; $F_{(4,24)} = 18.151$, $p < 0.001$). Although accuracy was unaffected by changes in the spatial scope of attention, subjects responded more slowly in the distributed condition than in the focused condition ($F_{(1,6)} = 7.159$ $p = 0.037$), consistent with the increased uncertainty of the target location. This selective influence of attention field size on RT, as opposed to accuracy, is consistent with our instructions that the subjects emphasize responding accurately.

SSVEP results

SSVEPs are well suited to evaluate the impact of changes in the spatial scope of attention on neural CRFs because they reflect synchronized activity pooled across neurons in visual cortex (Regan 1989; Rager and Singer, 1998; Srinivasan et al., 1999), and models such as the NMA make predictions regarding changes in the gain pattern of neural activity at the population level under the assumption that individual neurons in the population share a similar dependence on stimulus contrast (Reynolds and Heeger, 2009). In addition, previous research has established that SSVEP signals are influenced by attention and thus provide a sensitive measure to study patterns of sensory gain modulation (Müller et al., 1998a,b, 2003; Kim et al., 2007). Figure 3*A* shows the scalp topography of the grand-averaged SSVEPs collapsed across the focused- and distributed-attention conditions and all stimulus contrast levels. We obtained reliable SSVEP responses for both 21.25 and 28.33 Hz stimuli that peaked over posterior–occipital regions contralateral to the stimulus. Note that the attention effects (third row) were slightly less lateralized than the responses in each condition considered in isolation; this occurred because responses to attended stimuli not only had a higher SNR, but were also slightly broader in their spatial distribution. Since the peak distribution of SSVEP responses for each stimulus frequency assignment varied slightly across individuals, we selected five focal EOIs for each frequency from each observer for further analysis (collapsing across contrast levels; Fig. 3*A*, bottom; see Materials and Methods).

The grand-averaged SSVEPs are plotted as a function of stimulus contrast and attention in Figure 4*A*: the focused-attention condition yielded a pattern that qualitatively resembles response

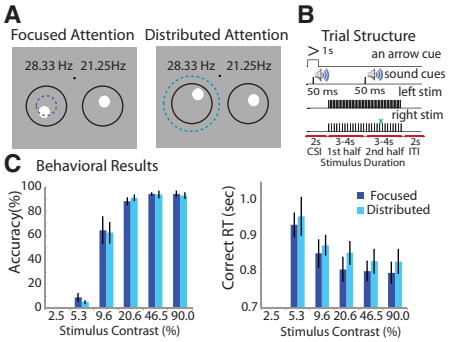

Figure 2. ***A***, The spatial attention task required either a focused- or distributed-attention strategy. In the focused-attention condition (left), the location of a small oriented-grating target was constrained to an area (a blue dotted ring, not shown in the actual display) that was smaller than the spatial extent of the nontarget disks (a black ring, not shown in the actual display). In the distributed-attention condition (right), the target could appear across a larger region of space (a cyan dotted ring, not shown in the actual display). ***B***, Trial structure. Each trial began with a 2 s arrow cue that instructed subjects to attend to either the left or the right stimulus, followed by a 50 ms auditory cue, and the pitch (high/low) instructed subjects to either adopt a focused- or distributed-attention strategy. A second auditory cue was then presented after a pseudorandomly selected interval of 3–4 s, and instructed the subjects to either maintain or switch their attention strategy. The small flickering nontarget disks in the lower left and lower right quadrants were updated at 21.25 and 28.33 Hz, respectively (or vice versa on one-half of the trials). The stimulus contrast was set to 2.5, 5.3, 9.6, 20.6, 46.5, or 90.0% on each trial. The ITI was 2 s. No target was presented on 75% of the trials, and these nontarget trials formed the basis for all subsequent analyses of the EEG signal. On the remaining 25% of the trials, a single square-wave grating target stimulus could appear briefly for 11.7 ms (green cross, bottom) in the first half of the trial, in the second half of the trial, or in both. ***C***, Behavioral accuracy (left) and reaction times for correct trials (right) as a function of stimulus contrast. Note that no correct responses were made when at the 2.5% contrast level, as the stimuli were nearly invisible. All error bars are ±1 SEM across subjects.

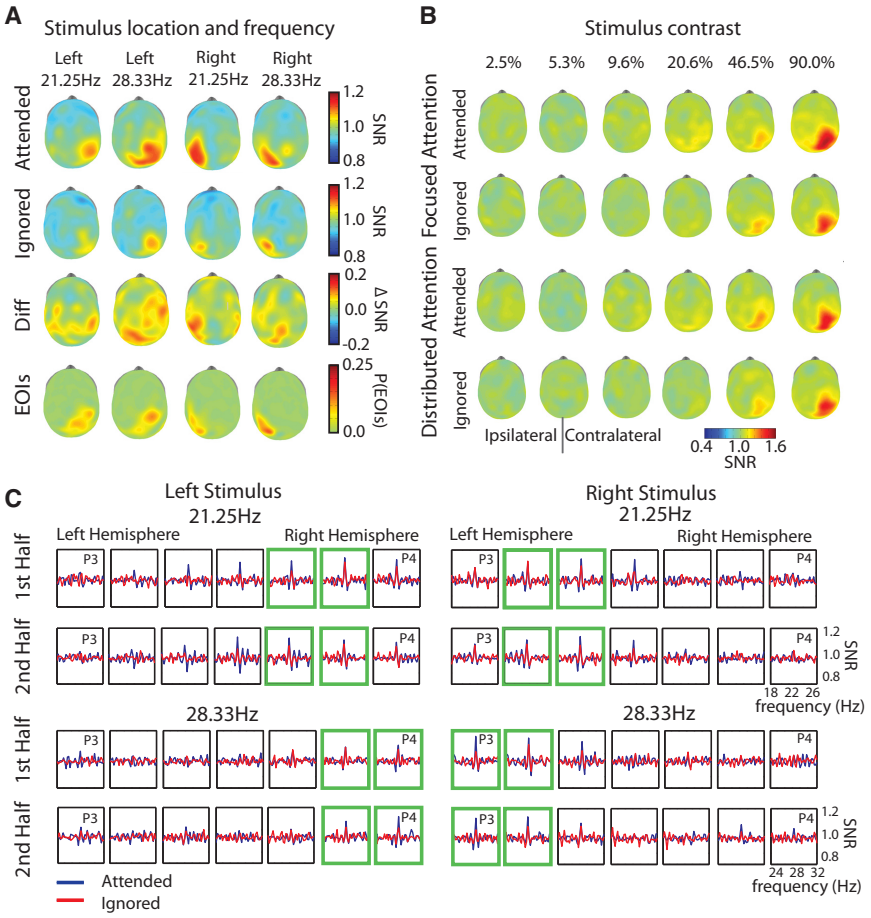

Figure 3. ***A***, Topographies of the grand-averaged SNR of the SSVEPs, collapsed across focused- and distributed-attention conditions, the first half and the second half of the trial, and all stimulus contrast levels. SSVEPs for attended (first row) and ignored (second row) stimuli peaked at posterior occipital sites contralateral to the stimulus that evoked the response. Attention boosted the SNR of the SSVEPs (third row). Five focal electrodes were selected separately for each frequency assignment and each stimulus location as EOIs. The fourth row shows the probability of each electrode being included as an EOI across all subjects. ***B***, Topographical maps for each attention condition and each stimulus contrast level. The plot is collapsed across stimulus frequencies and stimulus locations. The left half and the right half of the head model correspond to electrodes ipsilateral and contralateral to the stimulus location, respectively. Consistent with the main CRF results (Fig. 4), the SNR of the SSVEP increases as a function of stimulus contrast. In the focused-attention condition, the response at the highest contrast level is most enhanced by attention. In contrast, responses to high-contrast stimuli are relatively attenuated in the distributed-attention condition, and response enhancement is most evident at midlevel contrasts instead. ***C***, Posterior–occipital view of the grand-averaged SNR of the SSVEPs for each stimulus frequency assignment during the first and second halves of the trial. Data were collapsed across focused- and distributed-attention conditions and across all stimulus contrast levels. Blue and red lines show the response to attended and ignored stimuli, respectively. For each frequency assignment, there are clear SSVEPs that are sharply tuned to the flicker frequency of each stimulus and that peak in posterior–occipital electrodes contralateral to the stimulus location. Green boxes highlight sets of electrodes that responded robustly to stimuli in each location and stimulus frequency assignment.

gain (left), and the distributed-attention condition yielded a pattern that qualitatively resembles contrast gain (right). As an initial evaluation of attention-related differences between the CRFs shown in Figure 4*A*, we performed a three-way repeated-measures ANOVA. There was a significant main effect of the locus of attention (response to attended versus ignored stimulus, $F_{(1,6)} = 15.287$, $p = 0.008$), a main effect of stimulus contrast ($F_{(5,30)} = 12.573$, $p < 0.001$), and an interaction between the locus of attention and stimulus contrast ($F_{(5,30)} = 6.584$, $p < 0.001$). In addition, there was a significant three-way interaction between the size of the attention field, the locus of attention, and stimulus contrast ($F_{(5,30)} = 8.972$, $p < 0.001$), demonstrating that changes in the size of the attention field lead to different patterns of CRF modulation. This pattern can also be qualitatively seen in the scalp distribution of the SSVEP SNR (Fig. 3*B*). Importantly, this pattern of results was reproduced when data from the first half (Fig. 4*D*) and the second half (*F*) of each trial were analyzed separately. Specifically, there was a significant main effect of the locus of attention (first half, $F_{(1,6)} = 9.690$, $p = 0.021$; second half, $F_{(1,6)} = 22.184$, $p = 0.003$), a main effect of stimulus contrast

(first half, $F_{(5,30)} = 10.345$, $p < 0.001$; second half, $F_{(5,30)} = 13.087$, $p < 0.001$), an interaction between the locus attention stimulus contrast (first half, $F_{(5,30)} = 3.878$, $p = 0.011$; second half, $F_{(5,30)} = 3.881$, $p = 0.008$), and an interaction between the size of attention field, the locus of attention, and stimulus contrast (first half, $F_{(5,30)} = 4.213$, $p = 0.005$; second half, $F_{(5,30)} = 3.869$, $p = 0.008$). Note that consistent results were observed when raw SSVEP amplitudes were analyzed as opposed to SNR (data not shown).

Although the ANOVA presented above confirms that there is an effect of attention field size on the CRFs, it does not directly address the selectivity of changes in terms of response or contrast gain. Therefore, we next fit a Naka–Rushton equation (Eq. 1) to the CRFs associated with each condition to evaluate the influence of attention field size on response gain (as indexed by the response amplitude model parameter, a; Fig. 4*C*, left) and contrast gain (as indexed by the semisaturation constant model parameter, C_{50}; Fig. 4*C*, right).

Using a bootstrapping procedure (see Materials and Methods), we found a significant two-way interaction between the size of the attention field and the locus of attention on the response amplitude parameter, a ($p < 0.0001$; Fig. 4*C*, left). This two-way interaction was primarily driven by higher response amplitude for attended compared to ignored stimuli in the focused-attention condition ($p < 0.0001$; this and all other p values associated with *post hoc* pairwise comparisons are Bonferroni corrected with $\alpha < 0.0063$), but not in the distributed-attention condition [not significant (n.s.), $p = 0.3986$]. We also observed higher response amplitude for attended stimuli in the focused-attention condition compared to the distributed-attention condition ($p = 0.0026$; Fig. 4*C*, left, compare dark blue, cyan bars). Finally, there was no significant difference in the response amplitude for ignored stimuli across the focused- and distributed-attention conditions (n.s., $p = 0.0448$; Fig. 4*C*, left, compare red, orange bars).

As shown in the right panel in Figure 4*C*, right, we also found a significant two-way interaction between the size of the attention field and the locus of attention on the semisaturation contrast parameter C_{50} ($p = 0.0021$). The interaction was primarily driven by a significant decrease in C_{50} for attended compared to ignored stimuli in the distributed-attention condition ($p = 0.0010$) and no difference in

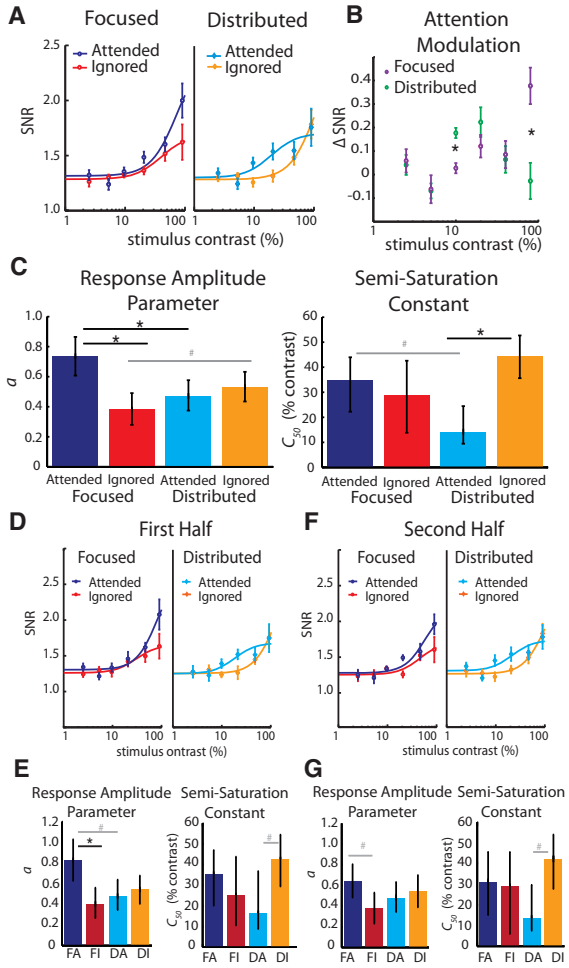

Figure 4. ***A***, CRFs based on the grand-averaged SNR ($N = 7$) associated with attended and ignored stimuli separately for the focused-attention (dark blue for the attended stimulus, red for the ignored stimulus) and distributed-attention conditions (cyan for the attended stimulus, orange for the ignored stimulus). The continuous curves represent fits based on a Naka–Rushton equation (see Materials and Methods). In the focused-attention condition, R^2 was 0.958 and 0.989 for attended and ignored responses, respectively. In the distributed-attention condition, R^2 was 0.835 and 0.987 for the attended and ignored responses, respectively. Focused attention led to a pattern of response gain (left), and distributed attention led to a pattern of contrast gain (right). ***B***, The attentional modulation for focused and distributed conditions (the difference between the data shown in left and right panels in ***A***) Asterisks indicate significant differences as assessed with by *post hoc t* test with Bonferroni correction for multiple comparisons (both $t_{(6)}$ values > 3.901; p values < 0.00833, two-tailed). ***C***, Results from the bootstrapping analysis demonstrating changes in the response amplitude parameter, a (left), and the semisaturation contrast, C_{50} (right), as a function of the size of the attention field and the locus of attention. The interaction between the size of the attention field and the locus of attention are significant for both a and C_{50}, with more pronounced response gain in the focused-attention condition and more pronounced contrast gain in the distributed-attention condition. ***D***, ***F***, Similar results were observed when data from the first half (***D***) and the second half (***F***) of each trial were analyzed separately. ***E***, ***G***, Pattern of results was also observed when data from the first half (***E***) and the second half (***G***) of each trial were analyzed separately. FA, Focused attended; FI, focused ignored; DA, distributed attended; DI, distributed ignored. For ***C***, ***E***, and ***G***, asterisks indicate significant differences as assessed with *post hoc* comparisons (Bonferroni corrected for 8 comparisons, all p values < 0.0063, two-tailed). Hash marks indicate differences without Bonferroni correction (all p values < 0.05). Error bars in ***A***, ***B***, ***D***, and ***F*** are ± 1 SEM across subjects. All error bars in ***C***, ***E***, and ***G*** represent 95% confidence intervals of the bootstrap distributions.

C_{50} between attended and ignored CRFs in the focused-attention condition (n.s., $p = 0.5302$). No significant differences were observed for attended stimuli in the focused-attention condition compared to the distributed-attention or for ignored stimuli in the focused-attention condition compared to the distributed-attention (n.s., $p = 0.0146$ and $p = 0.0642$, respectively).

Overall, these results demonstrate that the CRFs associated with attended stimuli undergo response and contrast gain in the focused-attention and distributed-attention conditions, respectively. Importantly, a similar pattern of amplitude and semisaturation parameters were observed when data from the first half (Fig. 4*E*) and the second half (*G*) of each trial were analyzed separately. Specifically, the interaction between the size of the attention field and the locus of attention is significant for both *a* (first half, $p = 0.0018$; second half, $p = 0.0225$) and C_{50} (first half, $p = 0.0147$; second half, $p = 0.032$), with more pronounced response gain in the focused-attention condition and more pronounced contrast gain in the distributed-attention condition.

fMRI results

To independently determine whether the spatial scope of attention was larger in the distributed compared to the focused-attention condition, we performed a control study using fMRI to examine the extent of activation within retinotopically mapped regions of early visual cortex. We tested two complementary predictions. First, we predicted that more voxels overall would be significantly active in the distributed compared to the focused-attention condition. Given that these areas are retinotopically organized, a higher proportion of significantly active voxels should correspond to a larger area of the visual field. Second, we reasoned that voxels showing the least activation in the focused-attention condition should undergo a relatively large increase in activation in the distributed-attention condition (compared to voxels that already showed a high activation level in the focused-attention condition). Again, this prediction is based on the retinotopic organization of these areas: voxels with spatial receptive fields near the center of the stimulus should respond strongly in both the focused and the distributed conditions, whereas voxels with a spatial receptive field that is farther from the center of the stimulus should respond more in the distributed compared to the focused-attention condition. Note that the first prediction concerns only voxels that show a significant positive response (i.e., does the total spatial extent of voxels passing a fixed threshold change with attentional demands?). In contrast, the second prediction concerns systematic changes in the responses of all voxels within a visual area, regardless of whether their responses are significantly higher than baseline in any given condition.

With respect to the first prediction, we observed a higher proportion of significant voxels in the distributed-attention condition compared to the focused-attention condition across most localizer-defined regions of V1, V2, and V3 (at an individual-voxel FDR-corrected threshold of $p < 0.05$; Fig. 5*A*, middle; 23 of 30 areas had a higher proportion of active voxels in the distributed compared to the focused-attention condition, where left and right V1, V2, and V3 were considered separately for each subject; $p < 0.005$ by sign test). Similar results were also obtained at FDR-corrected individual-voxel thresholds of $p = 0.10$ (Fig. 5*A*, left) and $p = 0.01$ (Fig. 5*A*, right), indicating that the result does not just reflect a thresholding artifact (all p values < 0.01 by sign test; Fig. 5*B*, results showing the higher proportion of voxels in the distributed- compared to focused-attention conditions across a wider range of t thresholds). Similar results were also observed when only responses in area V1 were considered. Note that only about ~40–50% of voxels were significant across the focused- and distributed-attention conditions. This is consis with the fact that the contrast of the stimulus used in the r fMRI experiment (20.03%) was lower than the contrast o localizer stimulus (100%), and the area of stimulation was also smaller than the size of the localizer (see Materials and Methods). Finally, note that for all analyses we first removed the mean of the BOLD response across the entire brain on a volume-by-volume basis, so the differences between the focused and distributed conditions in unlikely to be related to changes in global activation levels associated with general arousal. In addition, Figure 5*C* shows representative activation maps from two subjects who participated in both the EEG and fMRI experiments. In the distributed-attention condition, there is a visibly broader patch of activation on the cortical sheet in left/right V1, V2d, and V3d compared to the focused-attention condition (Figure 5*C*, orange–yellow color represents significance above baseline; $p < 0.05$, FDR corrected).

We next tested our second prediction that the least active voxels in the focused-attention condition should undergo the largest positive change in the distributed-attention condition. To assess this possibility, we examined the response in all voxels within each localizer-defined ROI to determine whether the least active voxels in the focused-attention condition became more active in the distributed-attention condition (as we would predict if the spatial scope of attention increased). We first sorted voxels in left and right V1, V2, and V3 from low to high based on β values (i.e., the GLM-estimated response magnitude) in the focused-attention condition. Because each participant had a different number of voxels in each ROI, we evenly sorted the data from each ROI into 20 bins. Then, we compared the averaged β values for voxels in each bin across the focused- and distributed-attention conditions (Fig. 5*D*). Across all subjects, voxels with relatively low activation (low β values) in the focused-attention condition showed significantly higher activation in the distributed-attention condition (Figs. 5*D*, far left bins marked by a red asterisks; $p < 0.05$, sign test across participants and visual areas, FDR-corrected). In contrast, voxels with higher activation in the focused-attention condition underwent a smaller change with attentional strategy (the far right bins; Fig. 5*E*, individual subject panels). Note that the modulation is primarily in voxels that have either negative or low positive β weights; however, the sign of the weight is only relevant with respect to the passive-fixation null trials (Stark and Squire, 2001), and so any increase (in this case, β values becoming less negative) is consistent with a more diffuse spatial response profile in the distributed-attention condition. In addition, note that the large response increases in voxels with a low β weight is not inconsistent with the data presented in Figure 5*A*, as the data in Figure 5*A* simply indicate that more total voxels fall above an FDR-corrected threshold in each condition (i.e., a small percentage of voxels shift from nonsignificant to significant when attention is diffuse). Thus, these two analyses provide consistent and complementary evidence that the spatial scope of attention changed as a function of our task instructions.

Discussion

Over the last several decades, spatial attention has been shown to modulate the contrast response functions of neurons in visual cortex in many different ways, with some studies suggesting response gain, others suggesting contrast gain, and still others suggesting a combination of both (McAdams and Maunsell, 1999; Reynolds et al., 1999, 2000; Di Russo et al., 2001; Martínez-

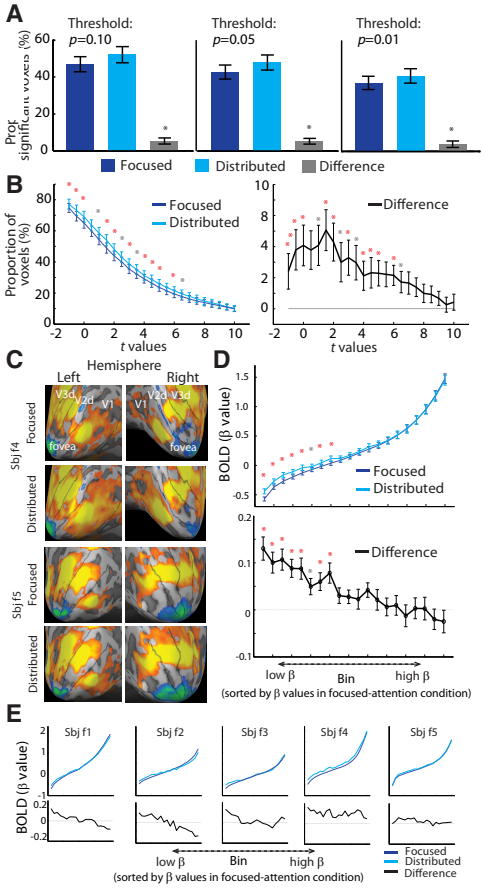

Figure 5. fMRI results independently address how the distributed-/focused-attention manipulation changed the spatial extent of activation in retinotopically organized regions of early visual cortex. ***A***, At an individual voxel threshold of $p = 0.05$ (FDR corrected) for determining a significant response (middle), we observed a higher proportion of significant voxels in the distributed-attention condition compared to the focused-attention condition across most V1, V2, and V3 regions of interest ($p < 0.005$ by sign test). Similar results were also obtained at FDR-corrected individual voxel thresholds of $p = 0.10$ (left) and $p = 0.01$ (right), indicating that the result does not just reflect a thresholding artifact (all p values < 0.01, sign test). Given that these areas are retinotopically organized, a higher proportion of voxels should translate into a broader spatial representation across the cortical surface in the distributed-attention condition. ***B***, The higher proportion of voxels in the distributed-attention condition compared to the focused-attention condition across V1, V2, and V3 was also observed across a wide range of t thresholds. ***C***, Representative activation maps from two subjects. In the distributed-attention condition, there is a visibly broader patch of activation on the cortical sheet in left/right V1, V2d, and V3d compared to the focused-attention condition (orange–yellow color represents significant voxels above the baseline; $p < 0.05$, FDR corrected). These data illustrate the effects reported in ***A*** and demonstrate that the experimental manipulation led to a larger attention field in the distributed-attention compared to the focused-attention condition. Critically, since the stimulus drive in our experiment was always fixed and the size of the attention field is larger in the distributed condition compared to the focused condition, the NMA predicts higher response gain and lower contrast gain in the focused condition compared to the distributed condition (see Fig. 1*A–E*, model simulations). ***D***, Voxels in left and right V1, V2, and V3 were sorted by the β values for the focused-attention condition (low to high) and evenly divided into 20 bins. The averaged β values for the focused- and distributed-attention conditions were compared across these 20 bins (left). Voxels with low activation in the focused-attention condition underwent a significant increase in activation in the distributed condition, but those with higher activation did not. The difference between the β values for distributed and focused conditions was significant (above zero) for bins with low β values, but not in bins with higher β values (bottom), suggesting that the spatial pattern of activity in the distributed condition is more diffuse compared to the focused condition. ***E***, The sorted β results (same as ***D***) in individual subjects. Red asterisks in ***B*** and ***D*** indicate significance, as determined by sign tests ($p < 0.05$, FDR corrected). Gray asterisks indicate uncorrected difference. Error bars in all figures are ± 1 SEM across all unilateral regions of interest from each subject (left/right V1, V2, and V3; 30 total ROIs).

Trujillo and Treue, 2002; Williford and Maunsell, 2006; Buracas and Boynton, 2007; Kim et al., 2007; Murray, 2008; Lee and Maunsell, 2009, 2010a,b; Carrasco 2011; Pestilli et al., 2011; Serences, 2011; Andersen et al., 2012; Fig. 1). In turn, the heterogeneous pattern of neural modulation is consistent with the wide variety of gain patterns inferred using psychophysical methods (Morrone et al., 2002, 2004; Carrasco et al., 2004; Ling and Carrasco 2006; Pestilli et al., 2007, 2009).

Previously, the NMA (Lee and Maunsell, 2009, 2010b; Reynolds and Heeger, 2009) offered a potential solution as to how these apparently inconsistent attentional gain patterns might arise via changes in the relative size of the stimulus and the attention field. The NMA generates the output of sensory neurons by multiplying the stimulus drive (E) from the classical excitatory RF with the attention field (A). This combined influence of the stimulus drive and attention (AE) is then divided by the suppressive drive (S), obtained from the convolution between AE and the nonclassical inhibitory receptive field. Given a fixed size of E and S, the size of the attention field (A) relative to the stimulus drive (E) will influence the pattern of gain of the modeled population responses. For example, an attention field smaller than the stimulus drive (focused attention) will lead to response gain because attentional gain enhances the entire stimulus drive, but only enhances the center of the suppressive field. In contrast, an attention field larger than the stimulus drive (distributed attention) will lead to contrast gain because attentional gain is applied equally to the stimulus drive and suppressive field. Consistent with this prediction, a *post hoc* survey of previous studies suggests that different patterns of gain modulation may be due to changes in the size of the attention field (Table 2). For example, Reynolds et al., 2000 used a large rectangular cue to direct animals' attention to a location that contained a smaller target stimulus. This display may have induced a relatively large attention field with respect to the stimulus, which is consistent with the observation of pure contrast gain. In contrast, other studies instructed animals to attend to a peripheral stimulus that was located on either the left or the right side of a video display (Williford and Maunsell, 2006; Lee and Maunsell, 2010a). The same location was attended for a long sequence of trials, and no physical cue or placeholder was used to mark the target position. In this case, the size of the attention field may have closely matched (or been smaller than) the size of the target, which is consistent with the observation of response gain in many cells.

Here, we used EEG to monitor SSVEPs in human subjects performing an attentionally demanding task in which the spatial scope of attention was systematically manipulated (focused vs distributed attention) while keeping the spatial extent of visual stimulation constant across trials. We found that highly focused spatial attention primarily enhanced neural responses to high-contrast stimuli (response gain), whereas distributed attention primarily enhanced responses to medium-contrast stimuli (contrast gain). Together, these data suggest that different patterns of

Table 2. A *post hoc* survey of studies examining the influence of attention on the gain pattern of neural CRFs

Studies	Stimulus type/stimulus size (visual angle)	Attention field size relative to the stimulus	Observed gain modulation			Visual area(electrode pc
			Response gain	Contrast gain	Additive gain	
Single-unit studies (macaque electrophysiology)						
Reynolds et al. (2000)	Bar-shaped grating, 0.4 × 1.5–2°	Larger (a cue box larger than a stimulus)		X		V4
Martínez-Trujillo and Treue (2002)	Random dot motion/variable	Larger or equal (monitor two stimuli in the same hemifield)		X		MT
Williford and Maunsell (2006)	Garbor patch/variable	Smaller or equal (sustain attention to a long sequence of stimuli/a small cue at the center of stimulus location)	X	X	X	V4
Lee and Maunsell (2010a)	Garbor patch, ~0.51° mean SD of Gaussian envelope	Smaller or equal (sustain attention to a long sequence of stimuli)	X			MT
ScalpEEG studies (large-scale human electrophysiology)						
Di Russo et al. (2001)	Square-shaped grating, 9 × 9°	Smaller or equal (sustain attention to a long sequence of large stimuli)	X			Posterior occipital electrodes
Kim et al. (2007)	Circular grating, 2.45° in radius	Smaller or equal (sustain attention to the long sequence of stimuli)	X			Posterior occipital electrodes
The present study	Circular disk flickering in a large stimulation area of					
Focused attention	4.90° in radius	Smaller (2.04° in radius)	X			posterior occipital electrodes
Distributed attention	4.90° in radius	Larger (6.54° in radius)		X		
fMRI studies (large-scale human hemodynamic response)						
Buracas and Boynton (2007)	Circular grating, 3.00° in radius	Smaller or equal (monitor one stimulus in each hemifield)			X	V1, V2, V3, MT+
Murray (2008)	Circular grating, 3.00° in radius	Larger or equal (monitor two stimuli in the same hemifield)			X	V1, V2, V3
Pestilli et al. (2011)	Circular grating					
Focused attention	2.45° in radius	Smaller or equal (monitor one stimulus in a quadrant)			X	V1, V2, V3, hV4
Distributed attention	2.45° in radius	Larger or equal (monitor four stimuli in the entire visual field)			X	

A post hoc survey of past studies suggests that different patterns of gain modulation may be due to differences in the size of the attention field relative to the size of the stimulus. The criteria used to estimate whether the size of attention is smaller, larger, or equal to the stimulus drive, based on task manipulation and the nature of the display across different studies, are shown in the parenthesis in the third column. Note that the spatial scope of attention seems to have no effect on the gain pattern of the CRFs measured by hemodynamic responses, unlike other electrophysiological measures (see Discussion).

neural modulation do not reflect fundamentally different neural mechanisms, but instead reflect changes in the spatial scope of attention.

It is possible that, in the distributed-attention condition, subjects' attention might be captured by high-contrast ignored stimuli on the opposite side of the display, and the attention field might actually extend across the vertical meridian to the ignored stimulus. In turn, this spread of attention to high-contrast ignored stimuli might attenuate any amplitude modulation (i.e., the *a* parameter from the Naka–Rushton equation) in the distributed-attention condition. However, we view this scenario as unlikely for two reasons. First, the stimuli were presented in different hemifields, and the spatial separation was large even with respect to the size of the attention field in the distributed-attention condition. Second, this account predicts that behavioral response times should be inflated when the ignored stimulus was high contrast and thus more salient, but no such differential inflation of response times was observed (n.s., $F_{(1,6)} = 0.034$, $p = 0.86$; Fig. 2*C*, right).

Interestingly, although the two types of CRF modulation that we report here (contrast gain and response gain) are generally consistent with previous observations from electrophysiological (Reynolds et al., 2000; Di Russo et al., 2001; Martínez-Trujillo and Treue, 2002; Kim et al., 2007; Lee and Maunsell, 2009, 2010a,b; Andersen et al., 2012) and psychophysical studies (Morrone et al., 2002, 2004; Carrasco et al., 2004; Ling and Carrasco 2006; Pestilli et al., 2007, 2009), several studies have now reported that the BOLD response measured using fMRI shows a purely additive shift such that the effects of attention on the BOLD response are constant across contrast levels (Buracas and Boynton, 2007; Murray, 2008; Pestilli et al., 2011; Table 2). Some authors have suggested that this additive effect may be due to the BOLD response pooling activity across neurons that show different attention effects, which would result in an aggregate response that more closely resembles an additive shift as opposed to either contrast or response gain (Williford and Maunsell, 2006; Pestilli et al., 2011). However, the SSVEP signal that we measured in the present study also pools signals across large neural populations, but we observed contrast and response gain effects that more closely resemble patterns typically observed in single neurons (Reynolds et al., 2000; Martínez-Trujillo and Treue, 2002; Lee and Maunsell, 2009, 2010a,b). Thus, the present data suggest that the SSVEP and fMRI measurements may tap into at least partially different signals associated with attentional modulation in visual

cortex. One possibility is that BOLD and SSVEP responses are differentially influenced by factors other than stimulus-evoked neural activity. For example, BOLD signals are highly sensitive to both stimulus-evoked and non-stimulus-evoked activity (Kastner et al., 1999; McMains et al., 2007; Murray, 2008; Sirotin and Das, 2009). Thus, relatively high BOLD responses to the attended low-contrast (and also 0% contrast) stimuli in past fMRI studies (Buracas and Boynton, 2007; Murray, 2008; Pestilli et al., 2011) may be largely attributable to anticipatory activity that is not directly evoked by the stimulus. In contrast, SSVEP signals, by definition, reflect stimulus-driven neural responses that are selectively entrained at the stimulus frequency (Regan 1989; Srinivasan et al., 1999; Rager and Singer, 1998; Müller et al., 1998a,b, 2003; Kim et al., 2007). Future studies could use multimodal imaging techniques (e.g., combining scalp-EEG SSVEPs and fMRI) to further examine the relationship between results obtained using these two imaging modalities.

Previous single-unit recording studies measuring neural CRFs have reported both response and contrast gain, fueling a long-running debate about the mechanisms of selective attention (McAdams and Maunsell, 1999; Reynolds et al., 1999, 2000; Martínez-Trujillo and Treue, 2002; Williford and Maunsell, 2006; Lee and Maunsell, 2009, 2010a,b). Here, we show that these discrepant modulatory effects can each be observed, depending on changes in the spatial extent of attention. This interaction between the size of the attention field and the gain pattern of the SSVEP-derived neural CRFs is consistent with a prediction of the NMA (Lee and Maunsell, 2009, 2010b; Reynolds and Heeger, 2009): a small attention field will result in relatively more response gain, and a larger attention field will result in relatively more contrast gain, given a constant stimulus drive (Fig. 1). However, it is important to note that the NMA is intentionally agnostic about other aspects of attentional modulation, such as the relationship between the size of the attention field and responses evoked by ignored stimuli, which the model assumes to be very far away from the focus of attention. For example, we observed modest, albeit nonsignificant, modulations of CRFs associated with ignored stimuli (Fig. 4*C*), and a similar observation was also reported in a previous psychophysical study (Herrmann et al., 2010). Since the NMA does not explicitly specify the exact spatial function that governs the attention field (Reynolds and Heeger, 2009), future studies will be required to determine how changes in the size and/or shape of the attention field mediate interactions between attended and ignored stimuli across the extent of the visual scene. That said, the present demonstration that changes in the size of the attention field can lead to a shift from response to contrast gain supports a key prediction of the NMA, and the general theoretical framework can be expanded as justified by new data.

References

Andersen SK, Müller MM, Martinovic J (2012) Bottom-up biases in feature-selective attention. J Neurosci 32:16953–16958. CrossRef Medline

Brainard DH (1997) The psychophysics toolbox. Spat Vis 10:433–436. CrossRef Medline

Breakspear M, Heitmann S, Daffertshofer A (2010) Generative models of cortical oscillations: neurobiological implications of the Kuramoto model. Front Hum Neurosci 4:190. Medline

Bridwell DA, Srinivasan R (2012) Distinct attention networks for feature enhancement and suppression in vision. Psych Sci 23:1151–1158. CrossRef

Bridwell DA, Hecker EA, Serences JT, Srinivasan R (2013) Individual differences in attention strategies during detection, fine discrimination, and coarse discrimination. J Neurophysiol 110:784–794. CrossRef Medline

Buracas GT, Boynton GM (2007) The effect of spatial attention on contrast response functions in human visual cortex. J Neurosci 27:93–97. CrossRef Medline

Carandini M, Heeger DJ (2011) Normalization as a canonical neural computation. Nat Rev Neurosci 13:51–62. Medline

Carrasco M (2011) Visual attention: the past 25 years. Vision Res 51:1484–1525. CrossRef Medline

Carrasco M, Ling S, Read S (2004) Attention alters appearance. Nat Neurosci 7:308–313. CrossRef Medline

Cavanaugh JR, Bair W, Movshon JA (2002) Nature and interaction of signals from the receptive field center and surround in macaque V1 neurons. J Neurophysiol 88:2530–2546. CrossRef Medline

Di Russo F, Spinelli D, Morrone MC (2001) Automatic gain control contrast mechanisms are modulated by attention in humans: evidence from visual evoked potentials. Vision Res 41:2435–2447. CrossRef Medline

Engel SA, Rumelhardt DE, Wandell BA, Lee AT, Glover GH, Chichilnisky EJ, Shadlen MN (1994) fMRI of human visual cortex. Nature [Erratum (1994) 370:106] 369:525. Medline

Freeman J, Simoncelli EP (2011) Metamers of the ventral stream. Nat Neurosci 14:1195–1201. CrossRef Medline

Garcia JO, Srinivasan R, Serences JT (2013) Near real-time feature-selective neural modulation in human cortex. Curr Biol 23:515–522. CrossRef Medline

Gattass R, Gross CG, Sandell JH (1981) Visual topography of V2 in the macaque. J Comp Neurol 201:519–539. Medline

Gattass R, Sousa AP, Gross CG (1988) Visuotopic organization and extent of V3 and V4 of the macaque. J Neurosci 8:1831–1845. Medline

Geisler WS, Albrecht DG (1997) Visual cortex neurons in monkeys and cats: detection, discrimination, and identification. Vis Neurosci 14:897–919. CrossRef Medline

Heeger DJ (1992) Normalization of cell responses in cat striate cortex. Vis Neurosci 9:181–197. CrossRef Medline

Herrmann K, Montaser-Kouhsari L, Carrasco M, Heeger DJ (2010) When size matters: attention affects performance by contrast or response gain. Nat Neurosci 13:1544–1559. CrossRef

Itthipuripat S, Garcia JO, Serences JT (2013) Temporal dynamics of divided spatial attention. J Neurophysiol 109:2364–2373. CrossRef Medline

Kastner S, Pinsk MA, De Weerd P, Desimone R, Ungerleider LG (1999) Increased activity in human visual cortex during directed attention in the absence of visual stimulation. Neuron 22:751–761. CrossRef Medline

Kim YJ, Verghese P (2012) The selectivity of task-dependent attention varies with surrounding context. J Neurosci 32:12180–12191. CrossRef Medline

Kim YJ, Grabowecky M, Paller KA, Muthu K, Suzuki S (2007) Attention induces synchronization-based response gain in steady-state visual evoked potentials. Nat Neurosci 10:117–125. CrossRef Medline

Lee J, Maunsell JH (2009) A normalization model of attentional modulation of single unit responses. PLoS One 4:e4651. CrossRef Medline

Lee J, Maunsell JH (2010a) The effect of attention on neuronal responses to high and low contrast stimuli. J Neurophysiol 104:960–971. CrossRef Medline

Lee J, Maunsell JH (2010b) Attentional modulation on MT neurons with single or multiple stimuli in their receptive fields. J Neurosci 30:3058–3066. CrossRef Medline

Ling S, Carrasco M (2006) Sustained and transient covert attention enhance the signal via different contrast response functions. Vision Res 46:1210–1220. CrossRef Medline

Martínez-Trujillo J, Treue S (2002) Attentional modulation strength in cortical area MT depends on stimulus contrast. Neuron 35:365–370. CrossRef Medline

McAdams CJ, Maunsell JH (1999) Effects of attention on orientation-tuning functions of single neurons in macaque cortical area V4. J Neurosci 19:431–441. Medline

McMains SA, Fehd HM, Emmanouil TA, Kastner S (2007) Mechanisms of feature- and space-based attention: response modulation and baseline increases. J Neurophysiol 98:2110–2121. CrossRef Medline

Morrone MC, Denti V, Spinelli D (2002) Color and luminance contrasts attract independent attention. Curr Biol 12:1134–1137. CrossRef Medline

Morrone MC, Denti V, Spinelli D (2004) Different attentional resources modulate the gain mechanisms for color and luminance contrast. Vision Res 44:1389–1401. CrossRef Medline

Müller MM, Picton TW, Valdes-Sosa P, Riera JR, Teder-Salejarvi WA, Hilly-

ard SA (1998a) Effects of spatial selective attention on the steady-state visual evoked potential in the 20–28 Hz range. Cog Brain Res 6:249–261. CrossRef

Müller MM, Teder-Sälejärvi W, Hillyard SA (1998b) The time course of cortical facilitation during cued shifts of spatial attention. Nat Neurosci 1:631–634. CrossRef Medline

Müller MM, Malinowski P, Gruber T, Hillyard SA (2003) Sustained division of the attentional spotlight. Nature 424:309–312. CrossRef Medline

Murray SO (2008) The effects of spatial attention in early human visual cortex are stimulus independent. J Vis 8(10):2 1–11. CrossRef

Pelli DG (1997) The VideoToolbox software for visual psychophysics: transforming numbers into movies. Spat Vis 10:437–442. CrossRef Medline

Pestilli F, Carrasco M (2005) Attention enhances contrast sensitivity at cued and impairs it at uncued locations. Vis Res 45:1867–1875. CrossRef Medline

Pestilli F, Carrasco M, Heeger DJ, Gardner JL (2011) Attentional enhancement via selection and pooling of early sensory responses in human visual cortex. Neuron 72:832–846. CrossRef Medline

Pestilli F, Viera G, Carrasco M (2007) How do attention and adaptation affect contrast sensitivity? J Vis 7(7): 9 1–12.

Pestilli F, Ling S, Carrasco M (2009) A population-coding model of attention's influence on contrast response: estimating neural effects from psychophysical data. Vision Res 49:1144–1153. CrossRef Medline

Rager G, Singer W (1998) The response of cat visual cortex to flicker stimuli of variable frequency. Eur J Neurosci 10:1856–1877. CrossRef Medline

Regan D (1989) Human brain electrophysiology: evoked potentials and evoked magnetic fields in science and medicine. New York: Elsevier.

Reynolds JH, Chelazzi L, Desimone R (1999) Competitive mechanisms serve attention in macaque areas V2 and V4. J Neurosci 19:1736–Medline

Reynolds JH, Pasternak T, Desimone R (2000) Attention increases sen…ity of V4 neurons. Neuron 26:703–714. CrossRef Medline

Reynolds JH, Heeger DJ (2009) The normalization model of attention. Neuron 61:168–185. CrossRef Medline

Serences JT (2011) Mechanisms of selective attention: response enhancement, noise reduction, and efficient pooling of sensory responses. Neuron 72:685–687. CrossRef Medline

Sereno MI, Dale AM, Reppas JB, Kwong KK, Belliveau JW, Brady TJ, Rosen BR, Tootell RB (1995) Borders of multiple visual areas in humans revealed by functional magnetic resonance imaging. Science 268:889–893. CrossRef Medline

Sirotin YB, Das A (2009) Anticipatory haemodynamic signals in sensory cortex not predicted by local neuronal activity. Nature 457:475–479. CrossRef Medline

Srinivasan R, Russell DP, Edelman GM, Tononi G (1999) Increased synchronization of neuromagnetic responses during conscious perception. J Neurosci 19:5435–5448. Medline

Stark CE, Squire LR (2001) When zero is not zero: the problem of ambiguous baseline conditions in fMRI. Proc Natl Acad Sci U S A 98:12760–12766. CrossRef Medline

Williford T, Maunsell JH (2006) Effects of spatial attention on contrast response functions in macaque area V4. J Neurophysiol 96:40–54. CrossRef Medline

Chapter 3, in full, is a reprint of the material as it appears in an article entitled "Changing the spatial scope of attention alters patterns of neural gain in human cortex" published in The Journal of Neuroscience 2014. Itthipuripat, S.; Garcia, Javier O.; Rungratsameetaweemana, Nuttida; Sprague, Thomas C.; Serences, John T., Society for Neuroscience, 2014. The dissertation author was the primary author of the manuscript. Supported by NIH Grant R01-MH092345 and a James S. McDonnell Foundation grant to J.T.S. and by NIH Grant R01-MH068004 to J.O.G. We thank Kimberly Kaye and Edward F. Ester for help with data collection, Anna Byers and Mary E. Smith for assistance with retinotopic mapping procedures, and John Reynolds, Timothy Q. Gentner, Edward Awh, Jeremy Freeman, and Scott Freeman for useful discussions.

Chapter 4:

Sensory gain outperforms efficient readout mechanisms in predicting attention-related improvements in behavior

Behavioral/Cognitive

Sensory Gain Outperforms Efficient Readout Mechanisms in Predicting Attention-Related Improvements in Behavior

Sirawaj Itthipuripat,[1] Edward F. Ester,[2] Sean Deering,[2] and John T. Serences[1,2]
[1]Neurosciences Graduate Program and [2]Department of Psychology, University of California, San Diego, La Jolla, California 92093

Spatial attention has been postulated to facilitate perceptual processing via several different mechanisms. For instance, attention can amplify neural responses in sensory areas (sensory gain), mediate neural variability (noise modulation), or alter the manner in which sensory signals are selectively read out by postsensory decision mechanisms (efficient readout). Even in the context of simple behavioral tasks, it is unclear how well each of these mechanisms can account for the relationship between attention-modulated changes in behavior and neural activity because few studies have systematically mapped changes between stimulus intensity, attentional focus, neural activity, and behavioral performance. Here, we used a combination of psychophysics, event-related potentials (ERPs), and quantitative modeling to explicitly link attention-related changes in perceptual sensitivity with changes in the ERP amplitudes recorded from human observers. Spatial attention led to a multiplicative increase in the amplitude of an early sensory ERP component (the P1, peaking ~80–130 ms poststimulus) and in the amplitude of the late positive deflection component (peaking ~230–330 ms poststimulus). A simple model based on signal detection theory demonstrates that these multiplicative gain changes were sufficient to account for attention-related improvements in perceptual sensitivity, without a need to invoke noise modulation. Moreover, combining the observed multiplicative gain with a postsensory readout mechanism resulted in a significantly poorer description of the observed behavioral data. We conclude that, at least in the context of relatively simple visual discrimination tasks, spatial attention modulates perceptual sensitivity primarily by modulating the gain of neural responses during early sensory processing

Key words: **attention; contrast discrimination; contrast response function; EEG; efficient readout; sensory gain**

Introduction

Spatial attention has been postulated to facilitate perceptual sensitivity via several mechanisms, including sensory gain (Moran and Desimone, 1985; Motter, 1993; Luck et al., 1997), noise modulation (Mitchell et al., 2007, 2009; Cohen and Maunsell, 2009) and the efficient "readout" of sensory representations (Palmer et al., 2000; Pestilli et al., 2011). However, it is unclear how much each of these mechanisms contributes to the relationship between attention-modulated changes in behavior and neural activity.

Sensory gain models (Fig. 1*A*) postulate that attention amplifies sensory signals evoked by attended stimuli. In a typical study, the magnitude of sensory responses is assessed as a function of stimulus contrast, yielding a contrast response function (CRF). Using this approach, attention has been shown to modulate the CRF in several ways: response gain, contrast gain, or a combination of both (Fig. 1*B–D*; Reynolds et al., 2000; Martínez-Trujillo and Treue, 2002; Williford and Maunsell, 2006; Buracas and Boynton, 2007; Kim et al., 2007; Murray, 2008; Lauritzen et al., 2010; Lee and Maunsell, 2010; Itthipuripat et al., 2014). The relationship between attention-related CRF and behavioral changes can then be assessed using simple linking hypotheses. For example, signal detection theory predicts that increasing the slope of CRFs, which would happen with multiplicative gain, should amplify the differential response evoked by stimuli rendered at slightly different contrast levels and lead to better discriminability (Fig. 1*A*). Similarly, regardless of the nature of gain modulations, a reduction in the trial-to-trial variability of neural responses should also lead to better discriminability (Fig. 1*E*).

In contrast to sensory gain and noise modulation accounts, a recent fMRI study reported that linking modulations of the fMRI response to behavior required an efficient readout mechanism that adaptively amplified the differential response evoked by target and nontarget stimuli (Fig. 1*F*). However, the generality of these findings is unclear as fMRI measures of attentional modulation are largely independent of stimulus intensity (Buracas and Boynton, 2007; Murray, 2008), and may be strongly influenced by the magnitude of top-down input to a region as opposed to changes in local spiking activity (Logothetis and Wandell, 2004).

Received June 4, 2014; revised Aug. 3, 2014; accepted Aug. 24, 2014.

Author contributions: S.I. and J.T.S. designed research; S.I., S.D., and J.S. performed research; S.I. and J.T.S. contributed unpublished reagents/analytic tools; S.I., E.F.E., and S.D. analyzed data; S.I., E.F.E., S.D., and J.T.S. wrote the paper.

This work was supported by National Institutes of Health Grant R01-MH092345 to J.T.S., by a James S. McDonnell Foundation grant to J.T.S, and by an Howard Hughes Medical Institute international student fellowship to S.I. We thank Suzanna K. Wong and Ivan Macias for help with data collection; Javier Garcia and Franco Pestilli for technical support; and Steven Hillyard, Franco Pestilli, Justin Gardner, Thomas C. Sprague, and Anna Byers for useful discussions.

The authors declare no competing financial interests.

Correspondence should be addressed to either of the following: Sirawaj Itthipuripat, Neuroscience Graduate Program, University of California, San Diego, 9500 Gilman Dr., La Jolla, CA 92093. E-mail: itthipuripat.sirawaj@gmail.com; or John Serences, Department of Psychology and Neuroscience Graduate Program, University of California, San Diego, 9500 Gilman Dr., La Jolla, CA 92093. E-mail: iserences@ucsd.edu.

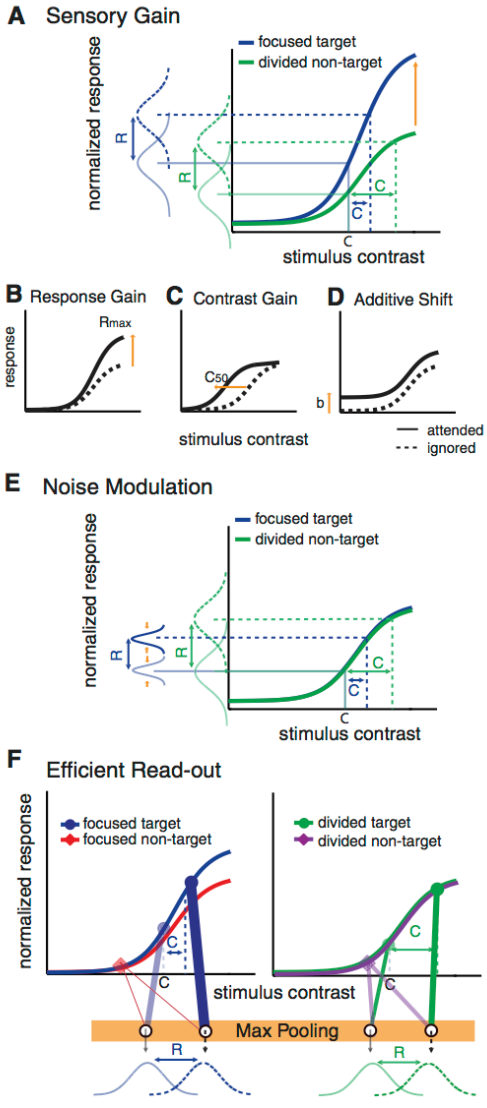

Figure 1. Competing theories of selective spatial attention. ***A***, The sensory gain model predicts that focused spatial attention amplifies neural responses evoked by visual stimuli of differing contrasts. According to the sensory gain model, increasing the slope of neural CRFs with attention will result in a reduction of the contrast increment (ΔC) that is required in the focused-attention condition, compared with the divided-attention condition. Importantly, this model makes an explicit assumption that neural gain in early sensory areas is sufficient to account for attention-related improvements in perceptual performance. ***B–D***, Note that many past studies have reported that spatial attention leads to a variety of gain patterns in the neural CRF: a multiplicative response gain (***B***), a contrast gain (***C***), or an additive baseline shift (***D***). Note that we use the term additive shift instead of additive gain here since gain is multiplicative by definition. ***E***, The noise modulation model predicts that focused spatial attention reduces trial-by-trial variability of neuronal responses and/or decreases correlated noises across neuronal populations. Under this scenario, if sensory gain modulations are insufficient to explain changes in psychophysical thresholds, changes in the noise parameter could be estimated to account for the observed behavioral changes. ***F***, The efficient readout model argues that attention does not strongly modulate responses in early sensory areas and neither sensory gain nor noise modulation could sufficiently account for attention-induced improvements in behavioral performance. Instead, attentional modulation is driven primarily by the efficient selection or readout of sensory signals in a manner that preferentially weights informative as opposed to noninformative sensory signals (Eq. 10, a max-pooling rule). In brief, the model will preferentially weight the stimulus that evokes a relatively large response compared with a stimulus that evokes a relatively small response, and consequently the stimulus evoking the larger response will increasingly influence downstream decision mechanisms.

Here, we quantitatively linked attention-related changes in contrast discrimination thresholds with changes in neural activity measured using electroencephalography (EEG). We focus on attention-related changes in the amplitude of two event-related potentials (ERPs): the P1, an early component thought to reflect sensory processing in early visual cortex (Van Voorhis and Hillyard, 1977; Woldorff et al., 1997), and the late positive deflection (LPD) component, which is thought to reflect decision-related processing (Hillyard et al., 1971; Squires et al., 1973, 1975a, 1975b). Consistent with sensory gain models, we found that increases in the amplitude of the P1 and LPD components were sufficient to explain attention-induced changes in psychophysical contrast discrimination thresholds, without a need to invoke noise modulation. In contrast, models that incorporated an efficient readout mechanism did not accurately capture the link between ERP modulations and behavior. The results suggest that, at least in relatively simple visual discrimination tasks, attention-related improvements in perceptual sensitivity are more closely linked to sensory gain.

Materials and Methods

Subjects. Seventeen neurologically healthy human observers (18–31 years old, nine females, two left-handed) with normal or corrected-to-normal vision were recruited from the University of California, San Diego (UCSD). All participants provided written informed consent as required by the local institutional review board at UCSD. All participants first underwent a 2.5 h behavioral training session where contrast discrimination thresholds were estimated using a staircase procedure (see below). Next, each subject participated in multiple sessions of the main EEG experiment (4–6 d over a period of 2–3 weeks). Each EEG session lasted ~3.5–4 h, including EEG preparation, data acquisition, and breaks. Data from one subject were discarded due to a failure to complete the experimental protocol (the subject withdrew after the second EEG session). Of the remaining 16 subjects, two subjects completed six EEG sessions (126 blocks, 7056 trials) and the rest completed four EEG sessions (84 blocks, 4704 trials).

Stimuli and task. Stimuli were presented on a PC running Windows XP using Matlab (Mathworks) and the Psychophysics Toolbox (version 3.0.8; Brainard, 1997; Pelli, 1997). Participants were seated 60 cm from the CRT monitor (which had a gray background of 34.51 cd/m^2, 85 Hz refresh rate) in a sound-attenuated and electromagnetically shielded room (ETS-Lindgren).

Participants performed a two-interval forced-choice contrast discrimination task (Fig. 2) similar to a procedure described by Pestilli et al. (2011). Each trial started with a red, green, or blue cue that instructed the subject to either covertly attend to the lower left or the lower right quadrant, or to attend to both quadrants. The relationship between cue color and attention condition was counterbalanced across participants. Trials in which the subject attended to either the left or the right quadrant were termed focused-attention trials, and trials in which the subject attended to both quadrants were termed divided-attention trials. The precue was 100% valid for the focused-attention trials, whereas the target was equally likely to appear in the left or right hemifield on divided-attention trials. The attention cue was presented for 500 ms and followed by a 400–600 ms blank interstimulus-interval (ISI). This ISI was followed by two suc-

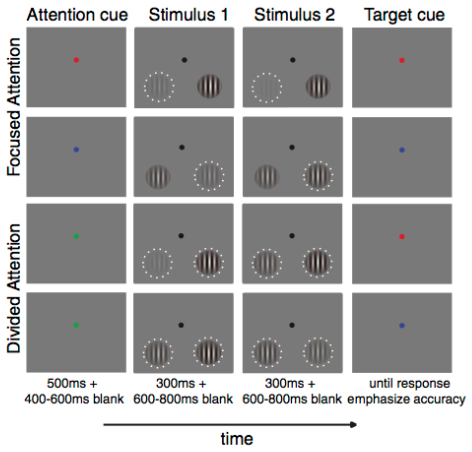

Figure 2. Experimental design. The two-interval forced-choice contrast discrimination task. Each trial started with an attention cue (a color cue, first column) instructing subjects to covertly attend to the lower left (a red cue) or right (a blue cue) quadrant (focused-attention conditions), or to both quadrants (a green cue, divided-attention condition). The white dotted rings in the second and third columns represent the spatial positions of the stimuli that the subjects were supposed to attend to (although they were not shown in the actual display). The attention cue was followed by two successive stimulus presentations, each consisting of two sinusoidal Gabor patches located in the lower left and right quadrants. The pedestal contrasts for each of the Gabor patches were randomly chosen from seven possible values (0–81.13% Michelson contrast). During one of the two stimulus intervals, a Gabor patch (either left or right) had a contrast increment (Δc) added to its pedestal contrast. After the second stimulus interval, a target cue appeared, informing subjects of the exact location of the target stimulus. Subjects reported whether the first or second stimulus presentation contained the target stimulus of higher contrast.

cessive stimulus presentations, with each presentation consisting of two sinusoidal Gabor patches (spatial frequency, 1.04 cycles/°; SD of a Gaussian window, 1.90°) located in the lower left and right quadrants (±8.58 and −7.63° from the horizontal and vertical meridians, respectively). Each stimulus pair was presented for 300 ms, followed by a 600–800 ms ISI. The pedestal contrasts of the two Gabor patches in each interval were randomly selected from seven possible values (0, 2.04, 4.26, 8.90, 18.61, 38.90, and 81.13% Michelson contrast). The stimulus contrast at each pedestal contrast level, except for the 0% contrast value, was jittered ±0.01 log contrast from the mean contrast value. For each trial, the orientations of the left and right Gabor stimuli were yoked and the orientation value was randomly drawn from a uniform distribution. During one of the two stimulus intervals, a small contrast increment (Δc) was added to one of the Gabors for the entire interval. After the offset of the second stimulus array, a postcue appeared to inform subjects which of the two stimuli contained this increment, and subjects reported whether the increment occurred during the first or second stimulus interval. Participants were instructed to prioritize accuracy, and no response deadline was imposed.

Each EEG session contained a total of 21 experimental blocks, which were broken up into three minisessions consisting of seven blocks each. Each minisession contained 392 trials across which all experimental conditions were counterbalanced—i.e., 2 (attention cues: focused, divided) × 2 (target locations: left, right) × 2 (target intervals: first, second) × 7 (pedestal contrast levels of target) × 7 (pedestal contrast levels of nontarget). Critically, Δc for each target pedestal contrast and each attention condition were adjusted after each minisession so that accuracy was maintained at 76% across all experimental conditions. Note that the contrast thresholds used in the first EEG minisession were obtained from the thresholds initially estimated in the 2.5 h behavioral training session using a staircase procedure that was applied independently for each attention condition and each pedestal contrast level. Specifically, three successive correct responses led to a 0.5% decrease in the Δc that defined the target stimulus, while one incorrect response led to a 0.5% increase in Δc. Trials from the first five reversals were excluded and the mean values of the contrast increments from remaining trials were used as contrast discrimination thresholds in the first EEG minisession.

Psychophysical analysis. To examine relationships between stimulus contrast and attention condition (i.e., focused vs distributed) we generated a set of threshold-versus-contrast (TvC) functions by plotting Δc as a function of pedestal contrast separately for each attention condition. We focused on data from the first six pedestal contrasts (0–38.90%) as we could not obtain stable Δc estimates at the highest pedestal contrast, due to scaling factors (i.e., the maximum contrast cannot be increased beyond 100%, so Δc was too small at the highest pedestal value).

Following previous studies (Nachmias and Sansbury, 1974; Legge and Foley, 1980; Ross et al., 1993; Boynton et al., 1999; Gorea and Sagi, 2001; Huang and Dobkins, 2005; Pestilli et al., 2011), we assumed that perceptual sensitivity (indexed via d') is limited by the differential neural response amplitude [$R(c + \Delta c) - R(c)$, or ΔR] divided by the magnitude of sensory noise (σ), as expressed in the following equation (Eq. 1):

$$d' = \frac{\Delta R}{\sigma} = \frac{R(c + \Delta c(c)) - R(c)}{\sigma}$$

where R is a hypothetical CRF that was estimated using the following Naka-Rushton equation (Eq. 2) (Geisler and Albrecht, 1997; Reynolds et al., 2000; Pestilli et al., 2011):

$$R(c) = G_r \frac{c^{s+q}}{c^q + G_c^q} + b$$

Here, G_r is a multiplicative response gain factor that determines the highest response amplitude of the CRF, G_c is a contrast gain factor that determines the horizontal position of the CRF, b is the baseline offset at 0% contrast, and s and q are exponents controlling how quickly the CRF rises and reaches an asymptote. Since G_r, ΔR, and σ are codependent (i.e., they all control the vertical shift of the TvC), we set ΔR and σ to 1. We also set b to zero since changing b would not affect the shape of the TvC. With the combination of the d' (Eq. 1) and Naka-Rushton (Eq. 2) equations, the contrast discrimination thresholds can be estimated based on the derivative (i.e., slope) of the hypothetical underlying CRF, as expressed in the following equation (Eq. 3):

$$\Delta c \approx \frac{\Delta R}{dR/dc}$$

where dR/dc is the derivative of the underlying CRF (Boynton et al., 1999).

We fit the TvC functions with Equations 1–3 with Matlab's fminsearch function (Nelder–Mead method; nonlinear least squares) to estimate a multiplicative response gain factor (G_r), a contrast gain factor (G_c), and two exponents (s and q) that describe the hypothetical CRF that best accounts for the observed TvC functions derived from the focused-attention and divided-attention conditions in each subject. Paired t tests were performed to examine the effects of focused and divided attention on the G_r, G_c, s, and q parameters. Note that this analysis attempts to recover the shape of the hypothetical CRF that best explains attention-related changes in contrast discrimination thresholds under the assumption that the behavioral data can be predicted by the differential response evoked by target and pedestal stimuli divided by the variability of responses at each pedestal level (and that variability is constant across all response levels).

EEG recording. EEG data were recorded with a 64 + 8-channel Biosemi ActiveTwo system (Biosemi Instrumentation) at a sampling rate of 512 Hz. The 64 channels were equally spaced across the EEG cap and covered the whole head from above the eyebrows to slightly below the inion. Two reference electrodes were placed at the mastoids. Vertical eye movements and blinks were monitored via four extra electrodes placed below and above the eyes. Horizontal eye movements were detected by another pair of electrodes, placed near the outer canthi of the eyes. Electrode imped-

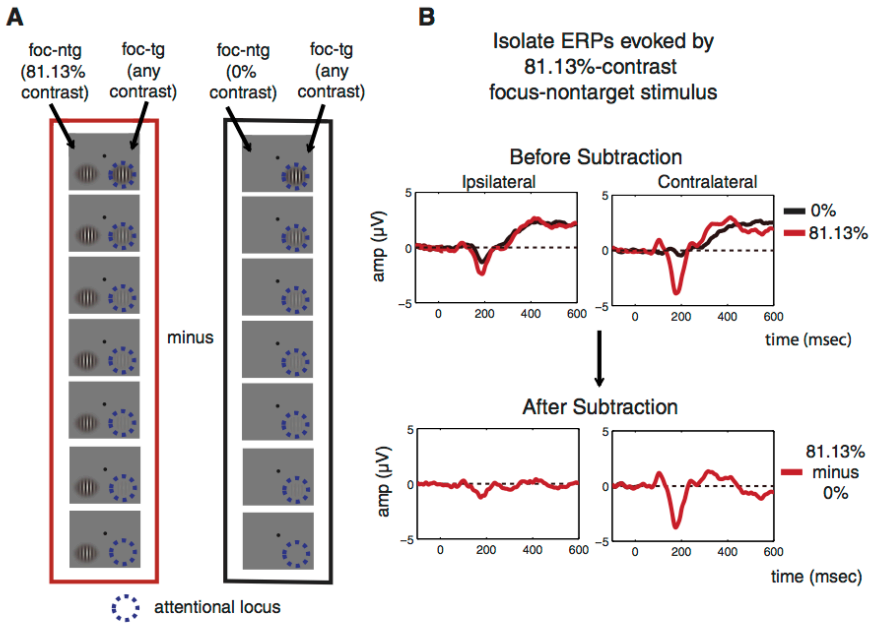

Figure 3. The ERP subtraction method. To isolate the ERP response evoked by stimuli in each experimental condition (i.e., each attention condition, each stimulus type, each stimulus location, and each stimulus interval), we subtracted the ERP evoked by the contralateral 0%-contrast stimulus from the ERP evoked by the stimulus of all other contrasts. In effect, this allowed us to use the response to a contralateral 0% stimulus as an index of how much effect a nonzero contrast ipsilateral stimulus had on the evoked response. ***A***, ***B***, An example of this subtraction method is presented in ***A*** where the ERP response contralateral to the focused-attention nontarget stimulus of 81.13% contrast on the left hemifield (termed the stimulus of interest) was to be extracted (***B***). In this case, the ERP response evoked by the left focused-attention nontarget stimulus of 0% contrast (***A***, right; ***B***, top, black traces) was subtracted from the ERP response evoked by the left focused-attention nontarget stimulus of 81.13% contrast (***A***, left; ***B***, top, red traces), resulting in the subtracted ERP response (***B***, bottom, red traces). Note that the stimulus paired with the stimulus of interest (in this case, the right target stimulus) could have any of seven contrast values. Therefore, the ERP response associated with the stimulus paired with the stimulus of interest should be subtracted out through this subtraction method.

ances were kept <20 kΩ, which is standard for this active-electrode system.

EEG preprocessing and analysis. The EEG data were preprocessed using a combination of EEGlab11.0.3.1b (Delorme and Makeig, 2004) and custom Matlab scripts. The continuous EEG data were first rereferenced to the algebraic mean of the two mastoid electrodes and then filtered by applying 0.25 Hz high-pass and 55 Hz low-pass Butterworth filters (third order). The data were then segmented into epochs extending from 195 ms before to 3437 ms after the trial onset (i.e., the attention cue onset). Artifact rejection was performed off-line by discarding epochs contaminated by eye blinks and vertical eye movements (>±80–150 μV deviation from zero; exact thresholds were determined on a subject-by-subject basis due to differences in amplitudes of eye blink and vertical eye movement artifacts), horizontal eye movements (>±75 μV deviation from zero), excessive muscle activity, or drifts using threshold rejection and visual inspection on trial-by-trial basis, which resulted in the removal of 17.46% (SD, 6.44%) of trials across all subjects.

Next, the artifact-free data were time-locked to the onset of the first and second stimulus presentations and the algebraic mean of the prestimulus baseline (−100–0 ms preceding stimulus onset) was subtracted from each epoch. The data were then sorted into 112 different bins: 2 (attention conditions: focused, divided) × 2 (stimulus intervals: first, second) × 2 (types of the stimulus of interest: target, nontarget) × 2 (locations of the stimulus of interest: left, right) × 7 (pedestal contrast levels). We arranged the electrode labels so that the electrodes that were contralateral and ipsilateral to the stimulus of interest were on the right and left hemispheres of the head model, respectively. Accordingly, we collapsed trials across target position and averaged all epoched EEG data to obtain ERPs. To subtract out the evoked potentials associated with the stimulus that was paired with the stimulus of interest and to minimize the potential effects of anticipatory ERPs, we subtracted the ERP evoked by a contralateral 0%-contrast stimulus in each stimulus-cue condition (focused target, focused nontarget, divided target, divided nontarget) from the ERPs elicited by stimuli of all other contrast levels in each condition (Fig. 3, schematic illustrating all signal processing steps; Talsma and Woldorff, 2005). Finally, we collapsed across ERPs evoked by the first and second stimulus presentations.

Previous work has shown that attentional modulation of N1 amplitudes (an early negative-going waveform in ERPs) can be confounded by modulations of the nearby P1 and LPD components (especially when bilateral displays are used; Mangun et al., 1987; Heinze et al., 1990; Luck et al., 1990; Lange et al., 1999; Störmer et al., 2009). Thus, our analyses focus on attention-related modulations of P1 and LPD component amplitudes. The P1 component is thought to index sensory gain in early visual cortex based on its timing (~80–130 ms poststimulus) and its putative origin in extrastriate visual cortex (Van Voorhis and Hillyard, 1977; Woldorff et al., 1997; Hillyard and Anllo-Vento, 1998). The LPD component, which is maximal above the parietal lobe, has been linked to the accumulation of sensory evidence and perceptual decision mechanisms (Hillyard et al., 1971; Squires et al., 1973, 1975a, 1975b; O'Connell et al., 2012). If early sensory gain is sufficient to explain attention-induced changes in behavior, we should be able to use signal detection theory to link attention-induced changes in P1 component amplitude with changes in psychophysical contrast discrimination thresholds. The predictive relationship between LPD component amplitude and behavior might also be expected if early sensory gain cascades to later processing stages.

To examine the pattern of attentional gain of the P1 component amplitude, we calculated the mean amplitude of the early positive P1 component across three contiguous contralateral posterior-occipital electrodes (PO3, P5, and P7 for right stimuli; PO4, P6, and P8 for left stimuli) across a 80–130 ms poststimulus window. These analyses were performed separately for each contrast level, attention condition, and stimulus type. We also identified and examined the mean amplitude of LPD components across three focal central posterior electrodes (P1, Pz, and P2) across a 230–330 ms poststimulus window. Next, the mean amplitudes of the P1 and LPD components for each attention condition were averaged across subjects and plotted as a function of stimulus contrast (for nontarget stimuli, the contrast value was the pedestal contrast; for target stimuli, the contrast value was the average between the pedestal contrast and the contrast value of the stimulus that contained the contrast increment, corresponding to the averaged physical contrast of the stimulus of interest across the two stimulus intervals). We then fit these functions with the Naka-Rushton equation (Eq. 2) to estimate the baseline (b), the maximum response (R_{max}), and the semisaturation [the contrast value at half the R_{max} (C_{50})] parameters using Matlab's fminsearch function. In this fitting routine, there were a total of 28 observed data points (seven contrast levels times four attention/stimulus-type conditions) and 14 free parameters (four attention/stimulus-type conditions times three free parameters G_r, G_c, and b), plus s and q exponents that were identical across all conditions. Since the G_r and G_c parameters control the response and contrast gain of the function where the contrast axis ranges from zero to ∞, the G_r and G_c parameters could in principle exceed the realistic range of stimulus contrast (0–100% contrast). Thus, instead of directly comparing G_r and G_c parameters across conditions, we obtained R_{max} and C_{50} parameters as they respectively capture response gain and contrast gain of the CRFs over the realistic range of stimulus contrast values.

Next, a bootstrapping procedure was used to assess differences between parameter estimates in each condition and to establish confidence intervals on the best fitting model parameters. First, we resampled subject labels with replacement. Next, we averaged the mean amplitudes of P1 and LPD components across the resampled subject labels to generate ERP CRFs for each experimental condition, and then we fit the grand-averaged ERP CRFs to estimate b, R_{max}, and C_{50} parameters. This resampling and fitting procedure was then repeated 10,000 times to create bootstrap distributions from which confidence intervals associated with each parameter were computed. To evaluate the main effect of attention condition (focused/divided), we compiled the bootstrap distribution of the differences between the estimated fit parameters in the focused-attention and distributed-attention conditions—i.e., focused (target plus nontarget) minus divided (target plus nontarget)—and computed the percentage of values in the tail of this distribution that were <0. Similarly, we tested the main effect of stimulus type (target/nontarget) by compiling the bootstrap distributions of the differences between the estimated fit parameters in the target and the nontarget conditions—i.e., target (focused plus divided) minus nontarget (focused plus divided). The interaction between attention condition and stimulus type was examined by comparing the bootstrap distributions of focused (target minus nontarget) minus divided (target minus nontarget). Finally, *post hoc* comparisons were performed to test for additional differences between pairs of conditions by evaluating bootstrap distributions of differences and then computing the percentage of the values in the tails of these distributions that were >0 or <0. We used two-tailed statistical tests to be conservative and all p values associated with *post hoc* comparisons were corrected by the Holm-Bonferroni method.

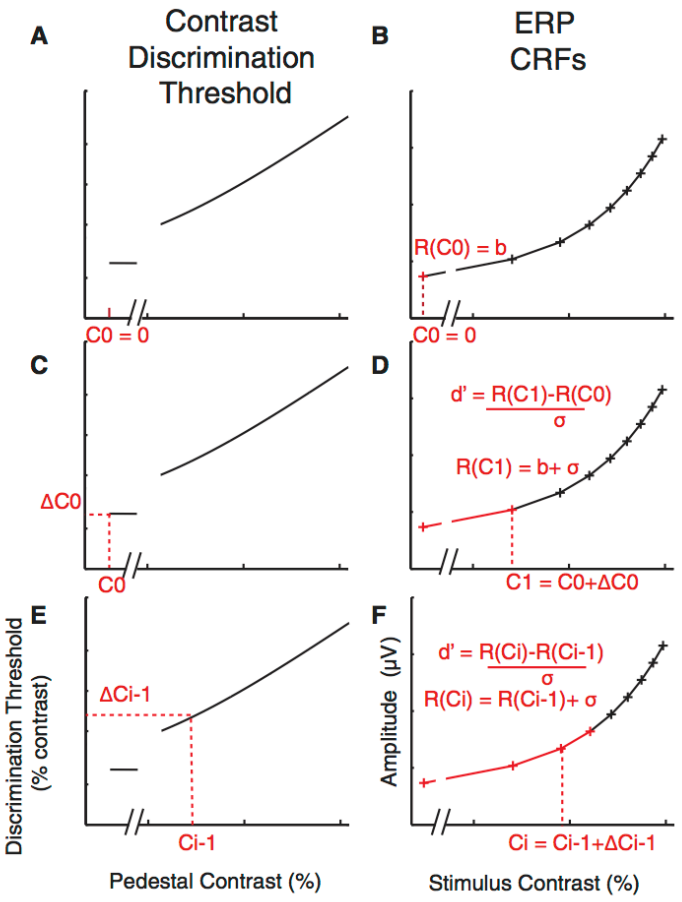

Figure 4. Testing the sensory gain model. To quantitatively evaluate whether the observed sensory gain in the ERP CRFs could sufficiently account for attention-induced changes in the contrast-discrimination thresholds, the TvC functions from the focused-attention and divided-attention conditions were interpolated (***A***, ***C***, and ***E***) and the ERP CRF (***B***, ***D***, ***F***) was estimated based on the interpolated TvC function using the combination of the signal-detection theory (Eq. 1) and Naka-Rushton functions (Eq. 2), given that $d' = 1$ (accuracy, ~76%; see step-by-step details in Materials and Methods).

Fit procedure for the sensory gain model. To quantitatively evaluate whether gain in the ERP response amplitudes in the P1 and LPD component windows could sufficiently account for attention-induced changes in contrast discrimination thresholds, we simulated the P1 and LPD component CRFs using the combination of the d' (Eq. 1) and Naka-Rushton (Eq. 2) equations (Fig. 4). The main parameters of interest were the baseline parameter of the simulated CRFs (b) and the noise parameter in the d' equation (σ; see similar method in Pestilli et al., 2011). Specifically, the TvC functions in the focused-attention and divided-attention conditions were first estimated using Equations 1–3. Then, we estimated

the P1 and LPD component CRFs for the divided condition based on the TvC function of the divided-attention condition. The fit routine started by setting the first point on the estimated CRF (c_0 = 0% contrast) to be a baseline parameter (b), for any given values of b and σ (Fig. 4*A*,*B*), as shown in the following equation (Eq. 4): $R(c_0) = b$.

The next contrast (c_1) for which a response was estimated was taken from the TvC function shown in the following equation (Eq. 5): $c_1 = c_0 + \Delta c_0$, where Δc_0 is the threshold at c_0 (Fig. 4*C*). Then, the response at c_1 was estimated using the d' equation (Eq. 1) as shown in the following equation (Eq. 6): $R(c_1) = b + \sigma$, given that $d' = 1$ (Fig. 4*D*). The next contrast was selected in the same way, shown in the following equation (Eq. 7): $c_i = c_{i-1} + \Delta c_{i-1}$, where i is the number of the current iteration that is >1. Accordingly, the response at c_i was estimated as the following equation (Eq. 8): $R(c_i) = R(c_{i-1}) + \sigma$. This procedure was continued until the entire CRF was estimated (Fig. 4*E*,*F*). Finally, the b and σ parameters were optimized by minimizing the least-squares error between the simulated CRFs and the observed P1 and LPD component CRFs in the divided-attention condition (the average between divided-attention target and nontarget conditions) using Matlab's fminsearch function. To test whether the multiplicative response gain of the ERP CRFs alone could account for changes in the TvC function, we estimated the P1 and LPD component CRFs for the focused-attention target, using the modeling routine described above with the b and σ parameters that are identical to those obtained from in the divided-attention condition.

To test whether allowing changes in the noise (σ) and baseline (b) parameters across the focused-attention and divided-attention conditions could significantly improve the fit of the P1 and LPD component responses, we estimated the P1 and LPD component CRFs derived from the focused-attention condition as we did above except that we allowed σ and b parameters to vary freely to find the best fit. The R^2 value obtained from the model with fixed σ and b parameters (reduced model) was then compared with the R^2 value from the model with free σ and b parameters in the focused-attention condition (full model), using an F test statistic as shown in the following equation (Eq. 9):

$$F(Df_1, Df_2) = \frac{R^2_{full} - R^2_{red}}{Df_1} \Big/ \frac{1 - R^2_{full}}{Df_2}$$

where R^2_{full} and R^2_{red} are obtained from the best fits of the full and reduced models, respectively. Df_1 is the number of parameters in the full model (four free parameters: σ and b for the divided-attention condition, and σ and b for the focused-attention condition) minus the number of the parameters in the reduced model (two free parameters: σ and b, shared across the divided-attention and focused-attention conditions). Df_2 is the number of observations (seven contrast levels times two attention conditions) minus the number of the free parameters in the full model minus one. The F distribution was then used to estimate the probability that the full model differed significantly from the reduced model.

To determine whether allowing the optimization of σ and b in the focused-attention condition led to a significant change in these parameters in the divided-attention condition, we used a bootstrapping procedure to establish confidence intervals on the best fitting model parameters (σ and b for the divided-attention condition, and σ and b for the focused-attention condition). First, we resampled subject labels with replacement. Next, we averaged the psychophysical contrast discrimination thresholds and the mean amplitudes of P1 and LPD components across the resampled subject labels to generate new TvC and ERP CRF functions for each experimental condition. Then, the TvC functions were interpolated using Equations 1–3. In turn, the interpolated TvC functions were used to estimate the ERP CRFs via the model as described in Figure 4 and σ and b for each of the attention conditions were optimized using Matlab's fminsearch function. To test the difference between σ parameters obtained from the divided-attention and focused-attention conditions, we compiled the bootstrap distribution of the differences between the estimated fit parameters in the focused-attention and the distributed-attention conditions, and computed the percentage of values in the tail of this distribution that were different from zero. An identical analysis was then performed for b parameters.

In addition, to examine the variability of the P1 and LPD component amplitudes across focused-target and divided-target conditions, we resampled half of the trials for each pedestal contrast level and each attention condition (focused-target and divided-target conditions) separately for individual subjects. The ERP for each pedestal contrast and each attention condition was obtained by averaging the stimulus-locked EEG data across these resampled trials and applying the subtraction method (Fig. 3). This resampling method was repeated 1000 times and the SEM amplitudes of these resampled and subtracted ERPs (P1 component from 80 to 130 ms and LPD component from 230 to 330) was obtained for each subject.

Fit procedure for the efficient readout model. First, we estimated the three CRFs (focused target, focused nontarget, and the average between divided target and nontarget) using the Naka-Rushton equation (Eq. 2), with G_r and G_c as free parameters for each of the three CRFs and q, s, and b parameters that were shared across the three CRFs. Since a max-pooling rule (Eq. 10; see below) requires overall response amplitudes to be positive values, the baseline values of the P1 and LPD component CRFs, which were slightly negative, were subtracted out from the CRFs so that all values on the CRFs were converted to positive numbers. This was done separately for the P1 and LPD component CRFs, and the resulting values formed the basis of the efficient readout model. Next, we simulated the performance of an ideal observer in 60,018 randomly generated trials (Fig. 5). These trials include 10,003 trials of each of the six trial types where the target contrast was 0, 2.04, 4.26, 8.90, 18.61, and 38.90% contrast, respectively (this ensures that the simulated performance of an ideal observer did not vary more than ~0.01% for each pedestal contrast level). Note that we focused on these six contrast levels where the accuracy was successfully equated across subjects (Fig. 2*B*). From these 10,003 trials, there were 1429 trials each where the nontarget contrast was 0, 2.04, 4.26, 8.90, 18.61, 38.90, and 81.13%, respectively. Then, for each simulated trial, we set the response of each stimulus type (target or nontarget) and stimulus interval (the interval that contains the contrast increment target) as a random draw from a Gaussian distribution whose mean was given by the mean amplitude of the interpolated P1 and LPD component CRFs at the corresponding contrast value and whose SD was the σ parameter in the d' equation (Eq. 1). The target (R_{tg}) and nontarget evoked responses (R_{ntg}) were then pooled into a single value (R_p) using the max-pooling equation expressed as follows (Eq. 10):

$$R_p = \frac{1}{2}\sqrt[k]{R^k_{tg} + R^k_{ntg}}$$

where k is an exponent that weights each of the responses to individual stimuli (k ranges from 1 to ∞). Next, we searched for the contrast increment value (Δc) that yielded 76% (or $d' = 1$) across the 10,003 simulated trials at each target contrast, assuming that an ideal observer would choose the interval that contained a larger pooled response as the interval that contained the target. To test how well we could estimate the TvCs based solely on the multiplicative response gain increase of the P1 and LPD component CRFs, we fixed k at 1 (i.e., equivalent to no differential weighting) and we optimized the σ parameter to find the best fit by minimizing the least-square error (this essentially amounts to the sensory gain model). To examine whether the max-pooling rule ($k > 1$) improves our ability to estimate attention-induced changes in behavior, we then allowed k to increase from 2 to 70 (the range of k used in this fitting routine is based on the best fit value (k = ~68) recently reported by Pestilli et al. (2011).

Results

Focused attention reduces psychophysical contrast discrimination thresholds

Figure 6*A* shows the mean response accuracy for each attention condition and each pedestal contrast level. By design, the Δc for each pedestal contrast and each attention condition were adjusted every seven blocks (i.e., the minimum number of blocks needed to ensure that all trial types were counterbalanced) to equate accuracy at a fixed level across attention conditions and

pedestal contrast levels. As a result, accuracy did not deviate significantly from 76% for the first six pedestal contrast levels [accuracy, 76.11 ± 0.64% (mean ± SEM across subjects)]. A 2 × 6 repeated-measures ANOVA with attention condition and stimulus contrast as within-subject factors revealed no effect of the attention cue ($F_{(1,15)} = 0.08$, $p = 0.78$), a marginal effect of stimulus contrast ($F_{(5,75)} = 2.28$, $p = 0.055$), and no interaction between these two factors ($F_{(5,75)} = 1.30$, $p = 0.27$). While these results suggest that accuracy was successfully matched across the first six contrast levels, the contrast increment at the highest pedestal contrast reached ceiling in most subjects (14 of 16 subjects), which prevented us from accurately estimating contrast discrimination thresholds (that is, when the pedestal contrast plus Δc reached 100%, and we were unable to increase contrast further). Thus, overall accuracy was lower for the highest contrast pedestal compared with lower contrast pedestals ($t_{(15)} = 4.28$, $p < 0.0001$). Because we were unable to equate the accuracy at the highest pedestal contrast, we focused all subsequent behavioral analyses on the first six pedestal contrast levels (0–38.90% contrast) for which task difficulty was successfully equated.

Given that accuracy was by design equated across the first six pedestal levels, the critical measure of the effects of attention on behavioral performance was the Δc required to achieve threshold performance at each pedestal contrast. We thus evaluated attention effects using a two-way repeated-measures ANOVA with attention condition and stimulus contrast as within-subject factors. Consistent with many previous studies (Nachmias and Sansbury, 1974; Legge and Foley, 1980; Ross et al., 1993; Gorea and Sagi, 2001; Huang and Dobkins, 2005; Pestilli et al., 2011), Δc significantly increased as a function of pedestal contrast (Fig. 6*B*; $F_{(5,75)} = 106.15$, $p < 0.0001$). Moreover, contrast discrimination thresholds were significantly lower in the focused-attention condition compared with the divided-attention condition ($F_{(1,15)} = 30.98$, $p < 0.0001$), demonstrating that subjects were more sensitive to small contrast changes in the focused-attention condition compared with the divided-attention condition. *Post hoc t* tests revealed that this pattern held across all six pedestal contrast levels that were considered in the analysis (all $t_{(15)}$'s ≥3.33, all p's ≤0.0045, Holm-Bonferroni corrected).

In addition, the combination of d' and Naka-Rushton equations (Eqs. 1–3) accurately predicted the observed contrast discrimination thresholds (Fig. 6*B*) in both the focused-attention [blue curve; $R^2 = 0.98 \pm 0.0034$ (mean ± SEM)] and the divided-attention conditions [green curve; $R^2 = 0.98 \pm 0.0034$ (mean ± SEM)]. Importantly, the downward shift of the TvC curves with focused attention was selectively driven by an increase in the multiplicative response gain factor (G_r) of the Naka-Rushton equation ($t_{(15)} = 4.92$, $p < 0.001$), which reflects an increase in the slope of the inferred CRFs in the focused-attention condition. Other parameters of the Naka-Rushton equation, including the contrast gain factor (G_c) and the exponents (q and s) did not differ across the focused-attention and divided-attention conditions (G_c: $t_{(15)} = 0.23$, $p = 0.82$; q: $t_{(15)} = 0.72$, $p = 0.50$; s: $t_{(15)} = 1.43$, $p = 0.17$). These results suggest that the effects of focused attention on the shape of the behavioral TvC curves can be best explained via changes in the multiplicative response gain of the hypothetical CRF. However, it is important to note that this effect of focused attention that was inferred solely on the basis of behavior can also be explained by alternative neural models (Pelli, 1985; Palmer et al., 2000; Mitchell et al., 2007, 2009; Cohen and Maunsell, 2009; Pestilli et al., 2011).

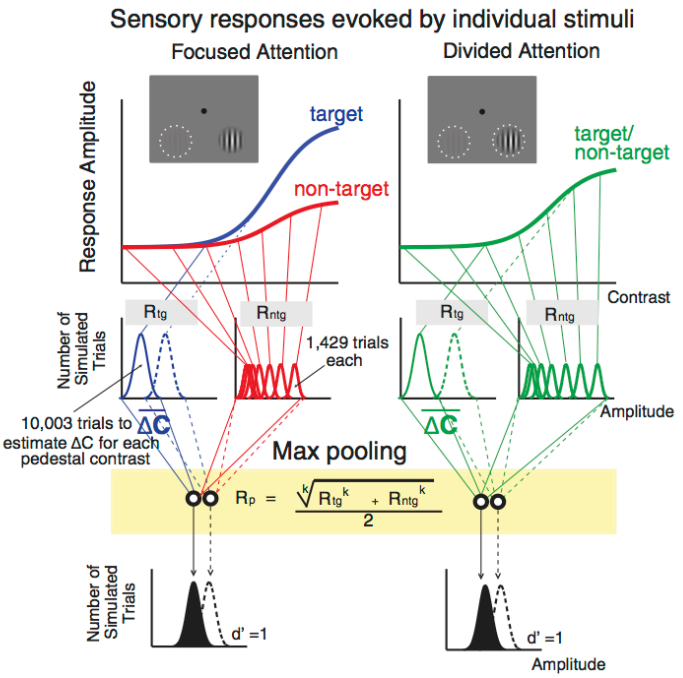

Figure 5. Testing the efficient readout model. Psychophysical contrast discrimination thresholds were estimated based on the CRFs measured by ERP responses (P1 and LPD components) using the max-pooling rule (Eq. 10; yellow box in the figure). The exponent of the max-pooling rule (k) determines the differential weight given to responses to target (R_{tg}) and nontarget stimuli (R_{ntg}) in each interval, which are later pooled into a single neural output (R_p). We used an ideal observer model that selected the interval with the highest R_p to determine the contrast increment value (Δc) that yielded 76% (or $d' = 1$) across 10,003 simulated trials at each target contrast. We first set $k = 1$ to examine how well sensory gain alone can estimate changes in the observed contrast thresholds. Finally, k was allowed to increase from 2 to 70 to determine whether the increase in differential weighting as implemented by the max-pooling rule is better at predicting changes in the behavioral data.

Focused attention enhances multiplicative response gain of visually evoked responses

The grand average of stimulus-locked ERPs (see Materials and Methods; Fig. 3) are shown in Figure 7*A* for each contrast level and combination of attention condition and stimulus type. In the posterior-occipital electrodes, we observed the lateralized P1 and N1 components peaking at ~80–130 and ~150–200 ms, respectively. These early components are followed by the LPD component peaking at ~230–330 ms over centroparietal electrodes. The timing (Fig. 7*A*) and topography (Fig. 7*B*) of each ERP com-

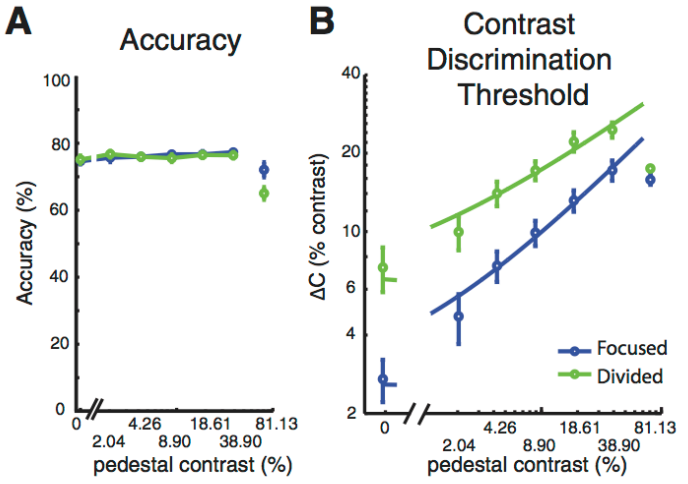

Figure 6. Psychophysical results. ***A***, Accuracy was successfully equated across attention conditions for the first six pedestal contrast levels by systematically changing Δc. Subjects performed poorly for the target of the highest contrast as we could not make Δc large enough at this pedestal (unconnected circles at 81.13% contrast). Thus, we focused the behavioral analysis on the first six pedestal contrast levels. ***B***, Psychophysical contrast discrimination thresholds at different pedestal contrast levels across focused-attention (blue circles) and divided-attention conditions (green circles). Smooth curves represent the fits of the TvC functions using a combination of signal detection theory (Eq. 1) and a Naka-Rushton equation (Eq. 2). Focused attention reduced discrimination thresholds, leading to a downward shift of the TvC. In turn, this downward shift in the TvC curve is consistent with a change in the multiplicative response gain parameter or the slope of the underlying CRF. Error bars in all figures indicate ±SEM across subjects.

ponent is consistent with previous reports of the P1, N1, and LPD components (Campbell and Kulikowski, 1972; Spekreijse et al., 1973; Van Voorhis and Hillyard, 1977; Wright and Johnston, 1982; Mangun and Hillyard, 1987, 1988, 1990, 1991; Heinze et al., 1990; Luck et al., 1990; Vassilev et al., 1994; Johannes et al., 1995; Hillyard and Anllo-Vento, 1998; Hillyard et al., 1998; Mangun and Buck, 1998; Lange et al., 1999; Noesselt et al., 2002; Schadow et al., 2007; Zimmer et al., 2010; Cravo et al., 2013). Note that previous work has shown that attentional modulation of N1 amplitudes can be confounded by modulations of the nearby P1 and LPD components (especially when bilateral displays are used; Mangun et al., 1987; Heinze et al., 1990; Luck et al., 1990; Lange et al., 1999; Störmer et al., 2009). Thus our analyses focus on attention-related modulations of P1 and LPD component amplitudes.

To assess the effect of attention on the gain pattern of neural CRFs, the mean amplitudes of the P1 and LPD components were plotted as a function of stimulus contrast (Fig. 8*A*,*D*). Overall, the Naka-Rushton equation explained a large proportion of the variance in the P1 (mean R^2, 0.92; 68% CI, 0.88–0.96) and LPD component CRFs (mean R^2, 0.95; 68% CI, 0.94–0.97). Neither attention (i.e., focused vs distributed) nor stimulus type (target vs nontarget) had an effect on the baseline or the C_{50} parameters (nor did these factors interact; Fig. 8*B*,*E*, left, right; baseline: all p's $\geq$ 0.21; C_{50}: all p's $\geq$ 0.15; note that all p values reported here and elsewhere for the ERP data are based on bootstrapping at the subject level). However, we did find that attention significantly modulated the response gain of the P1 and LPD component CRFs (the R_{max} parameter; Fig. 8*B*,*E*, middle).

For the R_{max} for the P1 component CRF (Fig. 8*A*–*C*), there was a significant interaction between attention condition and stimulus type ($p = 0.0022$). *Post hoc* pairwise comparisons (two-tailed) with the Holm-Bonferroni correction revealed that this interaction was driven by a higher R_{max} for focused-attention targets compared with focused-attention nontargets (blue vs red lines; $p = 0.0026$) and compared with divided-attention targets (blue vs green lines; $p = 0.015$). In addition, the R_{max} for divided-attention nontargets was significantly higher than the R_{max} associated with focused-attention nontargets (purple vs red lines; $p = 0.020$). We did not find any difference in R_{max} between target and nontarget stimuli in the divided-attention condition (green vs purple lines; $p = 0.35$).

For the R_{max} for the LPD component CRF (Fig. 8*D*–*F*), we observed a significant main effect of stimulus type (target/nontarget; $p < 0.0001$) and a significant interaction between attention condition and stimulus type ($p < 0.0001$). *Post hoc* pairwise comparisons (two-tailed) with Holm-Bonferroni correction revealed that this interaction was driven by a higher R_{max} for focused-attention targets compared with focused-attention nontargets (blue vs red lines; $p < 0.0001$) and compared with divided-attention targets (blue vs green lines; $p = 0.0086$). In addition, R_{max} for divided-attention nontargets was significantly higher than R_{max} for focused-attention nontargets (purple vs red lines; $p = 0.0018$) and R_{max} for divided-attention targets was significantly higher than R_{max} for divided-attention nontargets (green vs purple lines; $p = 0.017$).

In sum, we observed that focused spatial attention primarily increased the slope of P1 and LPD component CRFs via a multiplicative response gain as indexed by R_{max}, and that there was no significant impact on other parameters, such as the baseline offset or the semisaturation constant. Importantly, the increases in multiplicative response gain of the P1 and LPD component CRFs with focused attention are qualitatively consistent with the effects of focused attention on the psychophysically measured TvC functions, which were also modulated in a manner that is suggestive of a multiplicative response gain in the hypothetical CRFs (see psychophysical results).

Sensory gain is sufficient to account for attention-related behavioral improvements

Although both the psychophysical and the ERP data are consistent with the sensory gain model depicted in Figure 1*A*, these two independent sources of information must be formally linked to directly test competing accounts of attentional selection. For example, the magnitude of sensory gain that we observe in the ERP data might be either too small or too large to accurately predict the magnitude of psychophysically measured attention effects (Cook and Maunsell, 2002; Cohen and Maunsell, 2009; Pestilli et al., 2011). If this turns out to be the case, then we might need to posit an additional readout mechanism to accurately characterize the behavioral data (Pestilli et al., 2011). In contrast, if the sensory gain model fits the data with a high degree of precision, then we may not need to invoke any additional readout mechanism.

Thus, we then tested a series of nested models that incorporate sensory gain and/or efficient readout to determine which model (or combination of models) most parsimoniously links the ERP-derived CRFs with the psychophysically measured TvC functions. To assess these models, we first estimated the contribution of pure sensory gain to behavioral performance using a quantitative framework based on signal detection theory, which assumes that behavioral contrast discrimination thresholds are directly related to the amplitude difference and the variability of stimulus-evoked responses in early visual cortex. Then, we combined this sensory gain model with a recently developed efficient readout model, which estimates the degree to which early sensory responses are differentially weighted by postperceptual decision mechanisms (Pestilli et al., 2011). This variant of a readout model is designed to ensure that responses evoked by attended stimuli contribute more to a decision variable than responses associated with irrelevant stimuli, even in situations where attention-related sensory gain is minimal.

To investigate the sensory gain model, we first fit the psychophysical contrast discrimination thresholds in the divided-attention condition using a combination of the d' (Eq. 1) and the Naka-Rushton equations (Eq. 2) to obtain a continuous TvC function (Fig. 9*A*, green curve). Then, we optimized the sensory noise parameter (σ) in Equation 1 and the baseline (b) parameter in Equation 2 to find the value of each parameter that best fit the P1 and LPD component CRFs using only data from the divided-attention condition. This procedure resulted in an excellent fit for both the P1 (Fig. 9*B*, green curve; $R^2 = 0.97$, $\sigma = 0.15$ μV, $b = -0.13$ μV) and LPD component CRFs (Fig. 9*C*, green curve; $R^2 = 0.89$, $\sigma = 0.44$ μV, $b = -0.57$ μV). To examine how well changes in multiplicative response gain of the P1 and LPD component CRFs (Fig. 8) could account for the observed behavioral improvements with attention (i.e., the downward shift of the TvC curves; Fig. 6*B*), we then estimated the P1 and LPD component CRFs for the focused-attention target based on the continuous TvC function associated with the focused-attention condition (Fig. 9*D*, blue curve). Importantly, we used the σ and b parameters that were previously estimated using only the psychophysical TvC and ERP data from the divided-attention conditions (Fig. 9*A–C*). We observed an increase in the slope of the estimated ERP CRF in the focused-attention conditions (Fig. 8*E,F*, blue solid curves) compared with the divided-attention conditions (green dotted curves). This slope increase of the estimated CRFs led to an excellent fit to the real ERP CRFs in the focused-attention condition (Figs. 9*E,F*, blue curves; P1 $R^2 = 0.93$; LPD $R^2 = 0.94$). These findings strongly suggest that a simple change in multiplicative response gain can sufficiently account for a high degree of attention-induced changes in both the psychophysical and the ERP data.

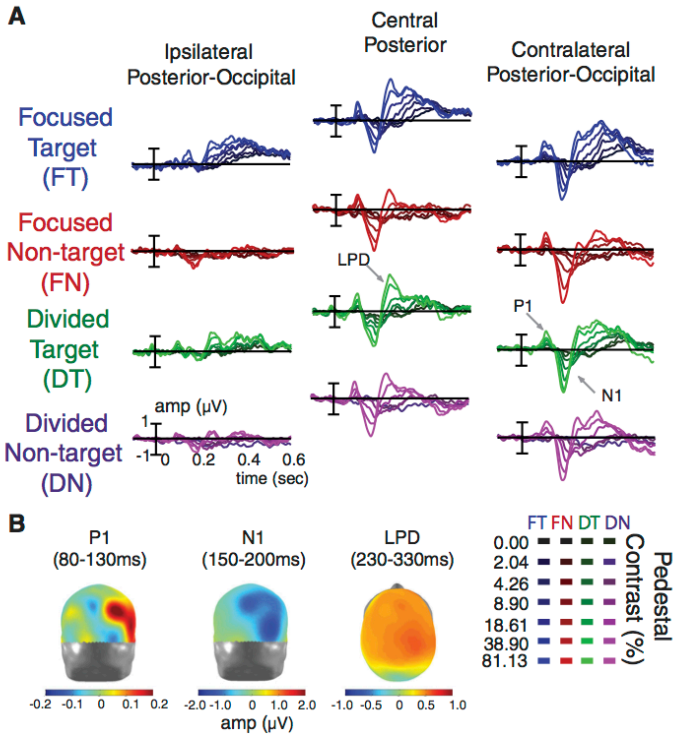

Figure 7. ERP responses and topographies. ***A***, Stimulus-locked ERPs (collapsed across the first and second intervals). The data were sorted into four main conditions: focused-attention target (i.e., attended stimulus in the focused-attention condition, blue), focused-attention nontarget (i.e., ignored stimulus in the focused-attention condition, red), divided-attention target (green), and divided-attention nontarget (purple). Shading of ERP traces represents the pedestal contrast of the driving stimulus (dark and bright colors represent low-contrast and high-contrast stimuli, respectively). The ERPs evoked by contralateral 0%-contrast stimuli in each condition were subtracted from the ERPs evoked by contralateral stimuli of all other contrast levels (Fig. 3). This subtraction was done to subtract out the evoked potentials associated with variable contrast ipsilateral stimuli paired with all other contralateral stimuli. We found early sensory positive (P1) and negative potentials (N1) peaking at the contralateral posterior-occipital electrodes in ~80–130 and ~150–200 ms temporal windows, respectively. These early components were followed by an LPD component peaking at ~230–330 ms in the central posterior electrodes. ***B***, The topographical maps of P1 (posterior view), N1 (posterior view), and LPD (dorsal view) components collapsed across all experimental conditions and all pedestal contrast levels. The data were arranged so that the electrodes on the left and right sides of the head models represented the electrodes that are ipsilateral and contralateral to the stimulus of interest, respectively.

In addition, we evaluated a more complex model in which the sensory noise (σ) and baseline parameters (b) were also allowed to vary freely between the divided-attention and the focused-attention conditions (yielding four free parameters: σ for divided attention, σ for focused attention, b for divided attention, and b for divided attention). We followed the same procedure outlined above in Figure 9*D–F* except that we now optimized the σ and b parameters to find the best fit to the P1 and LPD component CRFs obtained in the focused-attention condition. This more complex model led to a slight improvement in the fit to the P1 component CRF (Fig. 9*G*, blue curve; $R^2 = 0.96$, $\sigma = 0.15$ μV, $b = -0.07$ μV) and to the LPD component CRF (Fig. 9*H*, blue curve; $R^2 = 0.94$, $\sigma = 0.45$ μV, $b = -0.52$ μV). However, this

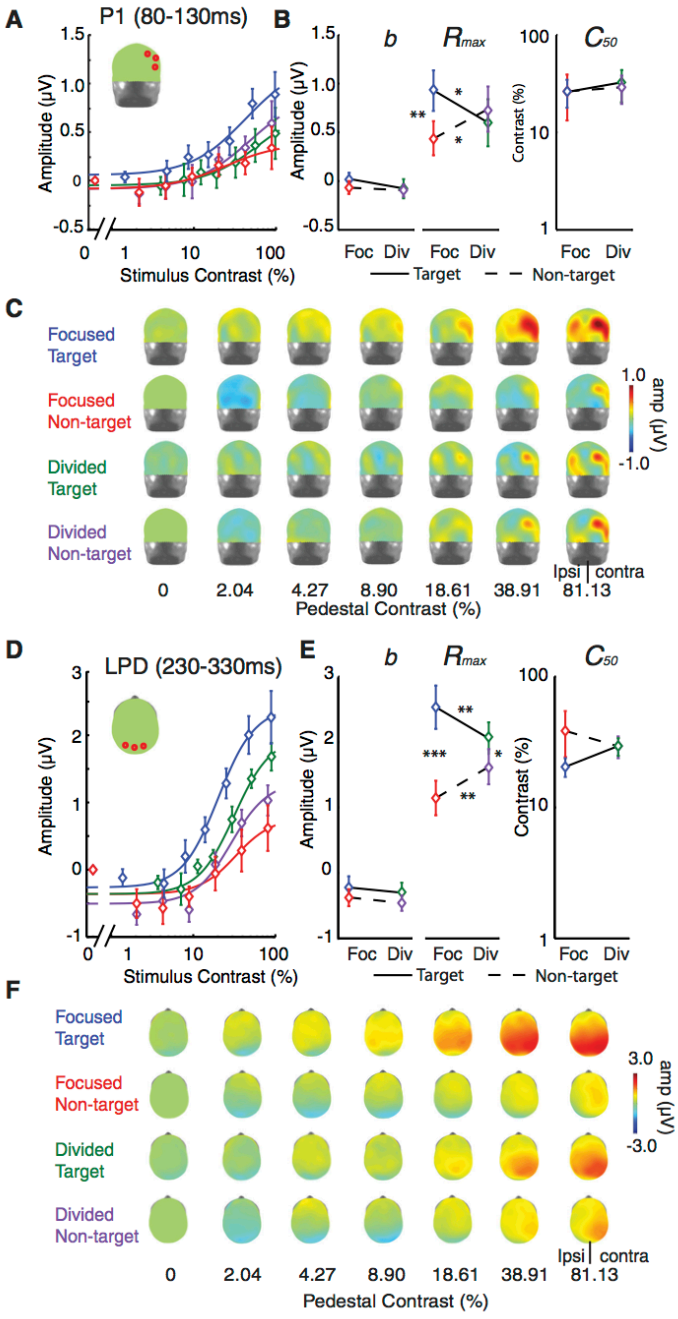

Figure 8. Multiplicative response gain increases with focused attention in ERP CRFs. ***A***, ***C***, ***D***, ***F***, The mean amplitudes of P1 (***A***) and LPD (***D***) components are plotted as a function of stimulus contrast (see corresponding topographical maps in ***C*** and ***F***, respectively). The CRFs for focused-attention targets (blue), focused-attention nontargets (red), divided-attention targets (green), and divided-attention nontargets (purple) were fit with a Naka-Rushton equation (Eq. 2). ***B***, ***E***, A bootstrapping analysis showed that the attentional enhancement on the P1 and LPD components was selectively driven by changes in the response amplitude parameter (R_{max}; ***B***, ***E***, middle), and the baseline (*b*, left) and the semisaturation contrast parameters (C_{50}, right) did not significantly change. Error bars in ***A*** and ***D*** indicate ±SEM across subjects. Error bars in ***B*** and ***E*** represent 68% confidence intervals from the bootstrapping analysis. *, **, and *** Indicate significance based on *post hoc* pairwise comparisons corrected by the Holm-Bonferroni method at $p < 0.05$, $p < 0.01$, $p < 0.001$, respectively.

improvement was not statistically significant (P1, $F_{(2,9)} = 2.29$, $p = 0.16$; LPD, $F_{(2,9)} = 0.85$, $p = 0.92$, nested *F* test) so the added complexity of the model with the increased number of free parameters was not justified. An additional bootstrapping analysis with resampled subject labels also revealed that this more complex model did not significantly change the values of the σ (Fig. 9*I*) or the *b* parameters (Fig. 9*J*) across the divided-attention and focused-attention conditions (σ of P1, $p = 0.92$; σ of LPD, $p = 0.98$; *b* of P1, $p = 0.46$; *b* of LPD, $p = 0.83$). This analysis suggests that changes in the sensory noise parameter and the baseline parameter are not necessary for explaining changes in behavior. Consistent with this notion, an additional analysis revealed no significant main effect of attention on the SD of the bootstrapping distribution of P1 ($F_{(1,15)} = 1.19$, $p = 0.29$) and LPD component amplitudes ($F_{(1,15)} = 0.0040$, $p = 0.60$; See Materials and Methods).

Sensory gain outperforms efficient readout

Thus far, a model in which only sensory gain varies between attention conditions can effectively link attention-related changes in behavioral TvCs and neural CRFs. However, we also asked whether a recently developed efficient readout model (Pestilli et al., 2011) could provide an even better account of the link between attention-related changes in neural CRFs and behavioral TvC curves. The model is based on the notion that the subject's task is to select the interval with the higher overall contrast. Thus, an ideal observer could compute the overall contrast across both stimuli in each interval and then select the interval associated with the higher mean contrast. To evaluate this model, we estimated the TvCs in the focused-attention and divided-attention conditions using a max-pooling equation (Eq. 10). In this equation, *k* is an exponent that weights each of the responses to indi-

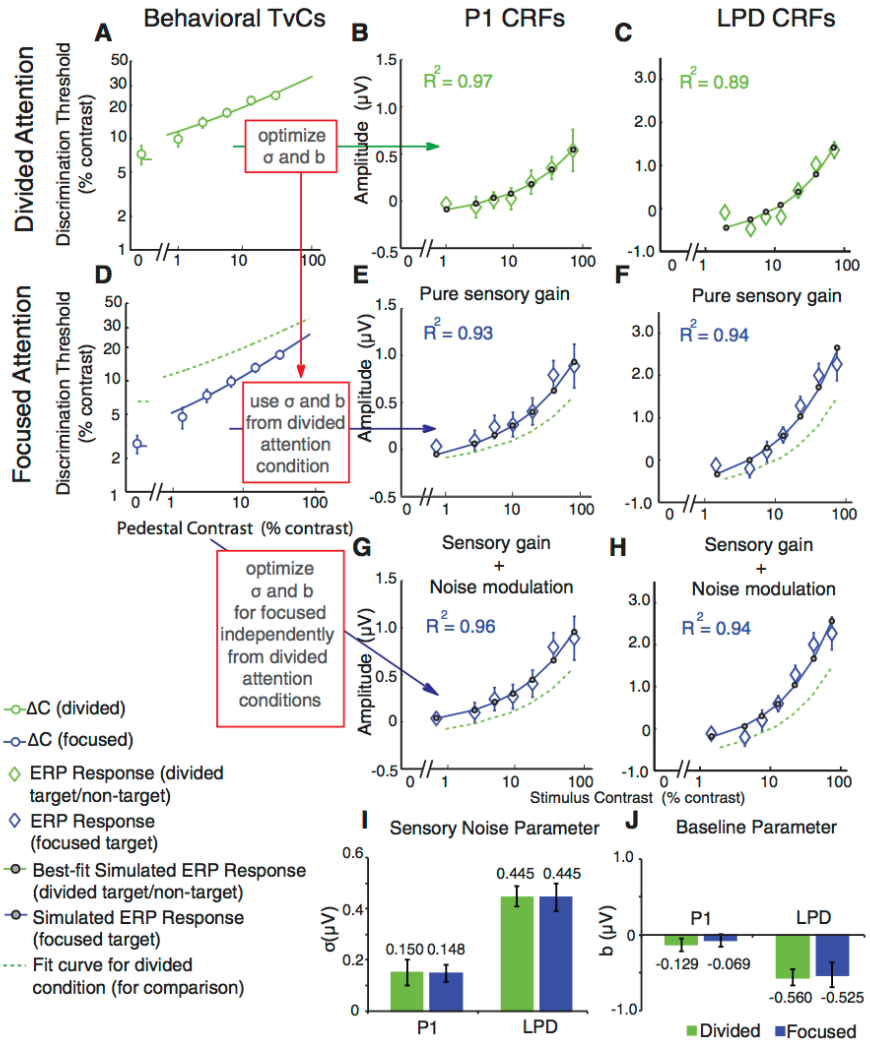

Figure 9. Sensory gain is sufficient to link neural and behavioral data. ***A–C***, The psychophysical TvC function in the divided-attention condition (***A***, green curve) was used to estimate P1 and LPD component CRFs (***B***, ***C***, green curves; Fig. 4, fitting procedure; see experimental procedures). Using the modeling routine in Figure 4, the sensory noise (σ) and baseline (b) parameters were optimized to yield the best fits for P1 and LPD component CRFs from the divided-attention condition, respectively. ***D–F***, To examine whether the multiplicative response gain increase in the P1 and the LPD component CRFs could sufficiently account for behavioral improvements with attention, the TvC function from the focused-attention condition (***D***, blue curve) was then used to estimate the P1 and the LPD component CRFs in the focused-attention condition (***E***, ***F***, blue curves) using the σ and b parameters obtained from the divided-attention condition (***A–C***). The simulation yielded excellent fits for both the P1 and the LPD component CRFs. To determine whether noise modulation improves the ability of the model to link neural and behavioral data, a similar analysis was also performed directly on data from the focused-attention condition by allowing the σ and b parameters in the divided-attention and focused-attention conditions to vary freely. ***G***, ***H***, This analysis yielded excellent fits for both the P1 (***G***) and the LPD (***H***) component CRFs. However, it did not significantly improve the fit. ***I***, ***J***, Moreover, a bootstrapping analysis on this later fitting procedure demonstrated there was no significant difference in σ (***I***) and b parameters (***J***) across divided-attention (green bars) and focused-attention conditions (blue bars). Error bars in ***A–H*** indicate ±SEM across subjects. Error bars in ***I*** and ***J*** indicate ±68% confidence intervals from the bootstrapping analysis.

vidual stimuli (k ranges from 1 to ∞). When $k = 1$, the responses are unmodified and are equal to the magnitude of their evoked responses (simple mean) and the model reduces to the standard sensory gain model described in the previous section. However, when $k > 1$, the stimulus that evokes a relatively large response will be overweighted compared with a stimulus that evokes a relatively small response, and consequently the stimulus evoking the larger response will increasingly influence downstream decision mechanisms (and as k approaches ∞, only the stimulus that evokes the largest response will contribute). Therefore, if a target-

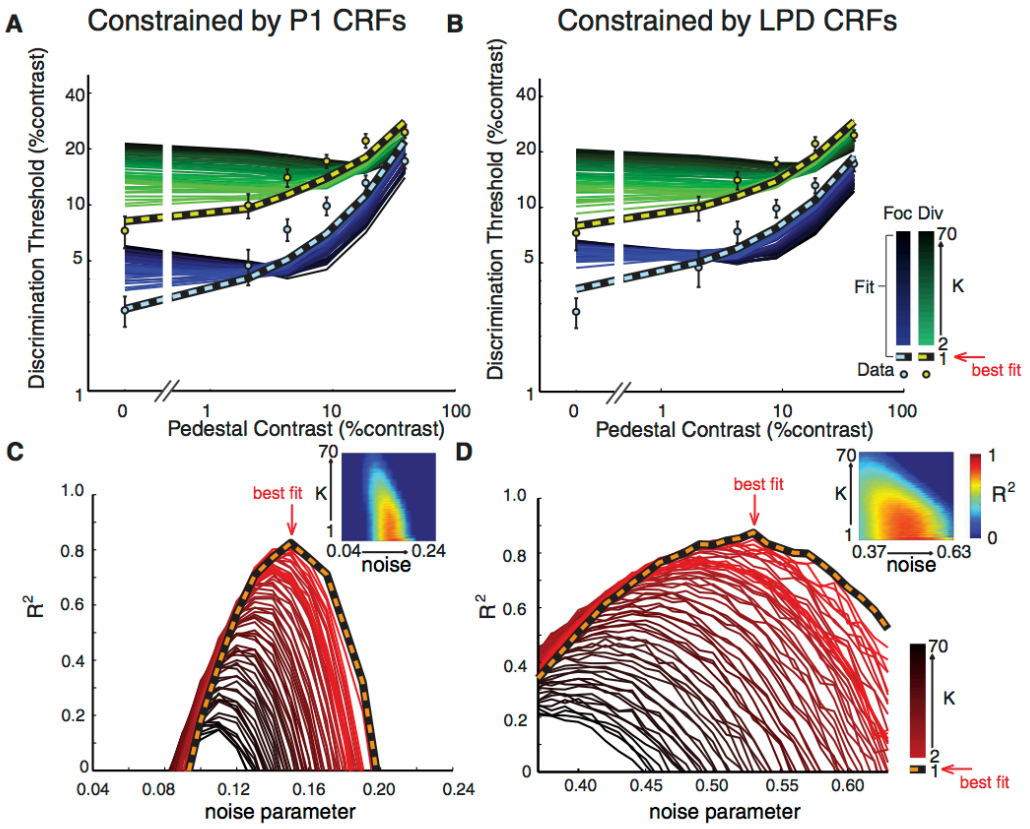

Figure 10. Direct comparison of the sensory gain and efficient readout models. ***A***, ***B***, To test whether the sensory gain model or efficient readout model is better at describing the relationship between the neural and behavioral data, we estimated the psychophysical contrast-discrimination thresholds with the max-pooling rule (Eq. 4), while constraining the fitting procedure with the P1 (***A***) and LPD (***B***) component CRFs. When the exponential weight in the max-pooling rule (k) was set to 1 (i.e., equivalent to the pure sensory gain model), the estimated TvC function fit very well with the observed psychophysical thresholds (light blue and black lines, focused-attention condition; light green and black lines, divided-attention condition). However, as k increased (i.e., implementing the max-pooling rule), the performance of the efficient readout model systematically declined. Specifically, the efficient readout model underestimated contrast thresholds when target stimuli had low pedestal contrasts and overestimated contrast thresholds when target stimuli had high pedestal contrasts. Error bars indicate ±SEM across subjects. The shading of the curves indicates the simulations at different k values (bright to dark colors for k of 2–70). ***C***, ***D***, Corresponding R^2 of the simulations shown in ***A*** and ***B***, respectively. Orange and black lines represent the goodness of fit when $k = 1$. Shading of the curves indicates R^2 at different k values (bright to dark colors for k of 2–70). Red arrows point to the k and noise values that yield the best fit ($k = 1$). Insets in ***C*** and ***D*** show the 2D plots of R^2 where x and y axes represent noise and k parameters in the fitting routine.

evoked response on a given trial is higher than a nontarget-evoked response, the pooling model will exacerbate this differential response in favor of the target response, and the interval containing the target will tend to be selected correctly. However, if a nontarget-evoked response on a given trial is higher than a target-evoked response, then this model will overweight the nontarget-evoked response and the probability of a correct response will decrease.

As shown in Figure 10*A–D*, without the max-pooling rule (i.e., $k = 1$), the model provided a good description of the observed behavioral data (striped curves) for both focused-attention and divided-attention conditions (R^2 of 0.82 and 0.87; σ of 0.15 and 0.53 μV for the P1 and LPD components, respectively). Conversely, the addition of the max-pooling rule (i.e., allowing k to adopt values >1) led to increasingly poor model performance that did not closely track the behavioral data (Fig. 10*A–D*; darker solid color curves for higher values of k). Under these circumstances ($k > 1$), the selection model overweights responses generated by any high-contrast stimulus in the display, and this degrades performance given that higher contrast stimuli may or may not be the target on a given trial.

Discussion

Several studies have demonstrated that spatial attention amplifies neural responses in early sensory areas (Haenny et al., 1988; Motter, 1993; Connor et al., 1997; Luck et al., 1997; McAdams and Maunsell, 1999; Reynolds et al., 2000; Martínez-Trujillo and Treue, 2002; Lee and Maunsell, 2009, 2010; Pooresmaeili et al., 2010; Sprague and Serences, 2013); however, very few of them have quantitatively linked these gain modulations with behavioral changes. As a result, almost all documented links between attention and behavior can be explained equally well by theories that invoke either noise modulation (Mitchell et al., 2007, 2009) or post-

sensory readout mechanisms (Pelli, 1985; Palmer et al., 2000; although see Cohen and Maunsell, 2009; Pestilli et al., 2011). Here, we examined the relative contributions of sensory gain, noise modulation, and readout to attention-dependent changes in perceptual sensitivity by simultaneously linking psychophysical and neurophysiological data using quantitative frameworks based on either signal detection theory or a combination of signal detection theory and efficient readout. We find that a model based solely on a multiplicative increase in the amplitude of the P1 and the LPD component-evoked potentials captures nearly all the variance in behavior, even in an absence of noise modulation. Moreover, this sensory gain model outperforms models that also incorporate an efficient readout mechanism.

Our results stand in contrast with a recent fMRI study (Pestilli et al., 2011), which found that attention induced an additive shift in hemodynamic CRFs. This additive shift cannot explain attention-related changes in TvCs via a sensory gain model, as changes in behavioral sensitivity are only predicted if the CRF slope changes. Note that we use the term additive "shift" instead of additive "gain" here since gain is multiplicative by definition. Alternatively, Pestilli et al. (2011) adopted a readout mechanism based on a max-pooling rule that uses exponentiation to increase differential responses evoked by pedestal and target stimuli. Unlike our study, the nontarget contrast values in Pestilli et al. (2011) by design were very close to the target contrast value. Thus, the additive shift in hemodynamic CRFs ensures that target-related responses will be higher than nontarget-related responses. As the exponent of the max-pooling rule increases, the contrast increment that defines the target will elicit a larger differential response and an ideal observer will more accurately discern the interval that contained the target. Accordingly, this max-pooling rule enabled them to accurately predict the relationship between attention-induced changes in TvCs and hemodynamic CRFs even without changes in slopes of the CRFs.

It is possible that a lack of quantitative evidence for sensory gain in Pestilli et al. (2011) may be due to the insensitivity of fMRI to detect attention-induced sensory gain changes. For example, it is known that attention-related additive increases in hemodynamic CRFs are independent of stimulus intensity (Buracas and Boynton, 2007; Murray, 2008), which is not typically observed in electrophysiological data (Reynolds et al., 2000; Di Russo et al., 2001; Martínez-Trujillo and Treue, 2002; but see Williford and Maunsell, 2006; Kim et al., 2007; Lauritzen et al., 2010; Lee and Maunsell, 2010; Itthipuripat et al., 2014). The stimulus-independent nature of hemodynamic responses is consistent with other reports showing large anticipatory/top-down effects of spatial attention on fMRI signals (Kastner et al., 1999; Ress et al., 2000; Serences et al., 2004; McMains et al., 2007; Sylvester et al., 2009) and this anticipatory/top-down modulation may not always be tightly associated with local neuronal activity (Sirotin and Das, 2009; Cardoso et al., 2012). Moreover, there is evidence from the clinical literature suggesting that fMRI may be insensitive to local changes in sensory gain, as presumed deficits in sensory gain in schizophrenic patients could be captured by EEG but not by fMRI (Calderone et al., 2013).

In contrast to fMRI studies (Buracas and Boynton, 2007; Murray, 2008; Pestilli et al., 2011), studies using EEG (Di Russo et al., 2001; Kim et al., 2007; Lauritzen et al., 2010; Wang and Wade, 2011; Itthipuripat et al., 2014) have shown various gain patterns resembling those measured using single-unit recording (Reynolds et al., 2000; Martínez-Trujillo and Treue, 2002; Lee and Maunsell, 2010). Among these studies, EEG does not typically exhibit an additive offset with attention and it appears to be sensitive to changes in sensory-evoked responses. This sensitivity to sensory responses enables us to assess the interaction of attention and stimulus-evoked responses to evaluate how well a model based on sensory gain can account for behavioral changes. We found that a multiplicative response gain of the ERP-based CRFs was sufficient to explain attention-related changes in behavior. As a result of this strong predictive relationship between ERP gain profiles and behavior, the implementation of a max-pooling rule impaired model fits, as little variance was left to be explained. Also note that by design, target and nontarget pedestal contrasts were fully crossed and independent. Thus a max-pooling rule would not always give more weight to the target-evoked response (e.g., when a low-contrast target paired with a high-contrast nontarget).

One resolution to the discrepancies between different measurements is offered by Hara et al. (2014), who argue that population-based metrics that index the activity from broadly tuned neurons will give rise to additive shifts with attention as observed in hemodynamic CRFs. In contrast, well-tuned cells, as is the case in most single-unit electrophysiology, will exhibit either response or contrast gain, which is thought to be determined by the relative size of the stimulus with respect to the scope of spatial attention as predicted by the normalization model of attention (Reynolds and Heeger, 2009; Herrmann et al., 2010; Itthipuripat et al., 2014). However, this possibility does not by itself offer a clear account for differences between fMRI and EEG, as EEG also provides a broad population-based activity. Further complicating matters, recent work using voltage-sensitive dye imaging (VSDI) also reported additive attention effects in monkey V1 (Chen and Seidemann, 2012). As suggested by Hara et al. (2014), each of these population-level measures (EEG, fMRI, and VSDI) might be differentially sensitive to well tuned and broadly tuned neurons, with EEG perhaps dominated more by responses from well tuned neurons. However, as mentioned above, it is also possible that EEG may be more sensitive to attentional modulations of local stimulus-evoked spiking activity, whereas fMRI and VSDI may be more sensitive to top-down signals. Consistent with this idea, fMRI has been suggested to be sensitive to capture synaptic inputs to particular cortical areas instead of spiking outputs from the areas (Logothetis, 2002, 2008; Logothetis and Wandell, 2004; Viswanathan and Freeman, 2007). Similarly, VSDI primarily captures the top-down inputs to V1 rather than the local modulations of spiking in V1 (Chen and Seidemann, 2012). In contrast to fMRI and VSDI, EEG has been closely associated with spiking activity in visual cortex (Whittingstall and Logothetis, 2009) and tightly linked to the perceived appearance of a stimulus (Campbell and Kulikowski, 1972; Störmer et al., 2009). Thus, it is possible that attentional modulation of stimulus-evoked spiking activity, which might be better captured by EEG, is more closely related to perceptual experience and its behavioral outcomes. Nonetheless, these attention-related changes in stimulus-evoked sensory responses are presumably being modulated by top-down attention signals, so understanding how different metrics of brain activity index different aspects of attentional modulation is crucial to develop a more complete understanding of cortical information processing.

Contrary to the sensory gain and efficient readout accounts, recent studies in monkeys have demonstrated that attention modulates neural noise. Attention has been shown to modulate the trial-by-trial variability of single neuron spike rates as well as pairwise correlations between neurons in early visual areas (Mitchell et al., 2007, 2009; Cohen and Maunsell, 2009; Niebergall et al., 2011; Herrero et al., 2013). These noise modulations

have been hypothesized to lead to a larger improvement in the signal-to-noise ratio (SNR) of neural populations compared with pure changes in sensory gain (Cohen and Maunsell, 2009; Mitchell et al., 2009). In our study, we found that sensory gain in ERPs could satisfactorily account for the observed behavioral improvements, even under the assumption that the trial-by-trial variability of ERP amplitudes is unaltered across attention conditions. Note, however, that our results are not necessarily inconsistent with observations from monkey data showing that attention does modulate neural noise, because EEG measures do not provide direct estimates of single-unit variability or population-level covariance measures (and the same limitation also applies for fMRI measures). Indeed, it is possible that attention-related modulations in neural noise might contribute to changes in ERP amplitudes. For example, if sensory neurons fire more consistently, and if changes in noise correlation improve the SNR of pooled neuronal signals, then these noise modulations may strengthen the synchronization across local neural populations and thus amplify the electrical dipole that generates an ERP on the scalp (Cooper et al., 1965; Gloor, 1985; Makeig et al., 2002; Murakami and Okada, 2006). Therefore, it is also possible that changes in the noise characteristics of underlying neural generators might influence attentional modulation of the P1 and LPD components.

References

Boynton GM, Demb JB, Glover GH, Heeger DJ (1999) Neuronal basis of contrast discrimination. Vision Res 39:257–269. CrossRef Medline

Brainard DH (1997) The psychophysics toolbox. Spat Vis 10:433–436. CrossRef Medline

Buracas GT, Boynton GM (2007) The effect of spatial attention on contrast response functions in human visual cortex. J Neurosci 27:93–97. CrossRef Medline

Calderone DJ, Martinez A, Zemon V, Hoptman MJ, Hu G, Watkins JE, Javitt DC, Butler PD (2013) Comparison of psychophysical, electrophysiological, and fMRI assessment of visual contrast responses in patients with schizophrenia. Neuroimage 67:153–162. CrossRef Medline

Campbell FW, Kulikowski JJ (1972) The visual evoked potential as a function of contrast of a grating pattern. J Physiol 222:345–356. Medline

Cardoso MM, Sirotin YB, Lima B, Glushenkova E, Das A (2012) The neuroimaging signal is a linear sum of neurally distinct stimulus- and task-related components. Nat Neurosci 15:1298–1306. CrossRef Medline

Chen Y, Seidemann E (2012) Attentional modulations related to spatial gating but not to allocation of limited resources in primate V1. Neuron 74:557–566. CrossRef Medline

Cohen MR, Maunsell JH (2009) Attention improves performance primarily by reducing interneuronal correlations. Nat Neurosci 12:1594–1600. CrossRef Medline

Connor CE, Preddie DC, Gallant JL, Van Essen DC (1997) Spatial attention effects in macaque area V4. J Neurosci 17:3201–3214. Medline

Cook EP, Maunsell JH (2002) Dynamics of neuronal responses in macaque MT and VIP during motion detection. Nat Neurosci 5:985–994. CrossRef Medline

Cooper R, Winter AL, Crow HJ, Walter WG (1965) Comparison of subcortical, cortical, and scalp activity using chronically indwelling electrodes in man. Electroencephalogr Clin Neurophysiol 18:217–228. CrossRef Medline

Cravo AM, Rohenkohl G, Wyart V, Nobre AC (2013) Temporal expectation enhances contrast sensitivity by phase entrainment of low-frequency oscillations in visual cortex. J Neurosci 33:4002–4010. CrossRef Medline

Delorme A, Makeig S (2004) EEGLAB: an open source toolbox for analysis of single-trial EEG dynamics including independent component analysis. J Neurosci Methods 134:9–21. CrossRef Medline

Di Russo F, Spinelli D, Morrone MC (2001) Automatic gain control contrast mechanisms are modulated by attention in humans: evidence from visual evoked potentials. Vision Res 41:2435–2447. CrossRef Medline

Gloor P (1985) Neuronal generators and the problem of localization in electroencephalography: Application of volume conductor theory to electroencephalography. J Clin Neurophysiol 2:327–354. CrossRef Medline

Gorea A, Sagi D (2001) Disentangling signal from noise in visual contrast discrimination. Nat Neurosci 4:1146–1150. CrossRef Medline

Haenny PE, Maunsell JH, Schiller PH (1988) State dependent activity in monkey visual cortex. I. Single cell activity in V1 and V4 on visual tasks. Exp Brain Res 69:245–259. CrossRef Medline

Hara Y, Pestilli F, Gardner JL (2014) Differing effects of attention in single-units and populations are well predicted by heterogeneous tuning and the normalization model of attention. Front Comput Neurosci 8:12. CrossRef Medline

Heinze HJ, Luck SJ, Mangun GR, Hillyard SA (1990) Visual event-related potentials index focused attention within bilateral stimulus arrays. I. Evidence for early selection. Electroencephalogr Clin Neurophysiol 75:511–527. CrossRef Medline

Herrero JL, Gieselmann MA, Sanayei M, Thiele A (2013) Attention-induced variance and noise correlation reduction in macaque V1 is mediated by NMDA receptors. Neuron 78:729–739. CrossRef Medline

Herrmann K, Montaser-Kouhsari L, Carrasco M, Heeger DJ (2010) When size matters: attention affects performance by contrast or response gain. Nat Neurosci 13:1554–1559. CrossRef Medline

Hillyard SA, Anllo-Vento L (1998) Event-related brain potentials in the study of visual selective attention. Proc Natl Acad Sci U S A 95:781–787. CrossRef Medline

Hillyard SA, Squires KC, Bauer JW, Lindsay PH (1971) Evoked potential correlates of auditory signal detection. Science 172:1357–1360. CrossRef Medline

Hillyard SA, Vogel EK, Luck SJ (1998) Sensory gain control (amplification) as a mechanism of selective attention: electrophysiological and neuroimaging evidence. Philos Trans R Soc Lond B Biol Sci 353:1257–1270. CrossRef Medline

Huang L, Dobkins KR (2005) Attentional effects on contrast discrimination in humans: evidence for both contrast gain and response gain. Vision Res 45:1201–1212. Medline

Itthipuripat S, Garcia JO, Rungratsameetaweemana N, Sprague TC, Serences JT (2014) Changing the spatial scope of attention alters patterns of neural gain in human cortex. J Neurosci 34:112–123. CrossRef Medline

Johannes S, Muente TF, Heinze HJ, Mangun GR (1995) Luminance and spatial attention effects on early visual processing. Cogn Brain Res 2:189–205. CrossRef

Kastner S, Pinsk MA, De Weerd P, Desimone R, Ungerleider LG (1999) Increased activity in human visual cortex during directed attention in the absence of visual stimulation. Neuron 22:751–761. CrossRef Medline

Kim YJ, Grabowecky M, Paller KA, Muthu K, Suzuki S (2007) Attention induces synchronization-based response gain in steady-state visual evoked potentials. Nat Neurosci 10:117–125. CrossRef Medline

Lange JJ, Wijers AA, Mulder LJM, Mulder G (1999) ERP effects of spatial attention and display search with unilateral and bilateral stimulus displays. Biol Psych 50:203–233. CrossRef

Lauritzen TZ, Ales J, Wade AR (2010) The effects of visuospatial attention measured across visual cortex using source-imaged, steady-state EEG. J Vis 10(14):1–17. CrossRef Medline

Lee J, Maunsell JH (2009) A normalization model of attentional modulation of single unit responses. PLoS One 4:e4651. CrossRef Medline

Lee J, Maunsell JH (2010) The effect of attention on neuronal responses to high and low contrast stimuli. J Neurophysiol 104:960–971. CrossRef Medline

Legge GE, Foley JM (1980) Contrast masking in human vision. J Opt Soc Am 70:1458–1471. CrossRef Medline

Logothetis NK (2002) The neural basis of the blood-oxygen-level-dependent functional magnetic resonance imaging signal. Philos Trans R Soc Lond B Biol Sci 357:1003–1037. CrossRef Medline

Logothetis NK (2008) What we can do and what we cannot do with fMRI. Nature 453:869–878. CrossRef Medline

Logothetis NK, Wandell BA (2004) Interpreting the BOLD signal. Annu Rev Physiol 66:735–769. CrossRef Medline

Luck SJ, Heinze HJ, Mangun GR, Hillyard SA (1990) Visual event-related potentials index focused attention within bilateral stimulus arrays. II. Functional dissociation of P1 and N1 components. Electroencephalogr Clin Neurophysiol 75:528–542. CrossRef Medline

Luck SJ, Chelazzi L, Hillyard SA, Desimone R (1997) Neural mechanisms of spatial selective attention in areas V1, V2 and V4 of macaque visual cortex. J Neurophysiol 77:24–42. Medline

Makeig S, Westerfield M, Jung TP, Enghoff S, Townsend J, Courchesne E, Sejnowski TJ (2002) Dynamic brain sources of visual evoked responses. Science 295:690–694. CrossRef Medline

Mangun GR, Buck LA (1998) Sustained visual-spatial attention produces costs and benefits in response time and evoked neural activity. Neuropsychologia 36:189–200. CrossRef Medline

Mangun GR, Hillyard SA (1987) The spatial allocation of visual attention as indexed by event-related brain potentials. Hum Factors 29:195–211. Medline

Mangun GR, Hillyard SA (1988) Spatial gradients of visual attention: behavioral and electrophysiological evidence. Electroencephalogr Clin Neurophysiol 70:417–428. CrossRef Medline

Mangun GR, Hillyard SA (1990) Allocation of visual attention to spatial locations: tradeoff functions for event-related brain potentials and detection performance. Percept Psychophys 47:532–550. CrossRef Medline

Mangun GR, Hillyard SA (1991) Modulations of sensory-evoked brain potentials indicate changes in perceptual processing during visual-spatial priming. J Exp Psychol Hum Percept Perform 17:1057–1074. CrossRef Medline

Martínez-Trujillo J, Treue S (2002) Attentional modulation strength in cortical area MT depends on stimulus contrast. Neuron 35:365–370. CrossRef Medline

McAdams CJ, Maunsell JH (1999) Effects of attention on orientation-tuning functions of single neurons in macaque cortical area V4. J Neurosci 19:431–441. Medline

McMains SA, Fehd HM, Emmanouil TA, Kastner S (2007) Mechanisms of feature- and space-based attention: response modulation and baseline increases. J Neurophysiol 98:2110–2121. CrossRef Medline

Mitchell JF, Sundberg KA, Reynolds JH (2007) Differential attention-dependent response modulation across cell classes in macaque visual area V4. Neuron 55:131–141. CrossRef Medline

Mitchell JF, Sundberg KA, Reynolds JH (2009) Spatial attention decorrelates intrinsic activity fluctuations in macaque area V4. Neuron 63:879–888. CrossRef Medline

Moran J, Desimone R (1985) Selective attention gates visual processing in the extrastriate cortex. Science 229:782–784. CrossRef Medline

Motter BC (1993) Focal attention produces spatially selective processing in visual cortical areas V1, V2 and V4 in the presences of competing stimuli. J Neurophysiol 70:909–919. Medline

Murakami S, Okada Y (2006) Contributions of principal neocortical neurons to magnetoencephalography and electroencephalography signals. J Physiol 575:925–936. CrossRef Medline

Murray SO (2008) The effects of spatial attention in early human visual cortex are stimulus independent. J Vis 8(10):2.1–2.11. CrossRef Medline

Nachmias J, Sansbury RV (1974) Letter: grating contrast: discrimination may be better than detection. Vision Res 14:1039–1042. CrossRef Medline

Niebergall R, Khayat PS, Treue S, Martinez-Trujillo JC (2011) Expansion of MT neurons excitatory receptive fields during covert attentive tracking. J Neurosci 31:15499–15510. CrossRef Medline

Noesselt T, Hillyard SA, Woldorff MG, Schoenfeld A, Hagner T, Jäncke L, Tempelmann C, Hinrichs H, Heinze HJ (2002) Delayed striate cortical activation during spatial attention. Neuron 35:575–587. CrossRef Medline

O'Connell RG, Dockree PM, Kelly SP (2012) A supramodal accumulation-to-bound signal that determines perceptual decisions in humans. Nat Neurosci 15:1729–1735. CrossRef Medline

Palmer J, Verghese P, Pavel M (2000) The psychophysics of visual search. Vision Res 40:1227–1268. CrossRef Medline

Pelli DG (1985) Uncertainty explains many aspects of visual contrast detection and discrimination. J Opt Soc Am 2:1508–1532. CrossRef

Pelli DG (1997) The VideoToolbox software for visual psychophysics: transforming numbers into movies. Spat Vis 10:437–442. CrossRef Medline

Pestilli F, Carrasco M, Heeger DJ, Gardner JL (2011) Attentional enhancement via selection and pooling of early sensory responses in human visual cortex. Neuron 72:832–846. CrossRef Medline

Pooresmaeili A, Poort J, Thiele A, Roelfsema PR (2010) Separable codes for attention and luminance contrast in the primary visual cortex. J Neurosci 30:12701–12711. CrossRef Medline

Ress D, Backus BT, Heeger DJ (2000) Activity in primary visual cortex predicts performance in a visual detection task. Nat Neurosci 3:940–945. CrossRef Medline

Reynolds JH, Heeger DJ (2009) The normalization model of attention. Neuron 61:168–185. CrossRef Medline

Reynolds JH, Pasternak T, Desimone R (2000) Attention increases sensitivity of V4 neurons. Neuron 26:703–714. CrossRef Medline

Ross J, Speed HD, Morgan MJ (1993) The effects of adaptation and masking on incremental thresholds for contrast. Vision Res 33:2051–2056. CrossRef Medline

Schadow J, Lenz D, Thaerig S, Busch NA, Fründ I, Herrmann CS (2007) Stimulus intensity affects early sensory processing: sound intensity modules auditory evoked gamma-band activity in human EEG. Int J Psychophysiol 65:152–161. CrossRef Medline

Serences JT, Yantis S, Culberson A, Awh E (2004) Preparatory activity in visual cortex indexes distractor suppression during covert spatial orienting. J Neurophysiol 92:3538–3545. CrossRef Medline

Sirotin YB, Das A (2009) Anticipatory haemodynamic signals in sensory cortex not predicted by local neuronal activity. Nature 457:475–479. CrossRef Medline

Spekreijse H, van der Twell LH, Zuidema T (1973) Contrast evoked responses in man. Vision Res 13:1577–1601. CrossRef Medline

Sprague TC, Serences JT (2013) Attention modulates spatial priority maps in the human occipital, parietal and frontal cortices. Nat Neurosci 16:1879–1887. CrossRef Medline

Squires KC, Hillyard SA, Lindsay PH (1973) Cortical potentials evoked by confirming and disconfirming feedback following an auditory discrimination. Percept Psychophys 13:25–31. CrossRef

Squires KC, Squires NK, Hillyard SA (1975a) Vertex evoked potentials in a rating-scale detection task relation to signal probability. Behav Biol 3:21–34. Medline

Squires KC, Squires NK, Hillyard SA (1975b) Decision-related cortical potentials during an auditory signal detection task with cued observation intervals. J Exp Psychol Hum Percept Perform 1:268–279. CrossRef Medline

Störmer VS, McDonald JJ, Hillyard SA (2009) Cross-modal cueing of attention alters appearance and early cortical processing of visual stimuli. Proc Natl Acad Sci U S A 106:22456–22461. CrossRef Medline

Sylvester CM, Shulman GL, Jack AI, Corbetta M (2009) Anticipatory and stimulus-evoked blood oxygenation level-dependent modulations related to spatial attention reflect a common additive signal. J Neurosci 29:10671–10682. CrossRef Medline

Talsma D, Woldorff MG (2005) Selective attention and multisensory integration: multiple phases of effects on the evoked brain activity. J Cogn Neurosci 17:1098–1114. CrossRef Medline

Van Voorhis S, Hillyard SA (1977) Visual evoked potentials and selective attention to points in space. Percept Psychophys 22:54–62. CrossRef

Vassilev A, Stomonyakov V, Manahilov V (1994) Spatial-frequency specific contrast gain and flicker masking of human transient VEP. Vision Res 34:863–872. CrossRef Medline

Viswanathan A, Freeman RD (2007) Neurometabolic coupling in cerebral cortex reflects synaptic more than spiking activity. Nat Neurosci 10:1308–1312. CrossRef Medline

Wang J, Wade AR (2011) Differential attentional modulation of cortical responses to S-cone and luminance stimuli. J Vis 11(6):1–15. CrossRef Medline

Whittingstall K, Logothetis NK (2009) Frequency-band coupling in surface EEG reflects spiking activity in monkey visual cortex. Neuron 64:281–289. CrossRef Medline

Williford T, Maunsell JH (2006) Effects of spatial attention on contrast response functions in macaque area V4. J Neurophysiol 96:40–54. CrossRef Medline

Woldorff MG, Fox PT, Matzke M, Lancaster JL, Veeraswamy S, Zamarripa F, Seabolt M, Glass T, Gao JH, Martin CC, Jerabek P (1997) Retinotopic organization of early visual spatial attention effects as revealed by PET and ERPs. Hum Brain Mapp 5:280–286. CrossRef Medline

Wright MJ, Johnston A (1982) The effects of contrast and length of gratings on the visual evoked potential. Vision Res 22:1389–1399. CrossRef Medline

Zimmer U, Itthipanyanan S, Grent-'t-Jong T, Woldorff MG (2010) The electrophysiological time course of the interaction of stimulus conflict and the multisensory spread of attention. Eur J Neurosci 31:1744–1754. CrossRef Medline

Chapter 4, in full, is a reprint of the material as it appears in an article entitled "Sensory gain outperforms efficient readout mechanisms in predicting attention-related improvements in behavior " published in The Journal of Neuroscience 2014. Itthipuripat, S.; Ester, Edward F.; Deering, Sean; Serences, John T., Society for Neuroscience, 2014. The dissertation author was the primary author of the manuscript. Supported by National Institutes of Health Grant R01-MH092345 to J.T.S., by a James S. McDonnell Foundation grant to J.T.S, and by a Howard Hughes Medical Institute international student fellowship to S.I. We thank Suzanna K. Wong and Ivan Macias for help with data collection; Javier Garcia and Franco Pestilli for technical support; and Steven Hillyard, Franco Pestilli, Justin Gardner, Thomas C. Sprague, and Anna Byers for useful discussions.